
du Treil, Lundin & Rackley, Inc.

240 North Washington Blvd., Suite 700
Sarasota, Florida 34236
Telephone: 941/366 2611
Facsimile: 941/366 5533

Writer's Direct Communications:
Telephone: 941/366 7434
e-mail: ron@dlr.com

July 30, 2004

Peter Doyle, Esquire
Chief, Audio Division, Media Bureau
Federal Communications Commission
445 12th Street, S.W.
Washington, DC 20554

Dear Peter,

On behalf of Star-H Corporation, the developer of the Kinstar AM antenna, and its manufacturer, Kintronic Laboratories, this is to request that the Audio Division issue a determination that, for purposes of processing construction permit and license applications, its efficiency and vertical radiation characteristics may be based on theoretical calculations using the procedures that are presently used by the FCC for conventional top-loaded AM tower antennas. Such calculations will use the physical height of the vertical radiating portion of the Kinstar antenna for the tower height along with the amount of top loading that is shown to be appropriate in the attached "Engineering Report for Experimental Station WS2XTR and Request for Application of 73.160(b)(2) for the Kinstar AM Transmitting Antenna for General Use by AM Radio Stations in the United States."

The field strength measurements which were made on the test antenna at 1680 kilohertz demonstrated that it met the minimum requirements for Class B, C, and D AM stations and had radiation closely agreeing with what would be predicted using the methods of the FCC Rules assuming its physical height and the amount of top loading that was determined by moment method modeling prior to its construction. The current distribution measurements that were made confirmed that the amount of top loading determined for the design was, indeed, correct. Additional current distribution measurements were made for different antenna tuning unit locations and configurations of the feed system and connections between the four vertical wires at their tops to support further moment method modeling analysis of how the current distributions of the wires might be effected by construction details and environmental factors, and whether they might impact the efficiency and/or vertical radiation characteristics of the Kinstar antenna under real-World conditions.

The report presents further moment method modeling results, using the latest NEC-4.1 techniques that are generally recognized as the best available for analyzing antennas of this type and that were confirmed to be accurate by the measurements that were made on the test antenna, studying what effects might be expected due to installation with imperfect dimensions, construction over non-uniform terrain, and operation under adverse weather conditions. It demonstrates that the departure of the Kinstar antenna's performance from the ideal thin-wire current distribution model assumed for AM antenna analysis is within the range typical of tower antennas that have been routinely authorized by the FCC for decades and that are presently in common use.

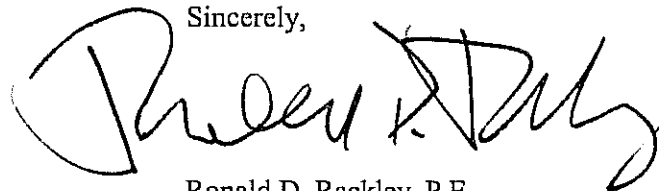
The calculations also show that the performance will not change significantly at any frequency within the AM band if its dimensions are scaled appropriately and that its unattenuated field efficiency will remain essentially constant over various ground types with the 120-radial, quarterwave ground system that it employs.

While the areas where access must be restricted to avoid excessive human electric and magnetic field exposure may be somewhat larger than for tower antennas of conventional height, the same practice of fencing the area around the base is applicable in the case of the Kinstar antenna. Conventional near-field measurement techniques may be used to evaluate the efficacy of the protection plan that is used.

Based on the foregoing, the Kinstar antenna may be employed by AM broadcasters - if standard FCC procedures for analyzing the performance of top loaded towers are used to determine their radiation characteristics - without compromising the present allocation system or adversely impacting service to the public. In fact, since it will be possible for AM stations that must relocate to areas where conventional towers are not allowed by local authorities to utilize Kinstar antennas, it is likely that local AM service may be preserved to a greater extent over time if Kinstar antennas are approved by the FCC. It is, therefore, requested that the FCC consider the Kinstar design to be a tower of the same physical height with the amount of top loading specified based on moment method modeling by its manufacturer over a conventional 120-radial, quarterwave ground system having a loop loss of 1.0 Ohm for the purpose of processing AM applications for construction permit. As modeling has confirmed that the amount of top loading remains essentially constant at the value demonstrated by the experimental station measurements for all frequencies within the AM band, it is also requested that current distribution measurements not be required with applications for license for Kinstar antennas.

If there are any questions with regard to the matters that have been raised, please let me know.

Sincerely,

A handwritten signature in black ink, appearing to read "Ronald D. Rackley". The signature is stylized and cursive, written over the word "Sincerely,".

Ronald D. Rackley, P.E.

dLR:2605A.2159

cc: Ms. Susan Crawford – MB, FCC
Mr. C. Norman Miller – MB, FCC
Ms. Ann Gallagher – MB, FCC
Mr. Ronald Chase – OET, FCC
Star-H Corporation
Kintronic Laboratories



**ENGINEERING REPORT FOR
EXPERIMENTAL STATION WS2XTR
AND
REQUEST FOR APPLICATION OF
47 CFR 73.160(b)(2)
FOR THE KINSTAR AM TRANSMITTING
ANTENNA FOR GENERAL USE BY AM
RADIO STATIONS
IN THE UNITED STATES**

Prepared By:

Michael W. Jacobs
STAR-H CORPORATION
LANCASTER, PENNSYLVANIA

Thomas F. King
KINTRONIC LABORATORIES
BRISTOL, TENNESSEE

July 30, 2004

Executive Summary

This report describes the results of detailed technical analysis along with extensive field tests conducted on the KinStar low-profile AM transmitting antenna developed by STAR-H Corporation and Kintronic Laboratories, Incorporated, and recommends how this new antenna should be considered within the framework of the rules of the Federal Communications Commission (herein "FCC") when used by radio stations in the United States.

Experimental and theoretical analysis of the antenna's operation and the methods underlying the FCC's rules regarding licensing of AM transmitting antennas have been conducted to ensure that the antenna's performance is completely understood and able to be characterized by the existing body of regulation.

In particular, this report will show the following key conclusions:

- The efficiency of the KinStar antenna **meets the minimum field requirements** of 73.189(b)(2)(ii) for Class B, C, and D broadcast stations in the United States.
- The elevation pattern radiation characteristics of the KinStar antenna are represented with sufficient accuracy by the formula of 73.160(b)(2) as a single top-loaded monopole antenna to **permit licensing for full-time operation**.
- All other operating characteristics of the antenna are within accepted practice for existing AM antenna systems and that there exist no safety, technical, or regulatory reasons to prevent stations from using the KinStar antenna in both daytime and nighttime operation anywhere in the United States, subject to the normal engineering and licensing process.

The broadcasting community has expressed its opinion that the availability of an efficient low-profile transmitting antenna will significantly benefit the AM radio service in the United States by allowing them an economical solution to siting difficulties and height restrictions. Further, use of the KinStar can result in improved service to the public by permitting transmitting facilities to be located closer to their service communities without presenting the undesirable visual appearance of a marked, lighted radio tower. Figure 1 shows a comparison of the height of the KinStar antenna versus that of a quarterwave tower monopole at the same operating frequency of 1680 kHz as used in the test program described in this report.

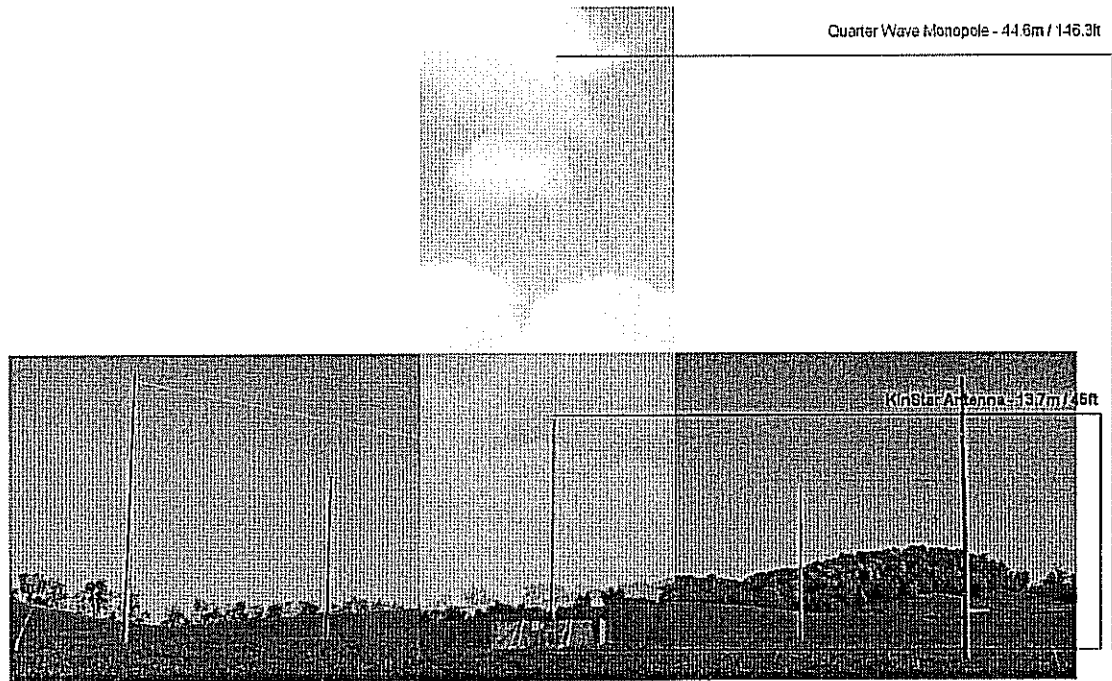


Figure 1 – Composite photograph of quarterwave tower and KinStar antenna at the WS2XTR test site, showing height comparison. Both antennas operate at 1680 kHz.

Table of Contents

Executive Summary..... 2
Table of Contents..... 4
Table of Figures..... 5
1.0 The KinStar Antenna..... 8
 1.1 Mechanical Design..... 10
 1.2 Radiation Pattern Performance..... 12
2.0 Field Testing of Antenna - Experimental Station WS2XTR.... 21
 2.1 Introduction..... 21
 2.2 Antenna Construction..... 22
 2.3 Testing Configurations..... 23
 2.4 Radial Proof Results..... 23
 2.5 Current Distribution Measurements..... 24
3.0 Environmental Effects Modeling..... 31
 3.1 Introduction..... 31
 3.2 Effects of Wind and Ice..... 31
 3.3 Ground Parameter and Frequency Effects..... 34
 3.4 Effects of Uneven Ground Under Antenna..... 37
4.0 Elevation Radiation Pattern..... 40
5.0 RF Exposure Safety Analysis..... 46
Appendix 1..... 54
Appendix 2..... 58
EXHIBIT A..... 62
EXHIBIT B..... 63

Table of Figures

Figure 1 - Composite photograph of quarterwave tower and KinStar antenna at the WS2XTR test site, showing height comparison. . .	3
Figure 2 - KinStar Antenna final design configuration.....	9
Figure 3 - Original KinStar antenna design.....	9
Figure 4 - Azimuth pattern of original "A" design.....	13
Figure 5 - Elevation pattern of original "A" design.....	14
Figure 6 - Azimuth pattern of final "B" design.....	15
Figure 7 - Elevation pattern of final "B" design.....	16
Figure 8 - Azimuth pattern of original "A" design.....	17
Figure 9 - Elevation pattern of original "A" design.....	18
Figure 10 - Azimuth pattern of final "B" design.....	19
Figure 11 - Elevation pattern of final "B" design.....	20
Figure 12 - KinStar antenna at WS2XTR test site.....	21
Figure 13 - Currents on KinStar Antenna Case A.....	27
Figure 14 - Currents on KinStar Antenna Case B.....	27
Figure 15 - Currents on KinStar Antenna Case C.....	28
Figure 16 - KinStar azimuth pattern circularity.....	30
Figure 17 - Impedance sweep of 1680 kHz KinStar "A" version antenna from 1640 to 1720 kHz over average ground with ¼" radial ice.....	32
Figure 18 - Impedance sweep of 1680 kHz KinStar "A" version antenna from 1640 to 1720 kHz over average ground with 1/2" radial ice.....	32

Figure 19 - Normalized elevation field pattern for KinStar antenna with 1/4" radial ice coating over perfect ground.....	33
Figure 20 - KinStar antenna with 0, 2', and 5' deflection in one pair of top loading wires.	34
Figure 21 - Elevation pattern showing horizontally polarized radiation component of KinStar antenna.....	38
Figure 22- Elevation pattern showing horizontally polarized radiation component of quarterwave monopole tower antenna.....	39
Figure 23 - Example of disagreements between 73.160 formulas and NEC models of selected AM broadcasting antennas.....	43
Figure 24 - E-field magnitude directly under top loading wire for 1680 kHz at 1 kW input power at a height of 2 meters (Permissible level is 614 V/m).....	47
Figure 25 - E-field in area halfway between two top loading wires (45 degrees) for 1680 kHz at 1 kW input power at a height of 2 meters (Permissible level is 614 V/m).....	47
Figure 26 - Magnetic field directly under top loading wire for an input power of 1 kW at a height of 2 meters (Permissible level is 1.63 A/m).....	48
Figure 27 - Magnetic field in between wires for 1680 kHz at 1 kW at a height of 2 meters (Permissible level is 1.63 A/m).....	48
Figure 28 - E-field directly under top loading wire for 1680 kHz at 50 kW input power at a height of 2 meters (Permissible level is 614 V/m).....	49
Figure 29 - Magnetic field directly under top loading wire for 1680 kHz at an input power of 50 kW at a height of 2 meters (Permissible level is 1.63 A/m).....	49
Figure 30 - Electric field directly under top loading wire for 550 kHz at an input power of 1 kW at a height of 2 meters (Permissible level is 614 V/m).....	50
Figure 31 - Magnetic field directly under top loading wire for 550 kHz at an input power of 1 kW at a height of 2 meters (Permissible level is 1.63 A/m).....	50

Figure 32 - Electric field directly under top loading wire for 550 kHz at an input power of 50 kW at a height of 2 meters (Permissible level is 614 V/m)..... 51

Figure 33 - Magnetic field directly under top loading wire for 550 kHz at an input power of 50 kW at a height of 2 meters (Permissible level is 1.63 A/m, threshold not shown)..... 52

Figure 34 - Magnetic field directly under top loading wire for 550 kHz at an input power of 50 kW at a height of 2 meters (Permissible level is 1.63 A/m)..... 52

Figure 35 - E -Field plot for 90 degree tower at 1680 kHz at 1 kW along radial at height of 2 meters (Permissible level is 614 V/m). 53

Figure 36 - H -Field plot for 90 degree tower at 1680 kHz at 1 kW along radial at height of 2 meters (Permissible level is 1.63 A/m)..... 53

1.0 The KinStar Antenna

This new antenna design is intended for use by medium frequency AM broadcasting stations in areas where height restrictions or public concern limits the use of 90-degree monopole structures. It consists of a vertical wire cage monopole structure, approximately 0.05 to 0.08 wavelengths tall, with horizontal top loading wires extending radially outward from the top ends of each wire in the monopole cage, with the entire structure operating over a standard quarter-wavelength 120-radial wire ground screen. The top load wires extend a sufficient distance as to cause the desired linear current distribution on the vertical cage wires.

An impedance matching network consisting of either a single lumped-element antenna tuning unit, or a unique system using specific length phase-matched semi-rigid coaxial transmission lines matches the antenna impedance to $50 + j0$ Ohms for connection to the radio station transmitter. Figure 2 shows the general arrangement of the wires in the antenna in the final lumped-element "B" configuration that is intended to be the primary model offered to broadcasters and for which permission for use is requested. Figure 3 shows the original antenna design which uses transmission line matching and which was tested at WS2XTR as the "A" configuration, and which shows slightly higher efficiency and may be preferred for some applications.

Both models have nearly identical current distributions and radiation characteristics. Table 1 presents typical dimensions of this antenna at various frequencies in the AM band. A full technical explanation of the operation of the antenna was presented at the 2002 IEEE Broadcast Symposium in Washington, DC, and is included here in an appendix as Exhibit A. A summary of the operating characteristics is presented here with results of full-scale testing and additional effects modeling in the following sections of this report.

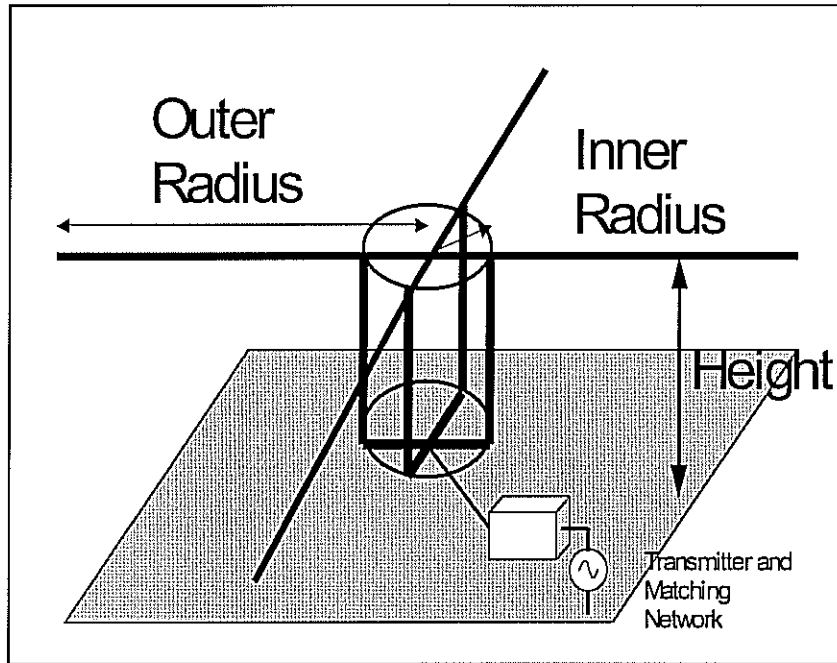


Figure 2 - KinStar Antenna final design configuration using lumped element matching and with top and bottom of vertical radiating wires connected together. Dimensions are shown in Table 1, below, for selected AM broadcast frequencies. All antenna wires are insulated from ground and supports. This design (less the connection at the top of the wires) was the KinStar "B" configuration in the WS2XTR test program

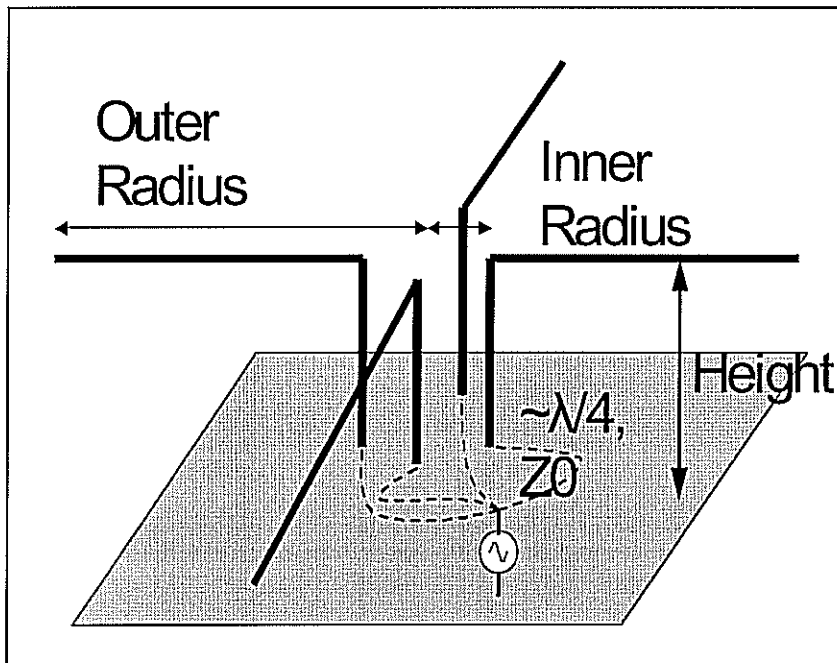


Figure 3 - Original KinStar antenna design using transmission line matching. Each wire is insulated in this configuration, which was tested at WS2XTR as configuration "A".

Table 1. Nominal KinStar Antenna Dimensions

Frequency	Height (ft)	Inner Radius (ft)	Outer Radius (ft)	1.5:1 Bandwidth (kHz)
550 kHz	136.3	16	306.6	16
1000 kHz	75	8.5	168.6	29
1680 kHz	44.9	5	100.1	49
General	Approx. 0.08 λ	Approx. 0.008 λ	Approx. 0.17 λ	2.9%

Note: Dimensions are based on scaling from optimized 1700 kHz design using transmission line matching and 4 vertical wires. Broadbanding of the matching network or the antenna dimensions can improve the bandwidth performance at the lower frequencies to meet IBOC transmitter requirements.

1.1 Mechanical Design

The KinStar antenna's height varies with frequency from 44.1 feet at 1700 kilohertz to about 140 feet at 530 kilohertz. This compares with a height of 146 to 464 feet for a quarterwave tower at the same frequencies. The benefits of the reduced height are both practical and cosmetic. Even at 530 kilohertz, the KinStar antenna will not require marking and lighting at most locations away from registered airports. This results in a cost savings by not requiring a lighting system with its concomitant maintenance and operational costs, along with eliminating the requirement for periodic structure repainting. By reducing the antenna height, the potential hazard to air navigation is reduced, thus increasing safety for aircraft which may find themselves operating at lower altitudes than normal. Cosmetically, the appearance of the antenna will be identical to that of common overhead electrical utility lines, and with its reduced height, the area from which the antenna is visible is significantly reduced. These factors should make it easier for stations to obtain local approval for construction than if they were installing a tall tower with flashing obstruction lighting.

The precise antenna dimensions are determined using computer optimization techniques applied to the NEC-4.1 (Numerical Electromagnetics Code) Method of Moments antenna modeling program. Use of computer optimization allows the KinStar to be designed to meet strict height and bandwidth requirements even as the percentage bandwidth requirement increases with decreasing operating frequency. The dimensions of the antenna, therefore, are not simply scaled with frequency, but can be specifically tailored for each application to best

meet bandwidth requirements while minimizing antenna height. The bandwidth requirements for digital IBOC and DRM transmission have been considered and can be met by the optimized KinStar design for all allocated AM frequencies in the United States.

Common overhead utility line construction materials and techniques are used in the construction of the antenna. For stations operating above approximately 1200 kilohertz, the antenna wires can be supported from a choice of wooden, metal, or concrete utility poles, or from short sections of a small cross-section tower. Below 1200 kilohertz, the required antenna height exceeds 70 feet and wooden poles become less available and more expensive, so the use of tower sections as supports is anticipated. Guying to screw-type ground anchors is practical when using utility poles, and if set carefully with sufficiently compacted backfill, the support poles can be placed directly in augured holes in the ground, resulting in a very low-cost installation. Stations located in coastal hurricane areas, or in areas subject to heavy ice accumulation, or with significant Emergency Alert System responsibilities may wish to opt for more substantial support structures to improve the antenna survivability in extreme weather situations. The vertical support structures will be equipped with a lightning rod and downconductor to a lightning ground to prevent damage to the supports from a lightning strike.

For most omnidirectional applications, the KinStar antenna will consist of a cage of four vertical wires arranged symmetrically around the center of the antenna. Each vertical wire will be connected at the top to a horizontal top loading wire that will extend from the center of the antenna out to the specified length to achieve the required top loading. This length is always shorter than the radius of the ground screen, so it does not impact the land area required for the antenna. At the center, all four horizontal wires will be connected together to provide a shunt path for the reduction of any asymmetrical currents which may arise as a result of inexact placement of supports or uneven terrain effects. For antennas using the lumped element matching method, the bottom of each vertical wire will also be tied together to allow a single feedwire from the antenna tuning unit to be used, as is common practice.

1.2 Radiation Pattern Performance

NEC modeling shows that the KinStar antenna, in both the "A" and "B" variants exhibits a completely omnidirectional azimuth radiation pattern as though radiated from a single vertical conductor. The elevation radiation pattern resembles that from a short constant current element. Figures 4 through 11 show the azimuth and elevation radiation patterns over perfect ground for both antenna variants at 530 kHz and 1680 kHz.

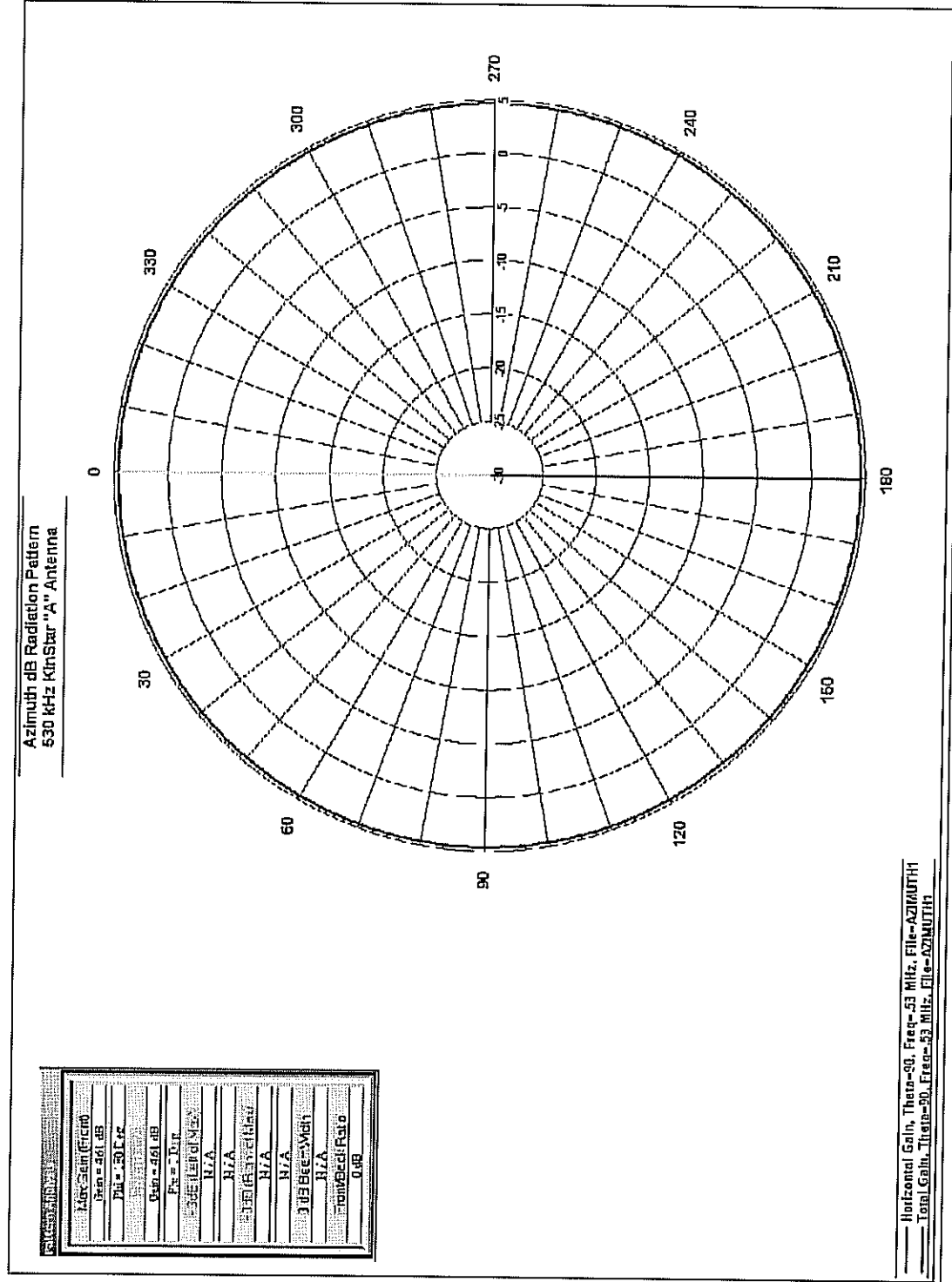


Figure 4 - Azimuth pattern of original "A" design using transmission line matching to isolated wire sections. Pattern is circular with gain of 4.61 dBi at 530 kHz over perfect ground. There is no radiated horizontally polarized component.

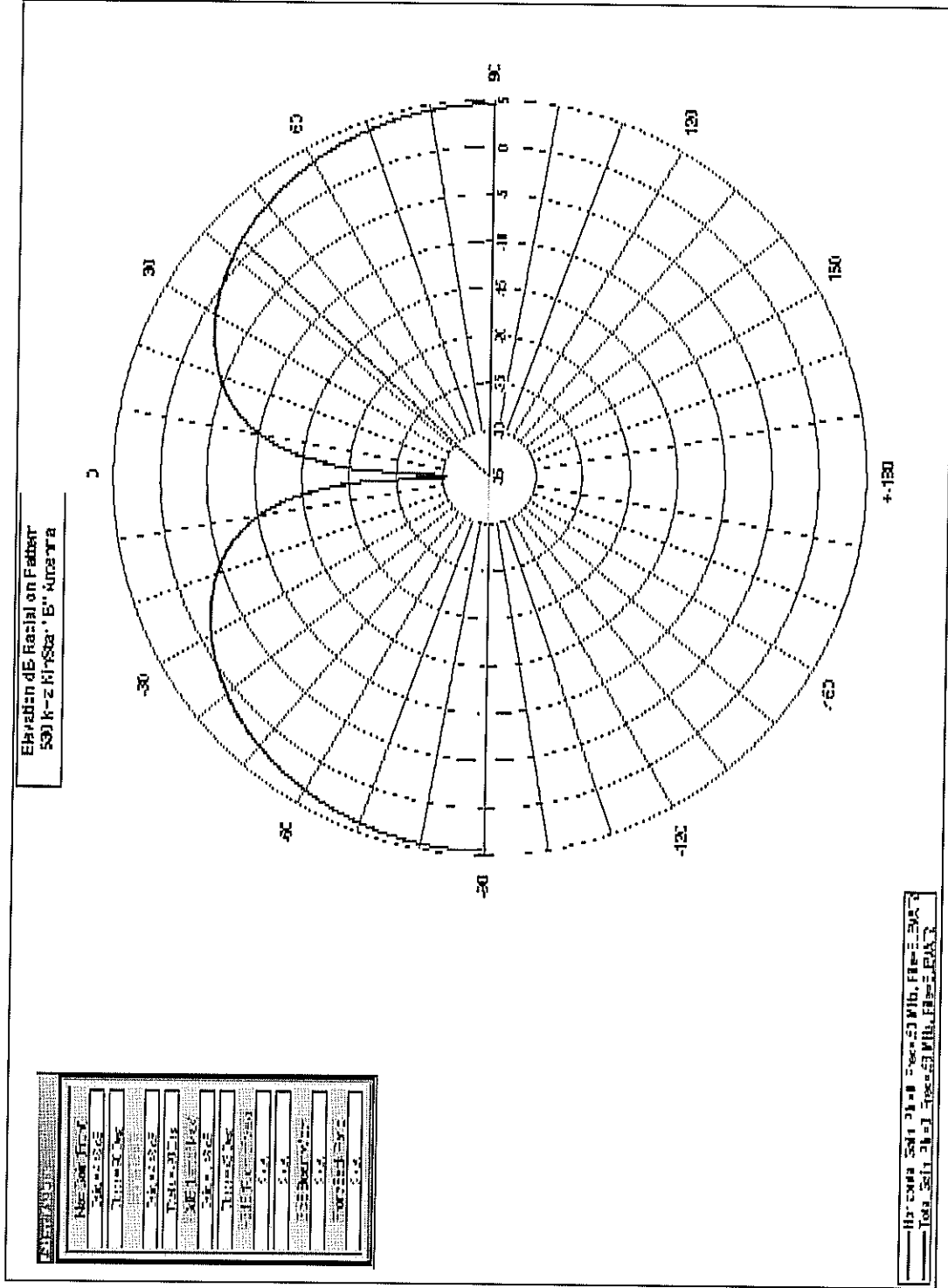


Figure 7 – Elevation pattern of final "B" design using lumped element matching to commoned wire sections. Pattern is sinusoidal with a half-power beamwidth of 43 degrees at 530 kHz over perfect ground. There is no radiated horizontally polarized component.

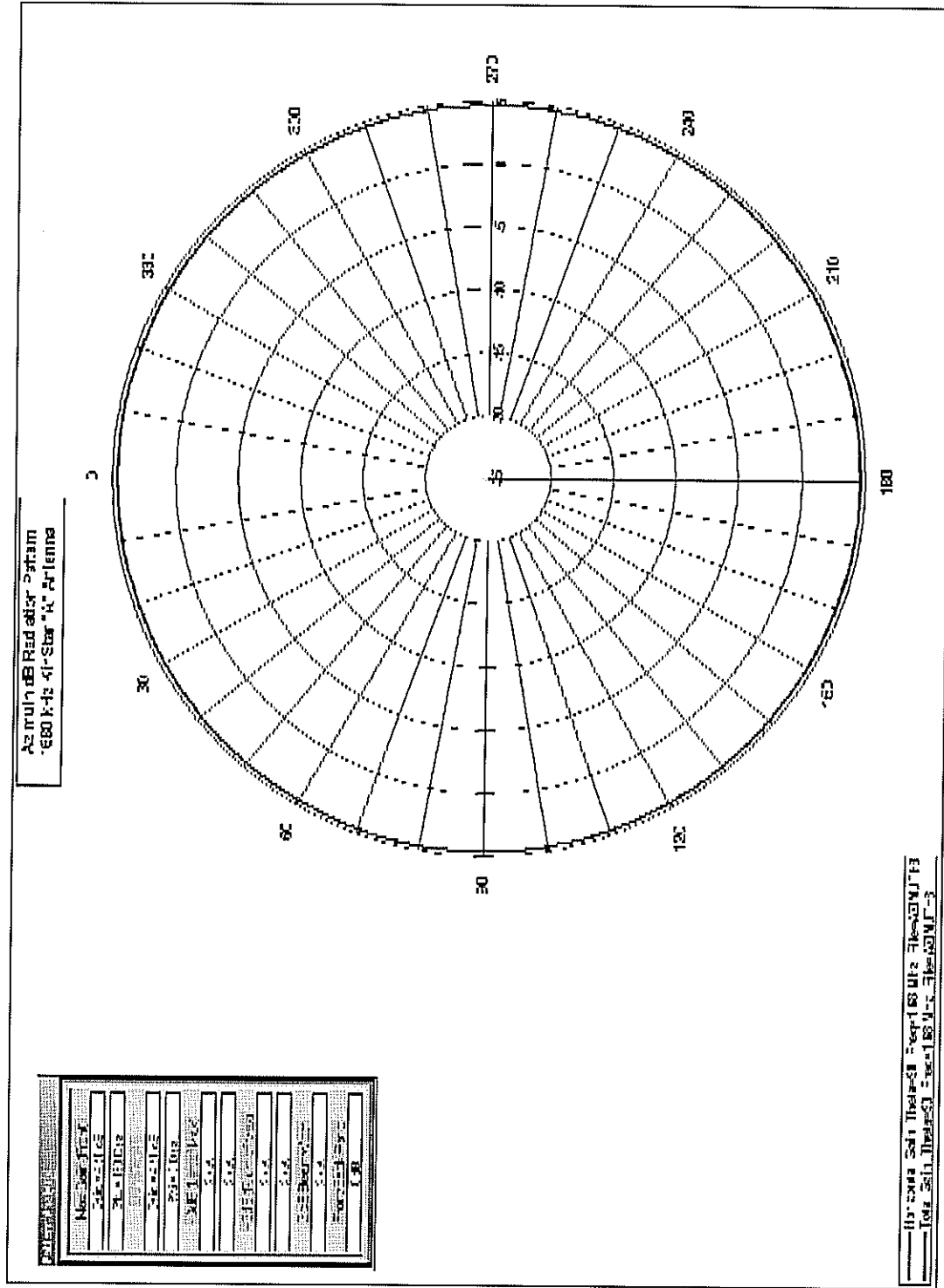


Figure 8 - Azimuth pattern of original "A" design using transmission line matching to isolated wire sections. Pattern is circular with gain of 4.61 dBi at 1680 kHz over perfect ground. There is no radiated horizontally polarized component.

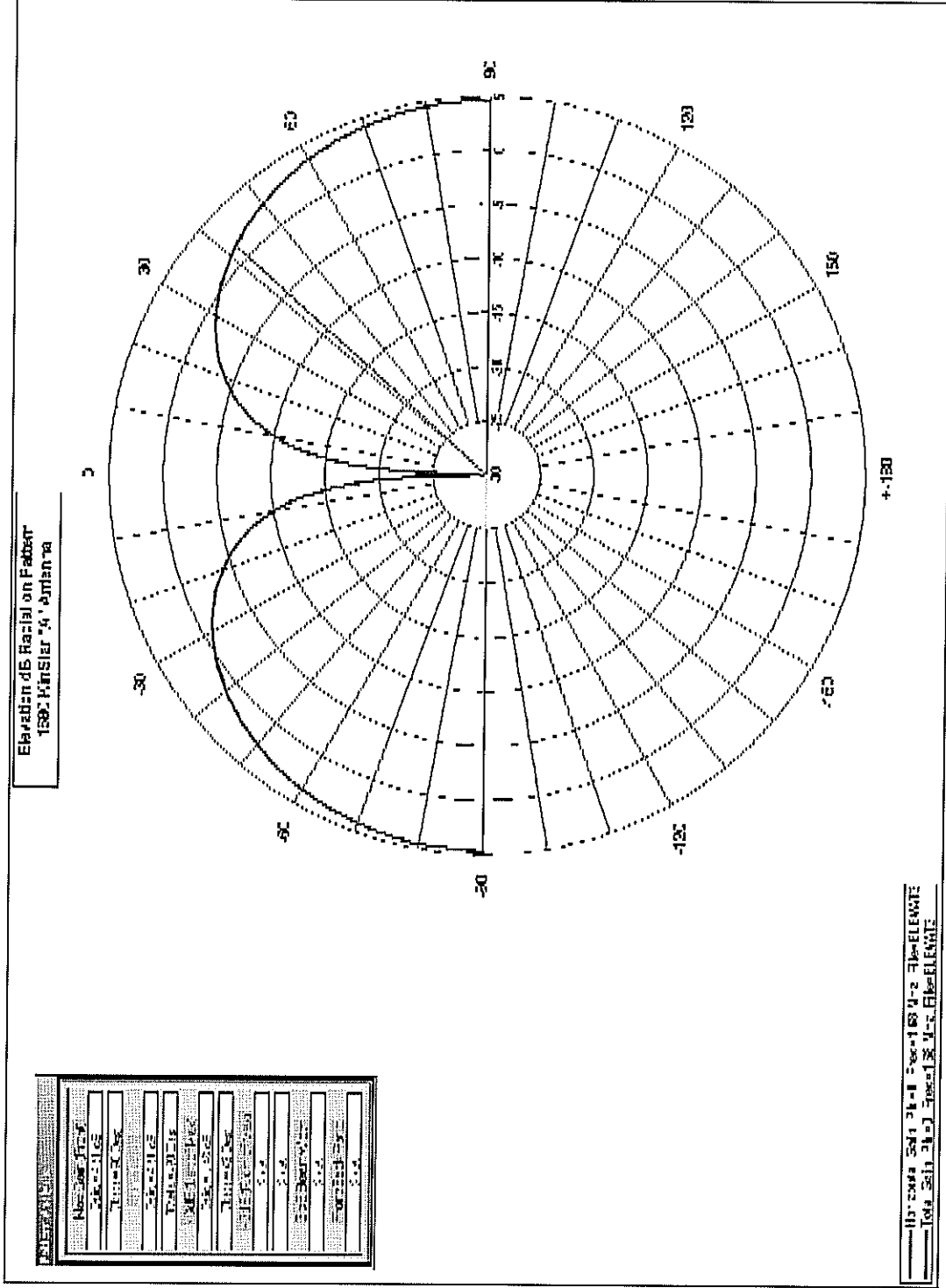


Figure 9 - Elevation pattern of original "A" design using transmission line matching to isolated wire sections. Pattern is sinusoidal with a half-power beamwidth of 42 degrees at 1680 kHz over perfect ground. There is no radiated horizontally polarized component.

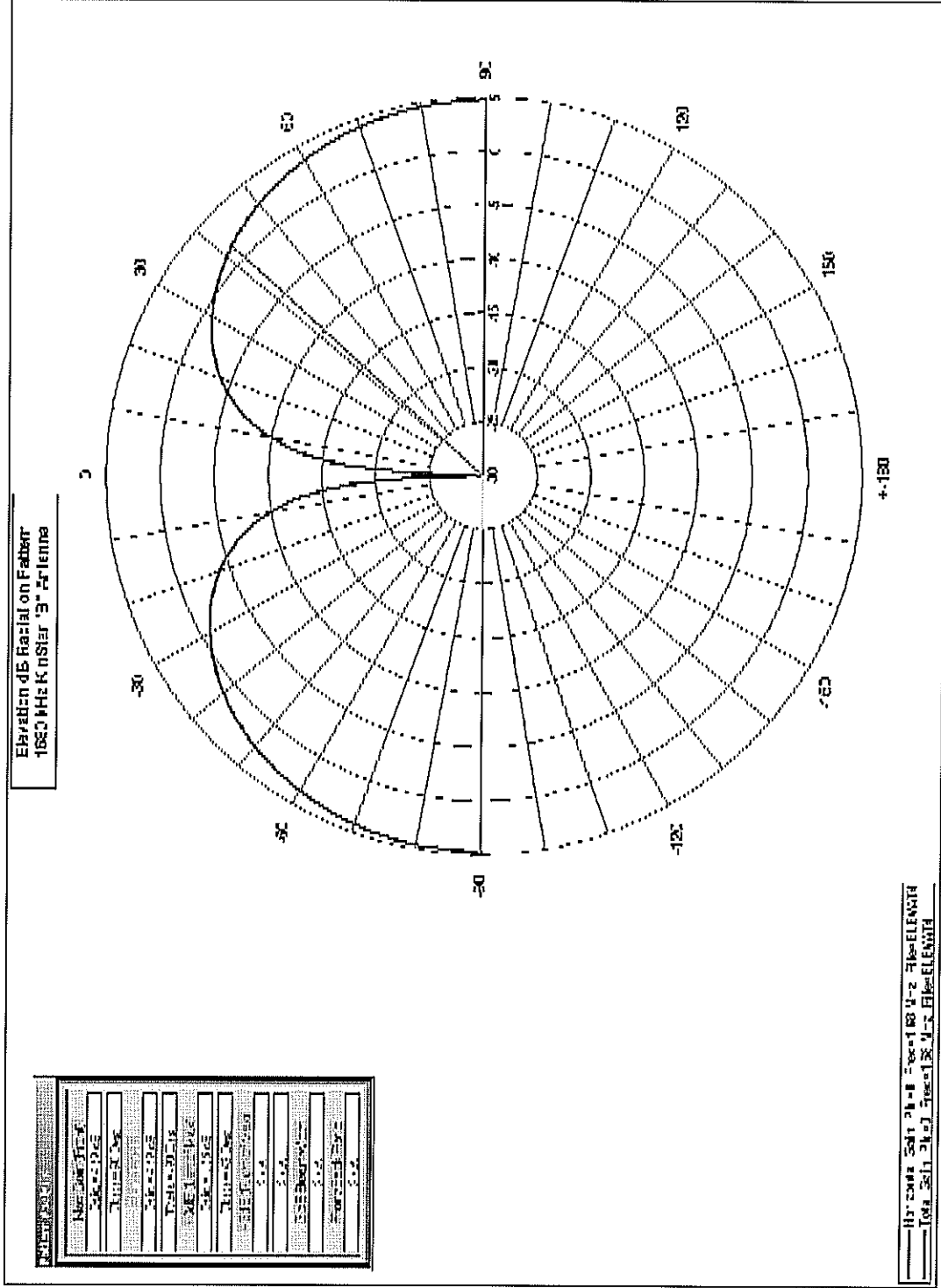


Figure 11 - Elevation pattern of final "B" design using lumped element matching to commoned wire sections. Pattern is sinusoidal with a half-power beamwidth of 42 degrees at 1680 kHz over perfect ground. There is no radiated horizontally polarized component.

2.0 Field Testing of Antenna - Experimental Station WS2XTR

2.1 Introduction

The KinStar antenna has been predicted by NEC-4.1 modeling to exceed the minimum efficiency requirements for class B, C, and D stations given in Section 73.189(b)(2)(i) of the FCC Regulations. The antenna does not meet the minimum height requirements of 73.190 Figure 7, so in accordance with 73.189(b)(5) a request was made for an experimental license to perform a complete field strength survey on an actual full-scale antenna. This request was granted and experimental license WS2XTR was issued for daytime-only testing at a frequency of 1680 kHz from a site in Evergreen, VA. The site was in an area of low rolling hills in an active alfalfa field. The test location was surrounded by farmland for several miles in all directions, and no large metal structures, towers, or high voltage utility lines were located nearby.



Figure 12 - KinStar antenna at WS2XTR test site. Vertical radiating and top loading wires have been enhanced for visibility. The pole structure is about 50 feet tall, and 105 feet in radius for operation at 1680 kHz to support the radiating antenna with a height of 45 feet and 100 foot radius. Each pole is approximately 55 feet long, with approximately 7 feet of that in the ground.

2.2 Antenna Construction

The antenna was constructed using wooden utility poles placed in augur-drilled holes directly in the ground of a rural alfalfa field, which was rented for the purpose of conducting this test. Installation of the antenna, once the ground system was completed, took a relatively short time, and could easily be completed in one day if a utility line construction bucket truck was used instead of having personnel climb the wooden poles. Uninsulated 3/8-inch diameter All-Aluminum Conductor (AAC) stranded cable was used for the vertical radiating and horizontal loading wires. Fiberglass rod insulators were used to insulate the antenna wires from the support poles and anchors. Each support pole was guyed in two directions to oppose the pull of the tension on the horizontal top loading wires. The wires were tensioned so that no sag was visible in the horizontals. The nominal design dimensions of the antenna for 1680 kHz were 44.97 feet high, with each vertical wire located 5 feet from the center and with the horizontal wires extending out 95.1 feet to an outer radius of 100.1 feet from the center. Construction of the antenna conformed to the 2002 National Electrical Safety Code.

The construction crew, either by error or by encountering rock below the surface, was unable to accurately place the four screw anchors for the vertical wires, with a typical error of approximately +1 foot in the inner radial distance (6 feet instead of 5). Table 2 compares the as-built dimensions of the antenna with those specified in the design. A photograph of the antenna, with the wires enhanced, is shown in Figure 12.

Table 2. Deviation of radial spacing of vertical radiating wire anchors, from design specification

Wire	Deviation from design spacing (Feet), approximate
1	1.1
2	0.8
3	0.3
4	1.1

2.3 Testing Configurations

Tests were conducted using two antenna feed configurations. These two configurations are shown in Figures 1 and 2. The Trial A configuration combined the use of four phase-matched and length-optimized sections of 50-Ohm 7/8" foam dielectric coaxial cables, one end of each of which was connected to the bottom end of each of the vertical antenna elements. The other ends of the cables were connected in parallel at the output of a simple lumped element "T" matching network. The Trial B configuration consisted of the use of a commoning ring at the top and bottom of the four vertical antenna elements with a single conductor connecting the bottom commoning element to the "T" matching network. This configuration results in the antenna wires behaving as a single fat top-loaded monopole antenna.

There was no significant difference in the radiation characteristics and electrical performance between the two methods, with the transmission line matching showing slightly higher efficiency than the top-loaded "fat" monopole approach. With broad-banding techniques, the top-loaded monopole configuration may offer wider bandwidth and higher power handling capabilities, while the transmission line matching system offers lower cost of implementation for low-power stations. Even with the transmission line matching, a simple T or L network of lumped elements was used to allow for easier tuning adjustment of the antenna impedance to match the feedline than having to adjust the lengths of the antenna wires or transmission lines.

A 400-Watt Nautel Ampfet transmitter was adjusted to apply 250 Watts of input power to the antenna and tuning system for testing. The transmitter and ATU were installed in two metal enclosures near the base of the antenna. The entire area was fenced off with wooden stockade fencing to prevent public contact with the wires or exposure to RF fields. Suitable warning signage was placed at the site to advise personnel of potential RF hazard areas.

2.4 Radial Proof Results

A complete six-radial proof of performance was conducted by Mr. Don Crane for each of the two antenna configurations and a reference quarterwave tower monopole at the same location using the same ground system. The

measured field strength data was then analyzed and reported by Mr. Ronald D. Rackley, P.E., of duTreil, Lundin, and Rackley, Inc., and is provided as Exhibit B in this document. Table 3 summarizes the results of the data analysis from Exhibit B, which shows that the measurements confirm fully the NEC-4.1 antenna efficiency predictions.

Table 3. Measured antenna efficiency and field values.

Antenna	Measured Field @ 1km	Equivalent Field with 1kW @ 1km	Average Radial Efficiency
Monopole Reference	153 mV/m	306 mV/m	1.00
KinStar Config. A	152 mV/m	304 mV/m	0.995
KinStar Config. B	150 mV/m	300 mV/m	0.980

(all values by duTreil, Lundin, and Rackley)

The predicted unattenuated field value for a 27.65 degree antenna, with 76.0 degrees of top loading to place the 90 degree point from the effective end at the center of its physical height and provide essentially uniform current along its vertical length, is 286.7 mV/M at one kilometer for one kilowatt input power and one ohm loss. This is within 0.5 and 0.4 dB of the measured field values of Configuration A and Configuration B, respectively.

2.5 Current Distribution Measurements

After completion of the field strength proof testing, it was decided to measure the current distribution on the vertical wires in order to be able to calculate the vertical radiation characteristics of the antenna. Kintronic Laboratories personnel constructed and calibrated a measurement and logging device, under the direction of Mr. Rackley, which consisted of a toroidal current transformer mounted on a Teflon tube with a battery-powered data logger. Individual vertical element current distribution measurements were conducted by routing the wire through the Teflon tube and raising the unit to the top of the element. The unit was then lowered in 2.5 foot increments with the transmitter on and the data logger operating continuously. Approximately 100 measurements were made on each vertical wire, resulting in a resolution of approximately 0.4 feet per measurement. The lowest 5

feet of the vertical wires consisted of the insulating rod and turnbuckle assembly, and thus carried no current and are not included in the measurement. Some opposing current is present in the ground straps from the coaxial cable endpoints at the base of the vertical wires, this can be assumed to be of equal magnitude and opposite phase to the first 5 feet of measured currents on the vertical wires. These ground straps were not present when testing with the lumped element matching network, however. NEC-4.1 modeling which placed the antenna feedpoint at the 5-foot above ground point did not show any difference in the vertical radiation pattern with that having the feedpoint 6 inches from the ground, so that the effect of the currents in the ground straps can be effectively ignored in calculating the vertical radiation pattern.

Initial evaluation of the current measurement results, shown in Figures 13 and 14 showed an unexpected asymmetry in the current magnitudes on the four vertical wires. Inspection of the site, and experience with other AM antenna systems suggested that the metal transmitter and ATU enclosures might have influenced the current distribution by being closer to two of the wires. These boxes were thus moved 16 feet outside the fenced area, thus reducing any coupling effects from the antenna wires. The current measurements were repeated for both antenna-matching configurations, and with the addition of having the horizontal wires shunted together at the tops of the vertical wires (a feature not included in the original antenna design). Table 4 summarizes each case for which current measurements were made.

Table 4. Antenna Test Configurations

Case	Matching Method	Wires Shunted	Comments
A	Transmission Line	No	Boxes inside fence
B	Lumped Element	Bottom Only	Boxes inside fence
C	Lumped Element	Bottom and Top	Boxes inside fence
D	Lumped Element	Bottom and Top	Boxes 16ft. Outside
E	Transmission Line	No	Boxes 16ft. Outside

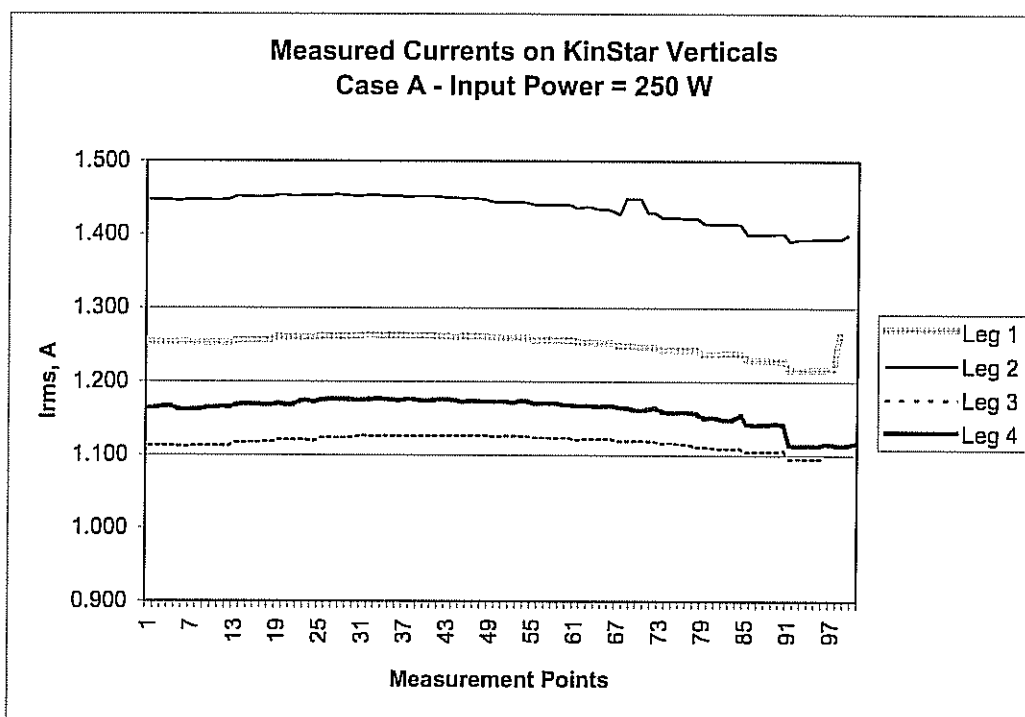


Figure 13 - Currents on KinStar Antenna Case A, with independent feeds to each leg of the antenna through transmission line matching sections and with all legs insulated.

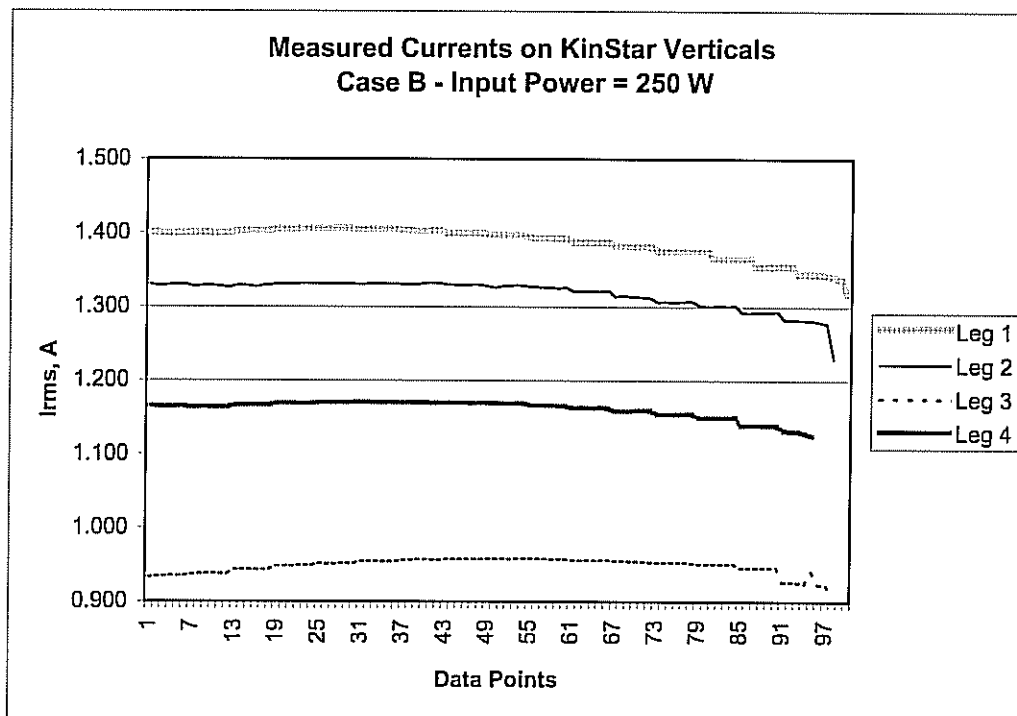


Figure 14 - Currents on KinStar Antenna Case B, with a common feed from lumped element matching network.

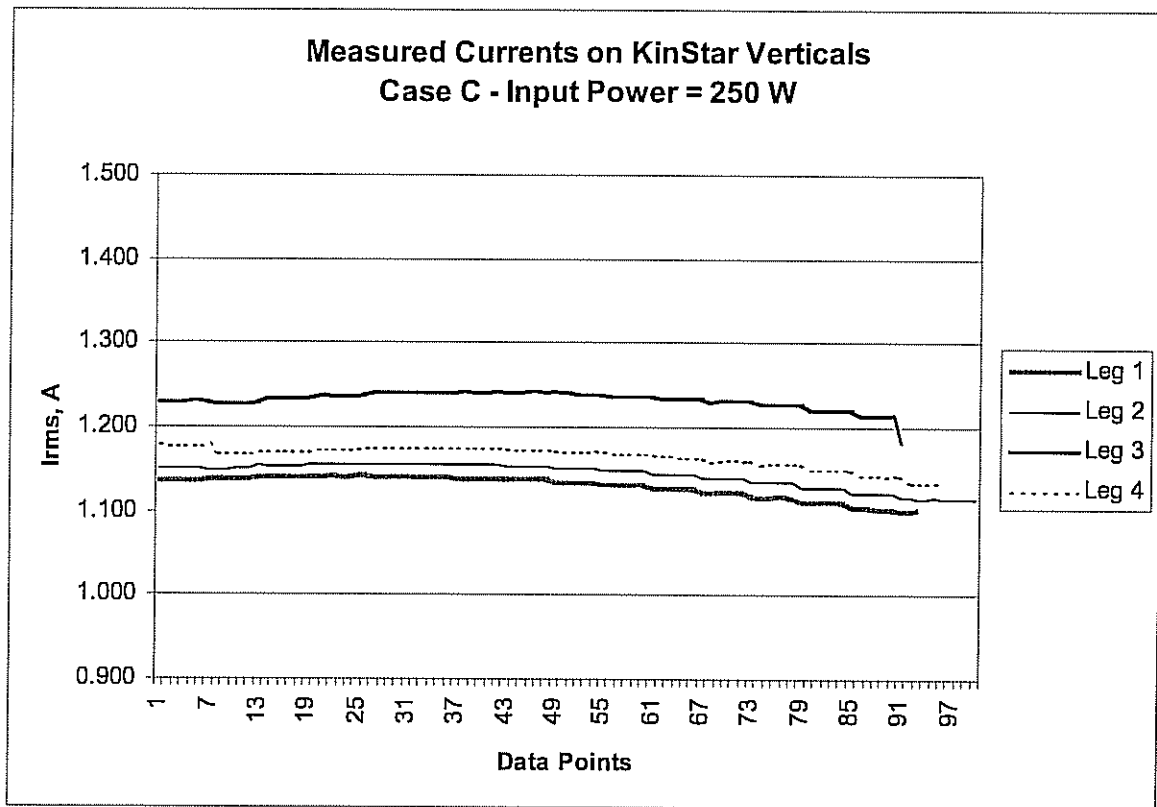


Figure 15 - Currents on KinStar Antenna Case C, with common feed from lumped element matching network and wires connected together at top and bottom of vertical radiating conductors. This shows significant equalization of currents compared with Case B above. This arrangement with the vertical wires connected at the top will be used in all KinStar installations as a precautionary measure to ensure that current symmetry is maintained as close as possible under all conditions.

These tests showed that proximity of the metal equipment cabinets did not cause the observed current asymmetry. Significant improvement in the current symmetry was seen for the test cases with the wires shunted at the top of the antenna, as shown in Figure 15. Later comparison with NEC-4.1 modeling data shows that the current asymmetry was most likely caused by a combination of the misplacement of the vertical wire anchors and the uneven terrain of the alfalfa field resulting in differing effectiveness of each top loading wire. While a surveyor was called in to stake the locations of the five support poles at approximately equal elevations, his survey of the site showed that several feet of variation were seen over the entire area covered by the ground system. Table 5

shows the average elevation variation along a line under each of the four top loading wires.

Table 5. Average ground elevations under horizontal wires.

Location	Average Elevation (Feet)	Difference from Center (Feet)
Center	100	-
Wire 1	99.33	-0.67
Wire 2	101.43	1.43
Wire 3	99.31	-0.69
Wire 4	98.79	-1.21

The concern for the uneven currents is not that it affects the azimuthal radiation pattern, indeed both the field measurement data and subsequent NEC-4.1 modeling showed that the vertical wires are so close together that they radiate effectively as a single vertical current element, as shown in Figure 16. Rather, in accordance with Kirchoff's current law, the currents on the horizontal loading elements are determined by the current magnitude at the top end of the vertical wires. When the horizontal wires are insulated from each other the current distribution on them is essentially sinusoidal, going from a maximum at the connection to the vertical down to zero at the outer end. The current maximum at the inner end of the horizontal is equal to that at the top end of the connected vertical wire, so efforts have to be made to ensure that the current distribution is evenly balanced throughout the structure.

Modeling shows that addition of the commoning ring at the top of the vertical wires has an equalizing effect on the horizontal element currents by redistributing any unequal currents which may tend to flow on the antenna. This feature will be incorporated in all KinStar antenna installations as a standard feature.

NEC modeling was used to study the unexpected unequal currents and to understand the causes. First, models were

made to recreate the observed current distribution for the insulated wire version (Case A). This model was then adapted to include the as-built dimensions including the actual vertical wire anchor positions. The modeling suggested that the offset of the wire base positions did not alone account for the observed current asymmetry. The modeling did verify, however, that connecting the four wires together at the top of the vertical radiating elements significantly improved the current differences and reduced any resulting horizontally polarized radiation by up to 6 dB compared with identical models without the top wires connected.

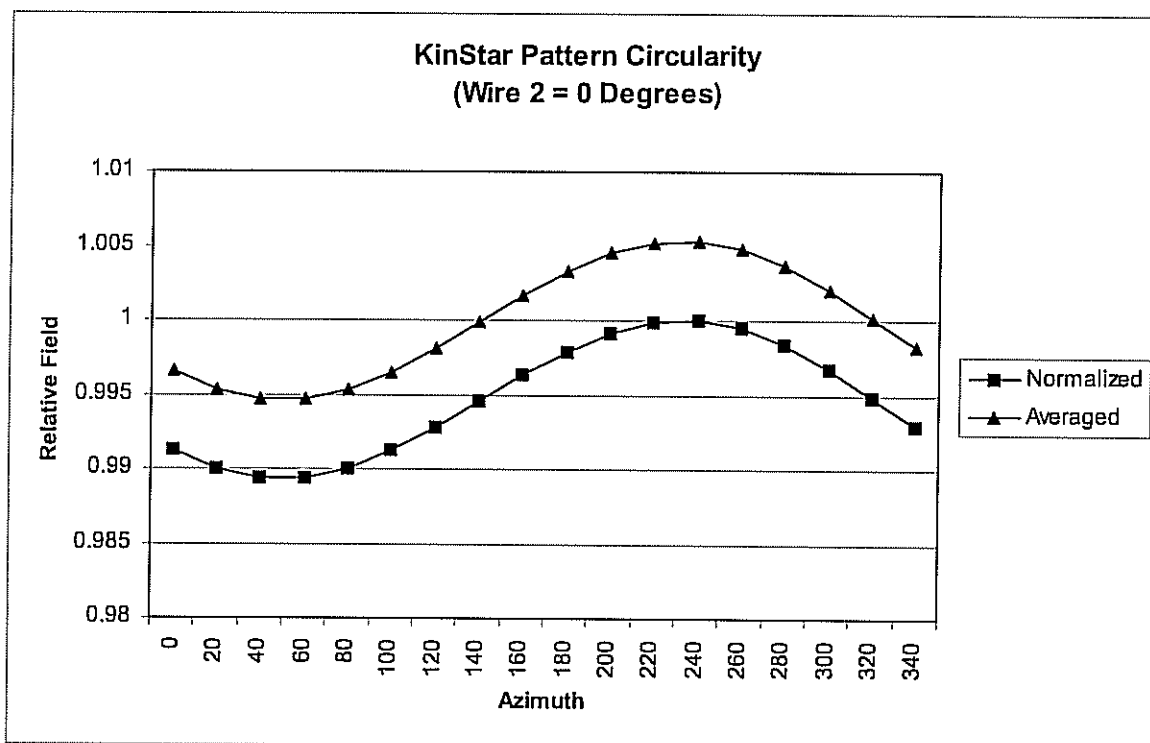


Figure 16 - KinStar azimuth pattern circularity at 0 degrees elevation calculated from the measured currents for Case A. Even with the significant asymmetry in the vertical wire currents, in the far-field (calculations were made for 1km distance) the field remains circular to within 0.6% for the worst observed case. This shows that the cage wire construction of the KinStar radiates essentially as a single vertical current element even in the uninsulated independent feedpoint version. For the proposed commercial version of the antenna, with the top of the vertical wires commoned together, the circularity error will be much reduced from this.

3.0 Environmental Effects Modeling

3.1 Introduction

NEC-4.1 modeling was also used to evaluate the effects of other expected environmental effects on the performance of the antenna. The KinStar is shown to respond to weather and environmental effects in a predictable manner that is consistent with the performance of other types of antennas. The antenna can operate normally in all anticipated survivable wind conditions and with up to $\frac{1}{2}$ " of radial ice (on $\frac{3}{8}$ " diameter radiating wires) before causing the transmitter protection circuitry to act due to the lowering of the antenna's resonant frequency. The efficiency of the KinStar is unaffected by local ground conditions or by operating frequency and is thus usable in all locations in the United States and on all allocated AM band frequencies.

3.2 Effects of Wind and Ice

Modeling shows that the impedance performance of the KinStar remains acceptable for all transmitter types with up to $\frac{1}{4}$ " of radial ice accumulation on the antenna wires. As the ice radius increases to beyond $\frac{1}{2}$ ", the impedance begins to deviate significantly as the antenna's resonant frequency drops, resulting in activation of transmitter protection circuitry. This situation is not different from the effects seen with significant ice accumulations on tower radiators and other antennas exposed to winter conditions. Because of the lighter weight construction techniques of the KinStar, it is expected to survive higher ice accumulations than many tower structures. Utility lines constructed of like materials typically do not fail due to ice unless a tree or other structure falls onto them.

Figures 17 and 18 show the impact on the matched input impedance of the antenna with $\frac{1}{4}$ and $\frac{1}{2}$ inch of radial ice. With $\frac{1}{4}$ inch of ice, the transmitter should be able to continue operation into the antenna. Figure 19 shows the elevation radiation pattern due to the effect of ice only. This shows no significant change in the radiation pattern.

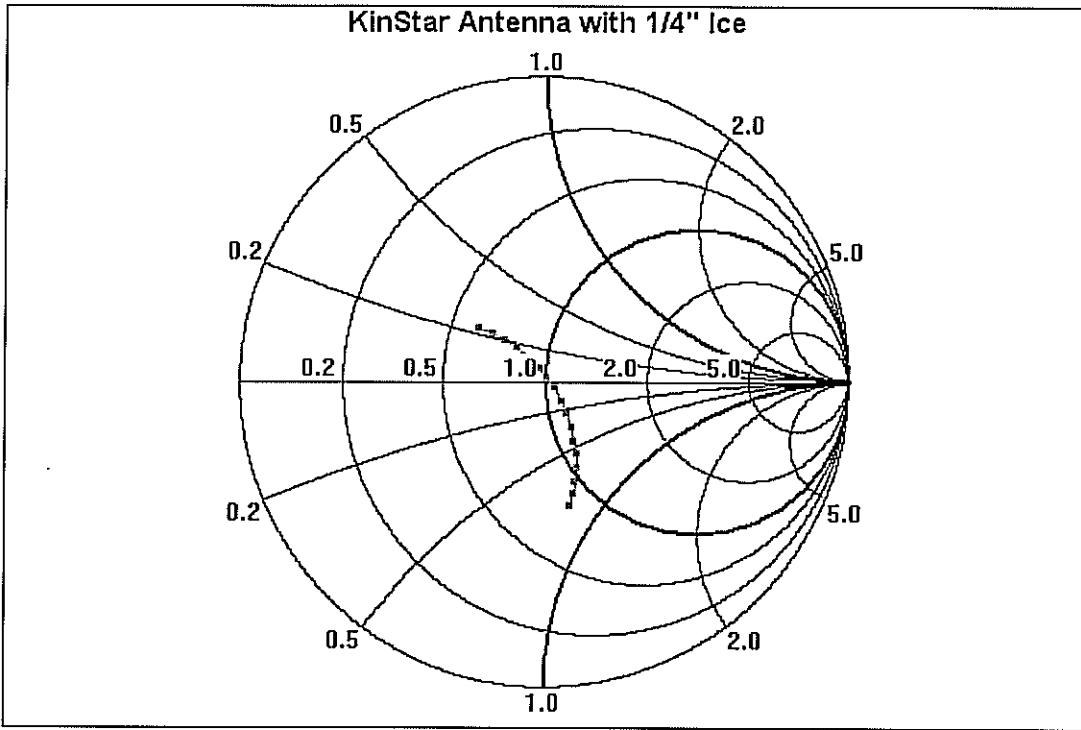


Figure 17 - Impedance sweep of 1680 kHz KinStar "A" version antenna from 1640 to 1720 kHz over average ground with 1/4" radial ice.

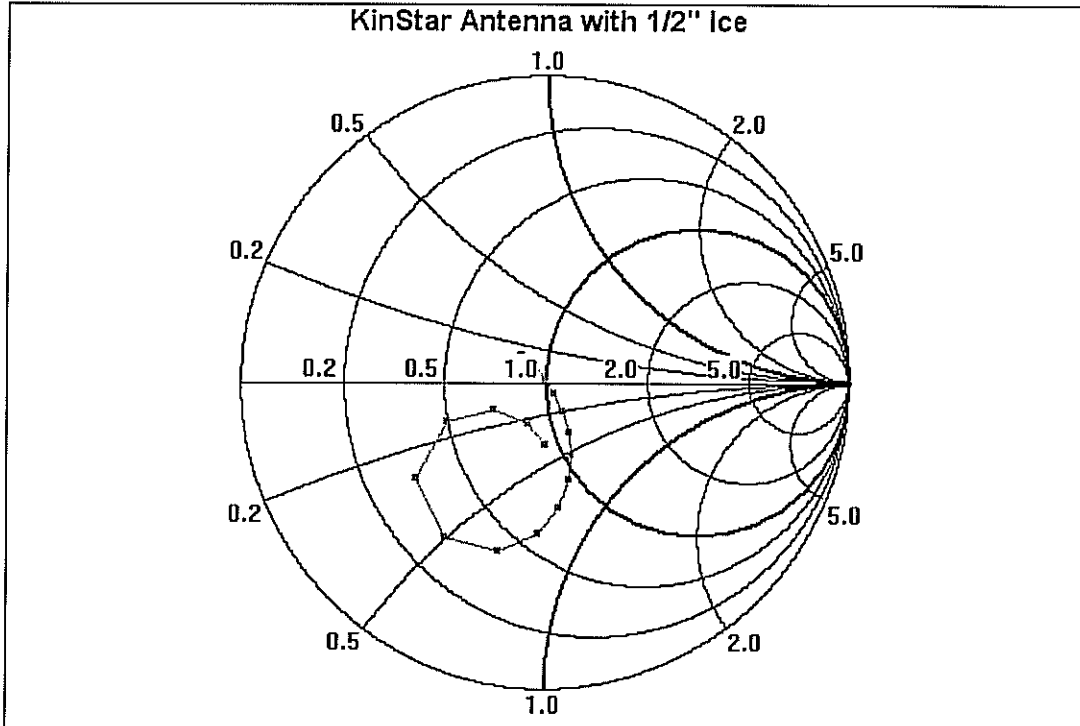


Figure 18 - Impedance sweep of 1680 kHz KinStar "A" version antenna from 1640 to 1720 kHz over average ground with 1/2" radial ice.

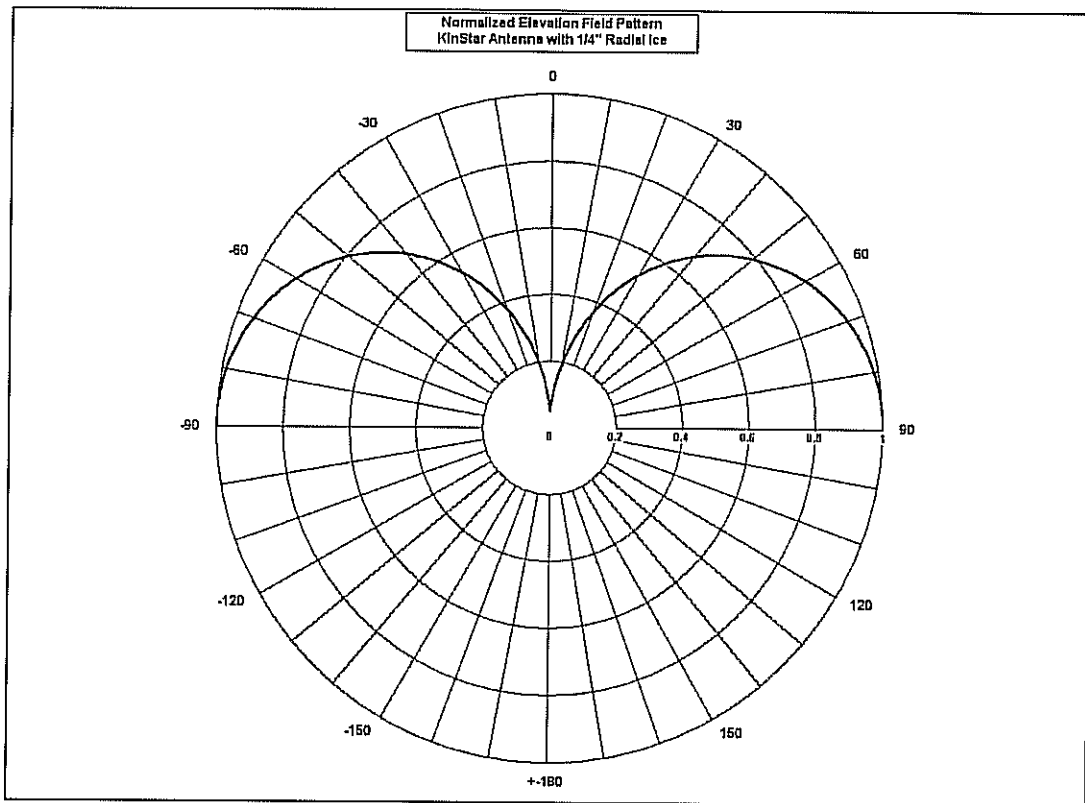


Figure 19 – Normalized elevation field pattern for KinStar antenna with 1/4" radial ice coating over perfect ground.

In high wind situations, the KinStar antenna wires will not significantly deform due to their installation with a high stringing tension, required to minimize sag in the horizontal wires, and their small surface area. During the course of the testing period in Virginia, no significant motion or displacement of the wires due to wind was observed. Should galloping or other undesired motion occur, dampening devices are commercially available for installation on the wires to reduce or eliminate this effect. Construction using high tensile strength aluminum (AAC) or aluminum coated steel reinforced wire (ACSR), depending on the span lengths, will allow the wires to be strung with sufficiently high tension during construction to minimize any significant wind deformation.

NEC modeling of the elevation radiation patterns shows that even with unexpectedly large wire deflections, the degradation to the radiation pattern is minimal. Figure 20 shows a comparison of the calculated elevation pattern with no wind, 2 feet of deflection, and 5 feet of deflection of

one pair of opposing top loading wires over perfect ground at 1680 kHz. The only effect is a very slight increase in the horizontally polarized radiation component, which even with 5 feet of deflection remains less than -32 dBi, over 36 dB below the peak lobe of the antenna pattern.

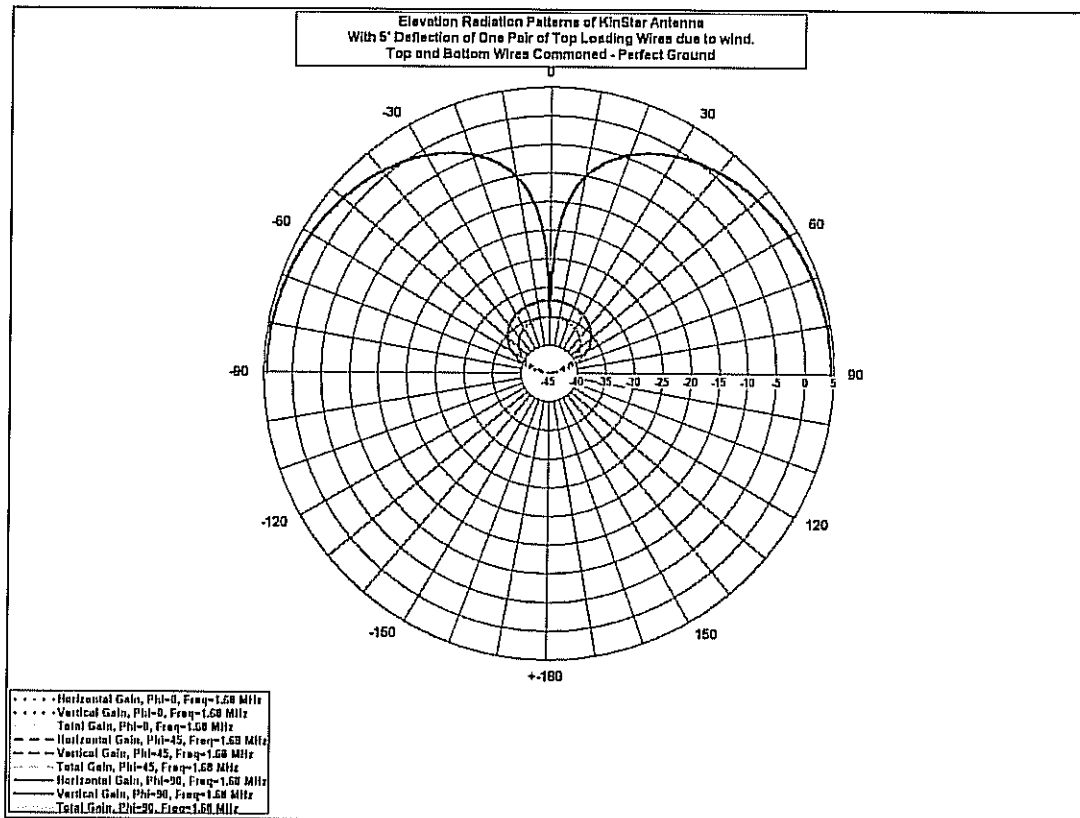


Figure 20 - KinStar antenna with 0, 2', and 5' deflection in one pair of top loading wires. This asymmetry results in some horizontally radiated component falling at most 35 dB below the main lobe of the antenna with 5' deflection, 40 dB below the main lobe with 2' deflection. No significant distortion to the main elevation pattern is seen with any deflection.

3.3 Ground Parameter and Frequency Effects

The field efficiency of the KinStar antenna is shown by NEC-4.1 modeling to not vary significantly with changes in ground constant values. NEC-4.1 uses the Sommerfeld-Norton method to model ground loss effects due to returning currents traveling through the ground. A parameter variation study was conducted to model the efficiency of the KinStar antenna over the AM frequency band with varying ground conditions. Models were tested at 530, 1000, and

1680 kHz over Perfect, Good, Average, Poor and Very Poor ground conditions at each frequency using the ground constants shown in Table 6. The models each included quarterwave copper #10 wire 120-radial ground screens located just above the surface of the ground, and included wire conductivity effects on the copper ground system and the aluminum antenna wires. A model of a one-quarter wavelength tall monopole triangular lattice tower, and a thin wire monopole were also analyzed for comparison. The RMS attenuated field for 1kW of input power for each model was calculated by NEC for the KinStar, and then compared with expected values from NEC calculations of thin quarterwave monopoles to find the resulting unattenuated field. The use of the model with the Perfect ground parameters allowed us to calculate correction factors to find the expected unattenuated field at the 1km point for each model.

In determining the field values at 530 kHz, modeling showed that the NEC calculated field at one kilometer from the antenna did not exhibit the expected roll-off with decreasing ground conductivity, so calculations for all antennas at this frequency were repeated at 10 kilometers to ensure that there was no residual nearfield effect. Results at 10km continued to show a slight increase in expected field strength for good ground conditions. This effect is small but consistent and represents either an artifact in the Sommerfeld-Norton formulas in the NEC program, or a possible real physical effect resulting from increasing penetration depth at lower frequencies. In any case, it is sufficiently small as to not significantly affect the key conclusion that the KinStar antenna retains its efficiency across the entire AM broadcast band.

The resulting calculated unattenuated 1km fields fell sufficiently close to the expected values that it is reasonable to conclude that there is no significant decrease in antenna or ground system efficiency with changes in frequency or ground characteristics. At all frequencies and ground conditions, the minimum efficiency requirements are met.

Table 7 summarizes the results of the NEC field modeling with varying ground conditions and frequencies. The complete data for all frequencies and ground constant values is given in Appendix 1. The results in Appendix 1 show that for the average ground case, the NEC predicted

fields for both the KinStar and the quarterwave monopole fall reasonably close to the expected values consistently across all frequencies. There are some minor differences at various ground and frequency combinations due to accumulated computational error or modeling variations, but a comparison of the modeling results and measured field data from the WS2XTR testing suggest that the NEC results tend to be conservative, lending confidence to the conclusion that antenna efficiency will meet or exceed predictions.

Table 6. Ground constant values used in modeling.

	Relative Permittivity	Conductivity (mS/m)
Perfect	-	∞
Good	15	30
Average	15	5
Poor	15	1
Very Poor	15	0.1

Table 7. Summary of calculated unattenuated fields with frequency over average ground conditions using NEC Sommerfeld-Norton calculations. All values in mVrms/m at 1km with 1kW input power to antenna.

Frequency	Calculated Unattenuated Field (average ground)			Perfect Ground with Ground Screen		
	Kinstar A	Kinstar B	QW Tower	Kinstar A	Kinstar B	QW Tower
1680	294.39	290.47	318.29	293.54	293.36	318.75
1000	291.33	286.25	315.80	290.43	290.30	317.70
530	285.41	277.96	306.37	283.88	286.65	314.00

In the case of the field test at WS2XTR, the overall measured unattenuated field was found to be 304 and 300 mV/m for the two test configurations, which agree within a few percent with the NEC predicted results shown here and suggest that the antenna efficiency as calculated by NEC is a conservative value. Since the NEC models consistently show the KinStar meeting the minimum field requirements of

73.189(b)(2)(ii), it is concluded that the KinStar antenna meets these requirements for all locations in the United States and that the efficiency of the KinStar antenna is independent of ground conditions and operating frequency when used with a suitable quarterwave or greater 120 radial ground system.

3.4 Effects of Uneven Ground Under Antenna

Efforts to model the effects of uneven terrain under the antenna yielded interesting results. These models relied on sloping half of the 120-wire radial ground screen above the plane of the model ground since NEC's only ground models are planar. The models suggest that some sloping ground conditions may result in asymmetric currents in both the antenna and ground system, resulting in a horizontal component to the radiation. As a check, the same sloping ground wire system was modeled with a quarterwave tower, showing the same result.

The monopole model also showed asymmetries in the ground wire currents (as expected). This resulted in a horizontal component to the radiated field as in the case of the KinStar model. This indicates that any antenna whose ground system is not perfectly planar can have some horizontally polarized radiation. It is always desirable to have the most level grade over the area of the ground screen for any AM broadcast antenna system, and this recommendation will be passed to stations interested in installing KinStar antennas, but it should not be considered an absolute requirement.

Figures 21 and 22 show the NEC results for the effect of a simulated sloping ground on the KinStar and a quarterwave tower monopole, respectively. The performance of the KinStar is no worse than that of the monopole, suggesting that the KinStar will respond to placement on uneven ground in a similar manner as more traditional antennas.

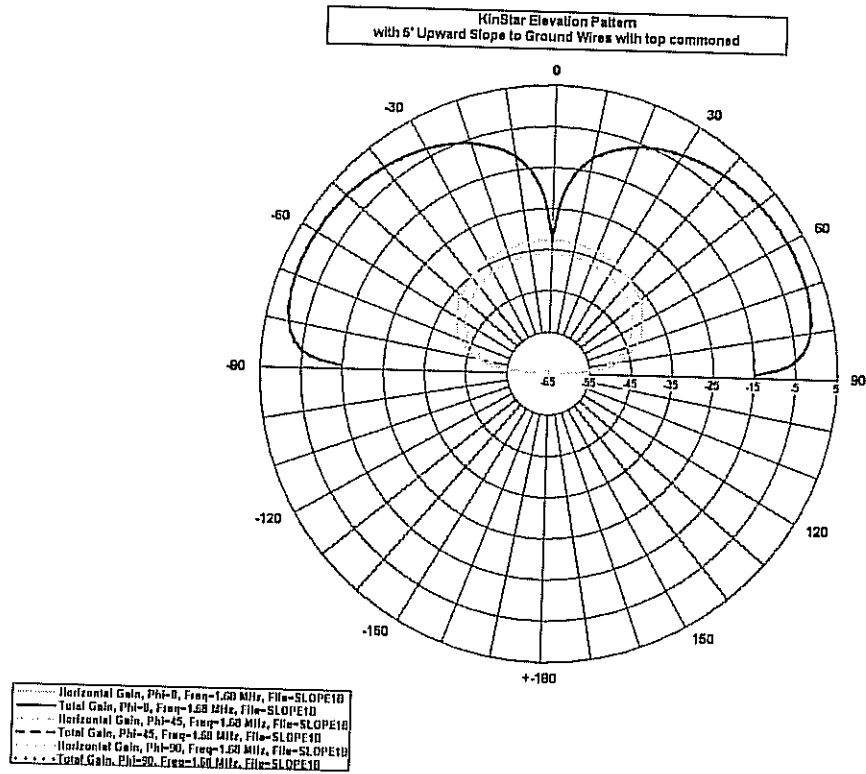


Figure 21 – Elevation pattern showing horizontally polarized radiation component of KinStar antenna (green trace) at least 35 dB below the pattern maximum due to effect of simulated sloping ground.

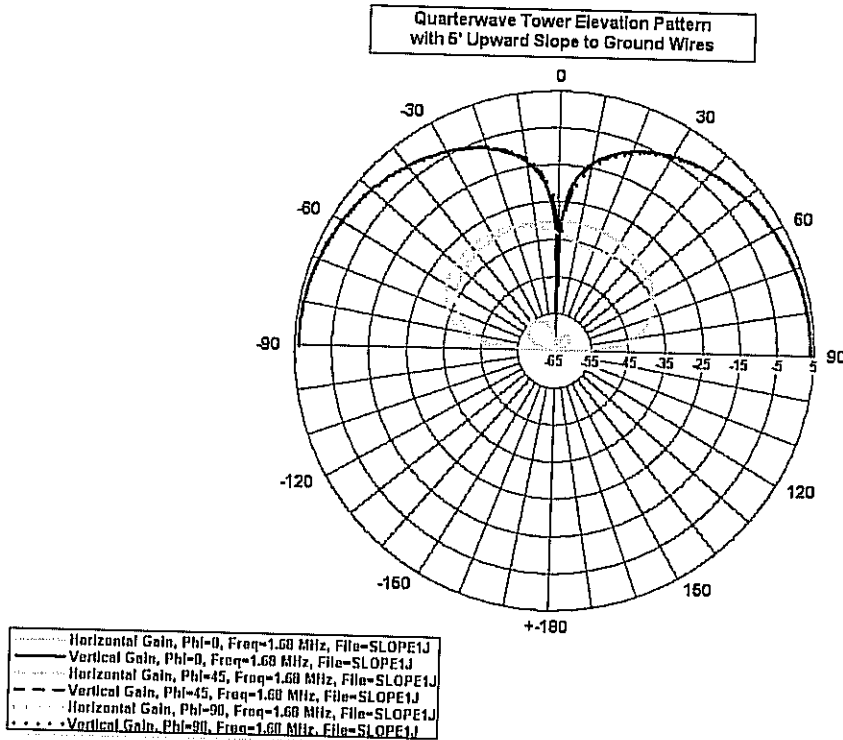


Figure 22- Elevation pattern showing horizontally polarized radiation component of quarterwave monopole tower antenna (green trace) at least 30 dB below the pattern maximum due to effect of simulated sloping ground. Result is similar to that seen with the KinStar.

4.0 Elevation Radiation Pattern

The KinStar antenna's elevation plane radiation pattern behaves almost exactly as predicted by the classical model of a short vertical constant current element having a cosine(theta) distribution, where theta is the elevation angle above the horizontal. The antenna produces a single radiation lobe aimed at the horizon with a deep null aimed directly overhead. The elevation pattern of a single KinStar antenna can be described by considering it as a single short monopole with a high degree of top loading, consistent with section 73.160(2) of the commission's rules.

$$f(\theta) = \frac{\cos B \cos(A \sin \theta) - \sin \theta \sin B \sin(A \sin \theta) - \cos(A + B)}{\cos \theta (\cos B - \cos(A + B))}$$

For the 1680 kHz KinStar antenna tested at WS2XTR, the physical height of the antenna, A, is 27.65 degrees, and inspection of the current distribution shows an effective electrical top loading of approximately 76 degrees. This results in a calculated relative field distribution as shown in Table 8. Agreement of results between the NEC calculated current distribution and the measurements from the WS2XTR test antenna is nearly perfect, showing the accuracy of the NEC modeling. It is thus possible to accurately confirm the effective electrical top loading value from any KinStar design using the NEC calculations for that antenna.

The current distribution measurement data, NEC-4.1 calculations, and radiation pattern and field proof data support the consideration of the antenna as a single radiating vertical current element. Inspection of the antenna dimensions and the current distribution readily yields A and B values suitable for application to equation 73.160(2). The construction of the KinStar "B" version is clearly seen as a top-loaded monopole structure, exactly as intended to be described in 73.160(2). Since the radiation performance of both the KinStar "A" version and KinStar "B" version are identical, both versions can be justifiably described in terms of A and B values for purposes of licensing.

Table 8 shows the elevation field ratio values as calculated by NEC-4.1 for the KinStar antenna over perfect ground, the application of 73.160(2), and from a derived

field calculation from the measured currents on the vertical wires of the WS2XTR antenna. The NEC-4.1 values show a higher relative field (broader elevation pattern) at higher angles than either the 73.160(2) formula or the derived field calculation. The NEC-4.1 calculation accounts for more terms, including effects of the relatively wide wire spacing in the antenna on the phase velocity, and thus produces a more accurate result than either of the other methods, which are based on mathematical approximations. The disagreement between the NEC-4.1 and the 73.160(2) results is under approximately 8% at the critical skywave interference angles below 60 degrees, and well under 5% below 40 degrees.

Table 8 - Comparison of Elevation Field Ratios

Angle	NEC-4.1 Prediction	73.160(2) Calculation	Calculation from Measured Currents	Percent Error between 73.160(2) and NEC-4.1
0	1	1	1	-
10	0.9871	0.9836	0.9848	0.350
20	0.9481	0.9353	0.9397	1.35
30	0.8827	0.8575	0.8660	2.86
40	0.7905	0.7535	0.7660	4.67
50	0.6720	0.6279	0.6428	6.56
60	0.5291	0.4852	0.5000	8.29
70	0.3655	0.3301	0.3420	9.67
80	0.1867	0.1670	0.1736	10.6

The NEC-4.1 calculated values have been verified with two independent alternative Method of Moments formulations, the MININEC Broadcast Professional program and the WIPL program. All agree on the calculated values shown here to better than 1 percent. The field ratios shown calculated from measured currents do not include phase data along the vertical extent of the wires. This calculation was based on the superposition of fields from the measured current elements and the as-built antenna geometry using a derivation of the following standard formula for the elevation pattern of a short constant current element:

$$E_{\theta} \approx j\eta \frac{\beta I_0 l e^{-j\beta R}}{4\pi R} \sin \theta [2 \cos(\beta h \cos \theta)]$$

The values calculated by the formula match those for the cosine distribution and are dominated by the sine(theta) component. Theta in this formula is measured according to the spherical coordinate system as being the angle from the zenith, not the horizon.

This difference between NEC-4.1 and the 73.160 formulas is observed not only with the KinStar, but also is consistent with observed differences for a number of other licensed antenna systems currently in common operation in the United States. Modeling data shows that these antennas tend to have large cross-section geometries (H/a ratio) relative to height, resulting in a modified phase velocity along the vertical axis of the structure compared with the usual thin wire approximation. This causes the phase distribution over the length of the antenna to increase over that for the thin wire case and changes slightly the elevation pattern of the antenna. Antenna models which show this effect include the KinStar, a wide-base tapered self-supporting tower, and the Blaw-Knox style of double pyramidal towers. All of these antennas show a deviation between the 73.160 calculated elevation pattern and the NEC calculated pattern similar to that seen with the KinStar, with some showing errors larger than seen with the KinStar. Studies showing the effect of H/a ratio on the elevation radiation pattern have been made by G.H. Brown, and more recently by V. Trainotti, and historical experience at WLW and other stations verifies this effect.

In actual practice, over locally varying ground conditions, the elevation pattern of any medium frequency antenna will differ somewhat from its predicted performance no matter what the approximation or modeling technique. Considering these factors, it is felt that the application of 73.160(b) will provide sufficient accuracy for calculation of nighttime skywave interference to permit 24-hour operation of the KinStar. Indeed, NEC-4.1 modeling demonstrates that the 73.160 formulas are applicable for the KinStar antenna with no greater degree of vertical radiation pattern uncertainty than is the case for other tower antennas that are routinely authorized and are in common use today. Examples of other antennas where the NEC calculated elevation pattern differs from the 73.160 calculated elevation pattern are shown in Figure 23.

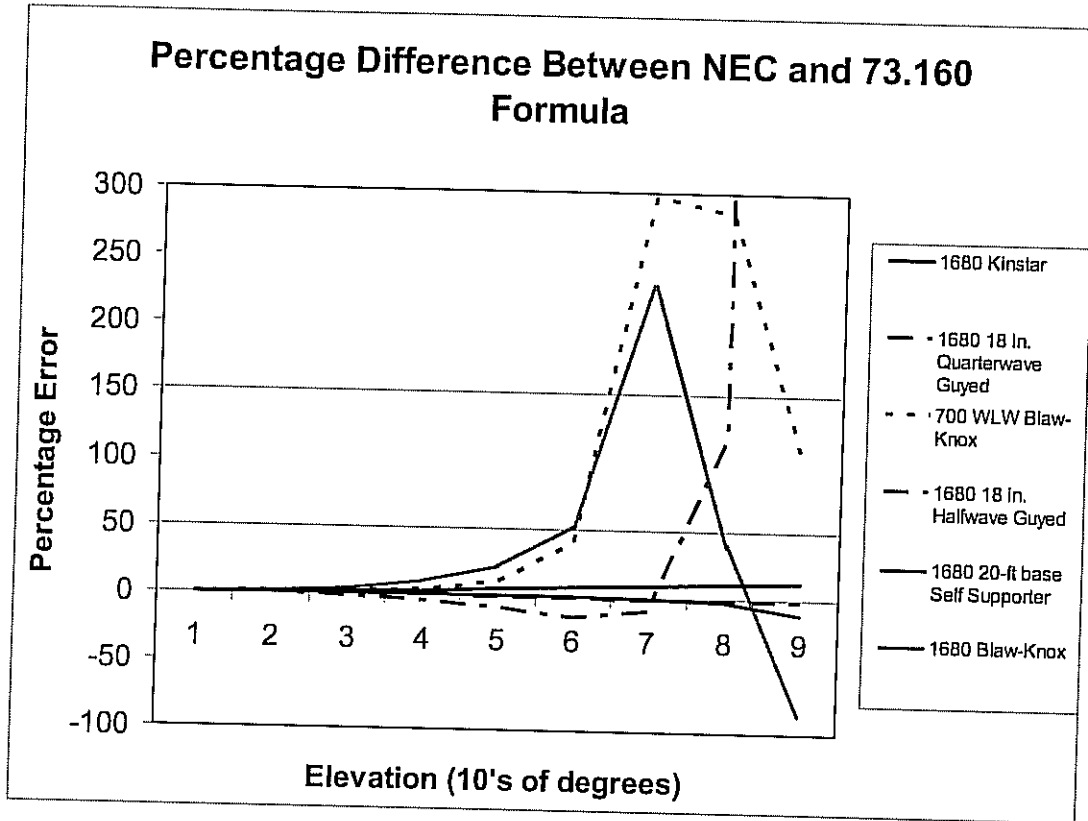


Figure 23 - Example of disagreements between 73.160 formulas and NEC models of selected AM broadcasting antennas. The KinStar error is small compared with large cross-section radiators such as wide-base self supporting towers and Blaw-Knox type antennas. See Appendix 2 for complete tables of elevation field patterns.

Tables of NEC-4.1 calculated field ratios, at 5 degree increments over both perfect and average ($\epsilon R=15$, $\sigma=5mS$) ground follow for both the KinStar A and B versions at 530 and 1680 kHz. Patterns for both versions of the antenna agree to within better than one percent.

**Table 9 - KinStar "A" Version Field Ratios
Calculated Using NEC-4.1 For Perfect and Average
Ground Conditions**

Angle	1680 kHz		550 kHz	
	Perfect	Average	Perfect	Average
0	1	1.26E-07	1	1.94E-07
5	0.996764	0.570873	0.996838	0.700932
10	0.987058	0.810635	0.987114	0.898286
15	0.970809	0.926173	0.970986	0.973737
20	0.947982	0.981114	0.948217	1
25	0.918507	1	0.918808	0.998959
30	0.882347	0.994041	0.882758	0.979267
35	0.839431	0.968944	0.839987	0.945079
40	0.789867	0.928142	0.790442	0.898639
45	0.733689	0.873857	0.734343	0.841373
50	0.671111	0.807655	0.671824	0.774332
55	0.602453	0.730849	0.603186	0.698415
60	0.528107	0.64465	0.528832	0.614502
65	0.448604	0.55022	0.449292	0.523503
70	0.364622	0.448831	0.365215	0.426418
75	0.276882	0.341726	0.277358	0.32433
80	0.18624	0.230273	0.186576	0.2184
85	0.093621	0.115876	0.093794	0.109862
90	1.9E-09	1.54E-08	4.23E-10	1.68E-07

Table 10 - KinStar "B" Version Field Ratios
 Calculated Using NEC-4.1 For Perfect and Average
 Ground Conditions

Angle	1680 kHz		550 kHz	
	Perfect	Average	Perfect	Average
0	1	1.26E-07	1	1.94E-07
5	0.996759	0.570967	0.996768	0.701047
10	0.987021	0.810758	0.987059	0.898398
15	0.970747	0.092625	0.97083	0.973807
20	0.947878	0.981175	0.948021	1
25	0.918354	1	0.918568	0.998863
30	0.882128	0.993917	0.882418	0.979084
35	0.83918	0.968751	0.839549	0.944799
40	0.789547	0.927893	0.789993	0.898275
45	0.73334	0.873542	0.733849	0.840944
50	0.670755	0.807303	0.671313	0.773866
55	0.602096	0.73049	0.602681	0.697946
60	0.527775	0.644311	0.528363	0.614062
65	0.448326	0.549948	0.448889	0.523133
70	0.364396	0.448625	0.364904	0.42615
75	0.276734	0.341618	0.277162	0.324187
80	0.186185	0.230279	0.186511	0.218403
85	0.093365	0.116011	0.093875	0.110024
90	0.000211	0.000315	3.19E-05	4.22E-05

5.0 RF Exposure Safety Analysis

The analysis is based on models of the KinStar antenna at 1 kW and 50 kW of power at 550 and 1680 kHz using the NEC-4.1 code and Sommerfeld-Norton ground approximation for average earth. The permissible exposure levels from 47 CFR § 1.1310 are 614 V/m for E-field and 1.63 A/m for H-field for both occupational and general public exposure. Since the physical size of the antenna is large, we need to evaluate both the electric and magnetic fields in the near field of the antenna, specifically in the areas in and around the vertical wires and under the horizontal loading wires where people might walk.

The electric and magnetic field exposures for the 1 kW KinStar antenna exceed allowable levels for both the general public and occupational exposure only in the immediate vicinity of the vertical wires. This area will require fencing to prevent contact and possible RF burns, as well as to protect the feedpoints from damage. An enclosed area containing the vertical wires would suffice.

At 50 kW, the E-field does not exceed permissible levels anywhere away from the vertical wires, but the H-field significantly exceeds the limit out to a radius of 12 meters at 1680 kHz and to 10 meters at 550 kHz, measured from the geometric center of the antenna. Personnel should not be within this radius while the antenna is transmitting. This area will require fencing and marking in accordance with the Commission's regulations. Personnel should also not contact the vertical wires while transmitting to avoid RF contact burns.

Standard fencing and marking procedures will be satisfactory for the KinStar antenna, although the areas requiring restricted access may be larger than for conventional towers. The areas to which access should be restricted may be based on either modeling data or post-construction field measurements.

Figures 24 through 33 show the NEC calculated fields for the 1 and 50 kW KinStar antennas at 1680 and 550 kHz. E and H-Field plots for a quarterwave monopole at 1kW follow the KinStar plots in Figures 34 and 35 for comparison. Note that the scales on the plots vary. These modeling results agree with the Mininec results shown in OET Bulletin 65 (revised).

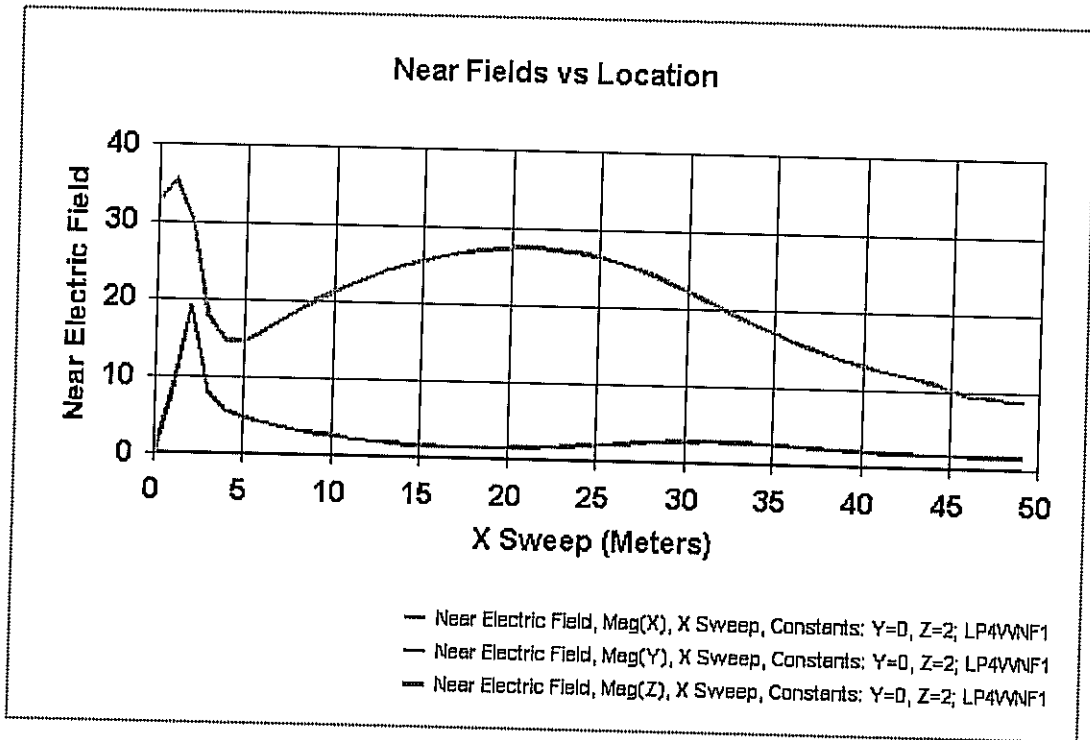


Figure 24 - E-field magnitude directly under top loading wire for 1680 kHz at 1 kW input power at a height of 2 meters (Permissible level is 614 V/m).

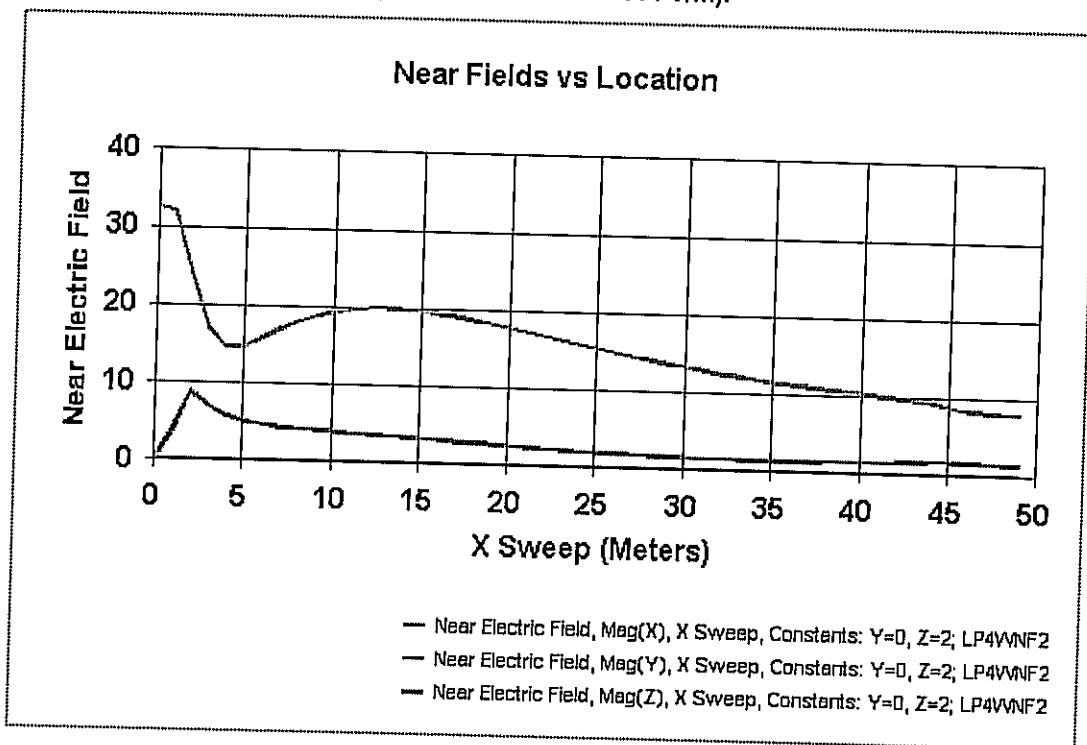


Figure 25 - E-field in area halfway between two top loading wires (45 degrees) for 1680 kHz at 1 kW input power at a height of 2 meters (Permissible level is 614 V/m).

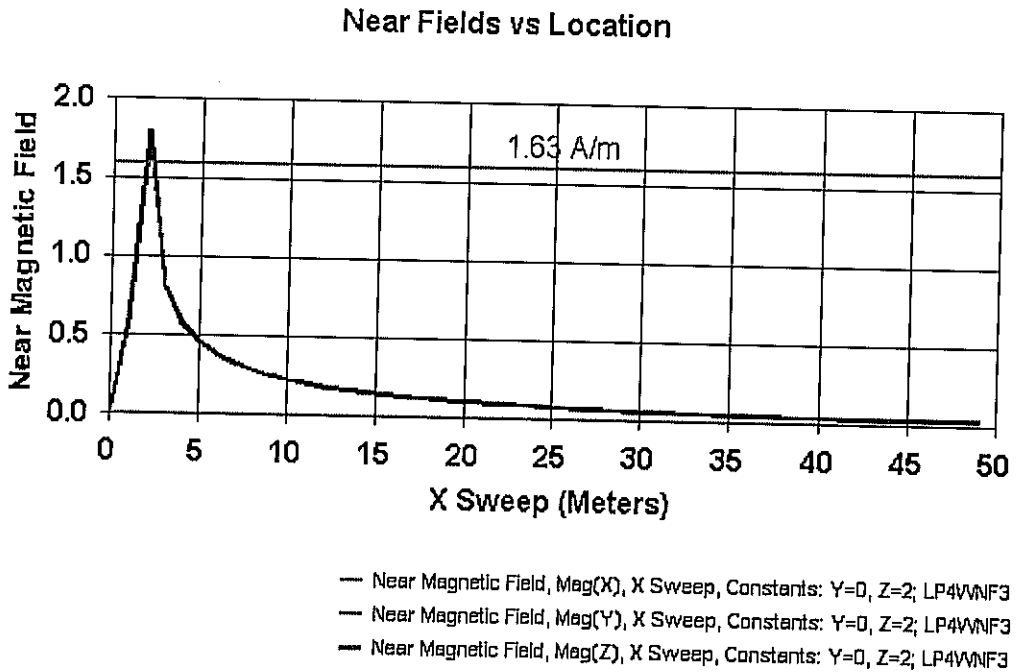


Figure 26 - Magnetic field directly under top loading wire for an input power of 1 kW at a height of 2 meters (Permissible level is 1.63 A/m).

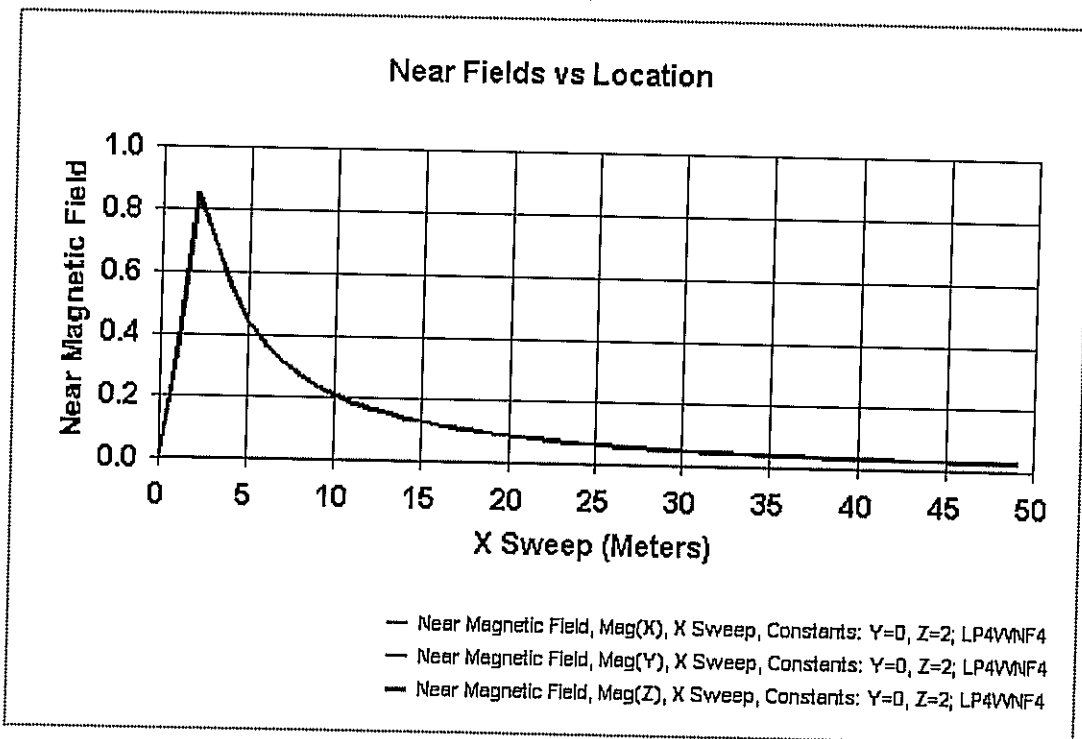


Figure 27 - Magnetic field in between wires for 1680 kHz at 1 kW at a height of 2 meters (Permissible level is 1.63 A/m).

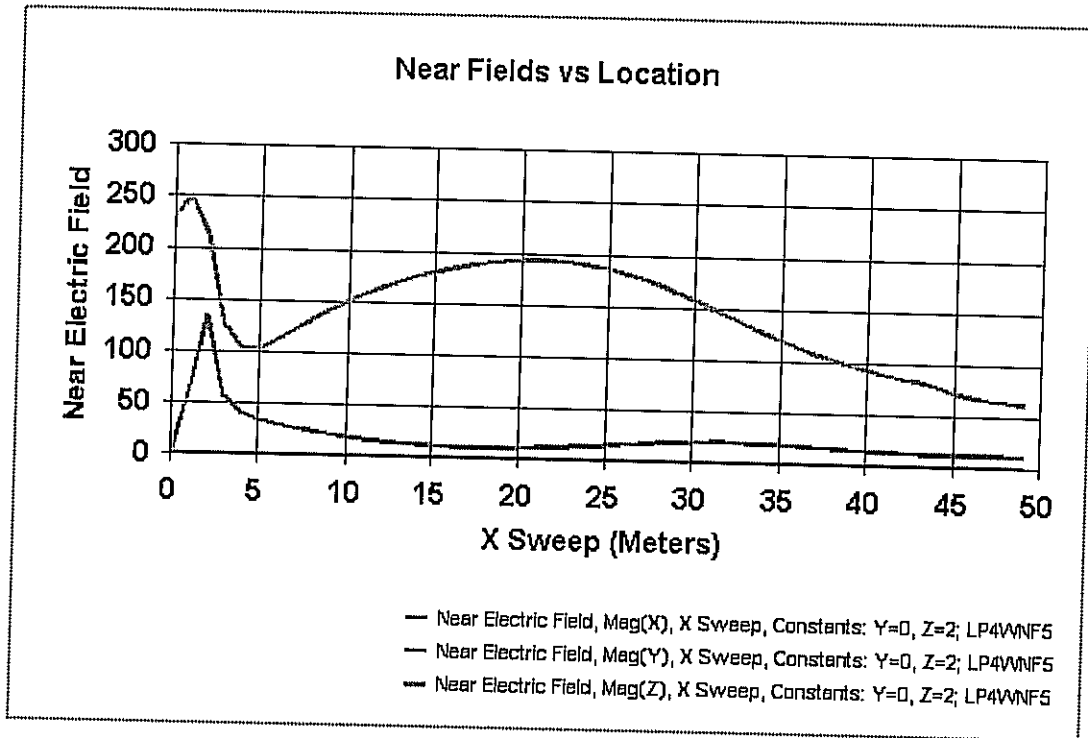


Figure 28 - E-field directly under top loading wire for 1680 kHz at 50 kW input power at a height of 2 meters (Permissible level is 614 V/m).

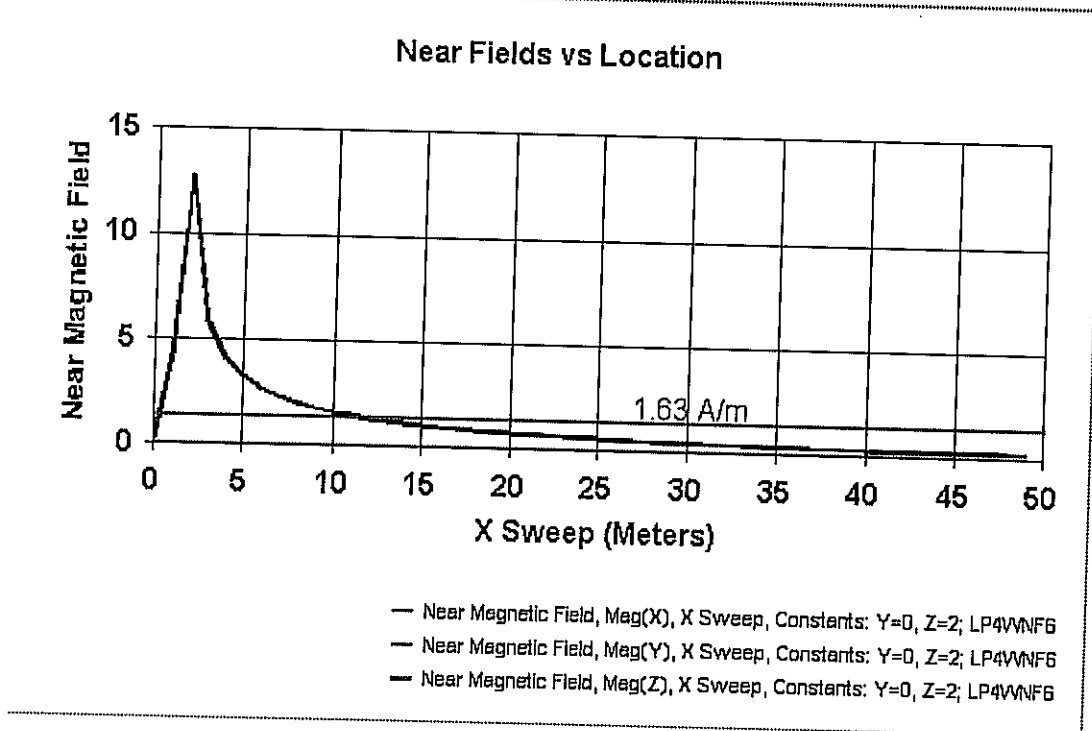


Figure 29 - Magnetic field directly under top loading wire for 1680 kHz at an input power of 50 kW at a height of 2 meters (Permissible level is 1.63 A/m).

Near Fields vs Location

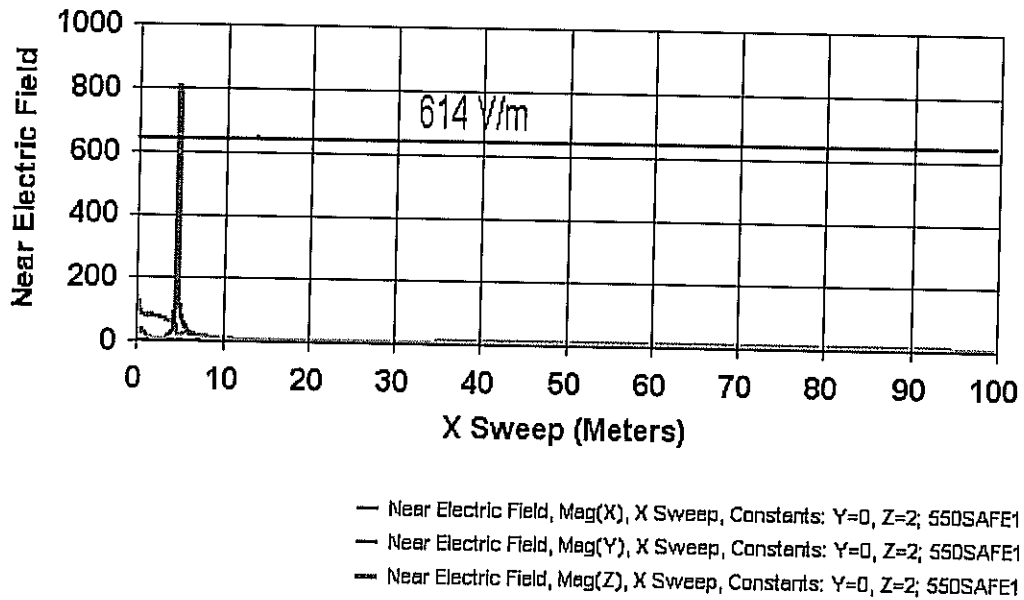


Figure 30 - Electric field directly under top loading wire for 550 kHz at an input power of 1 kW at a height of 2 meters (Permissible level is 614 V/m).

Near Fields vs Location

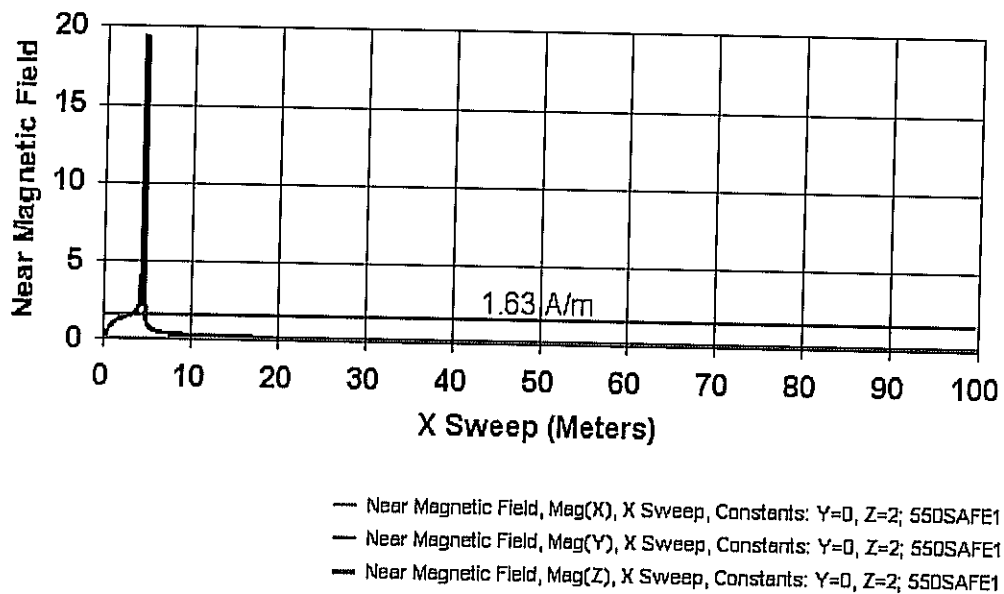


Figure 31 - Magnetic field directly under top loading wire for 550 kHz at an input power of 1 kW at a height of 2 meters (Permissible level is 1.63 A/m).

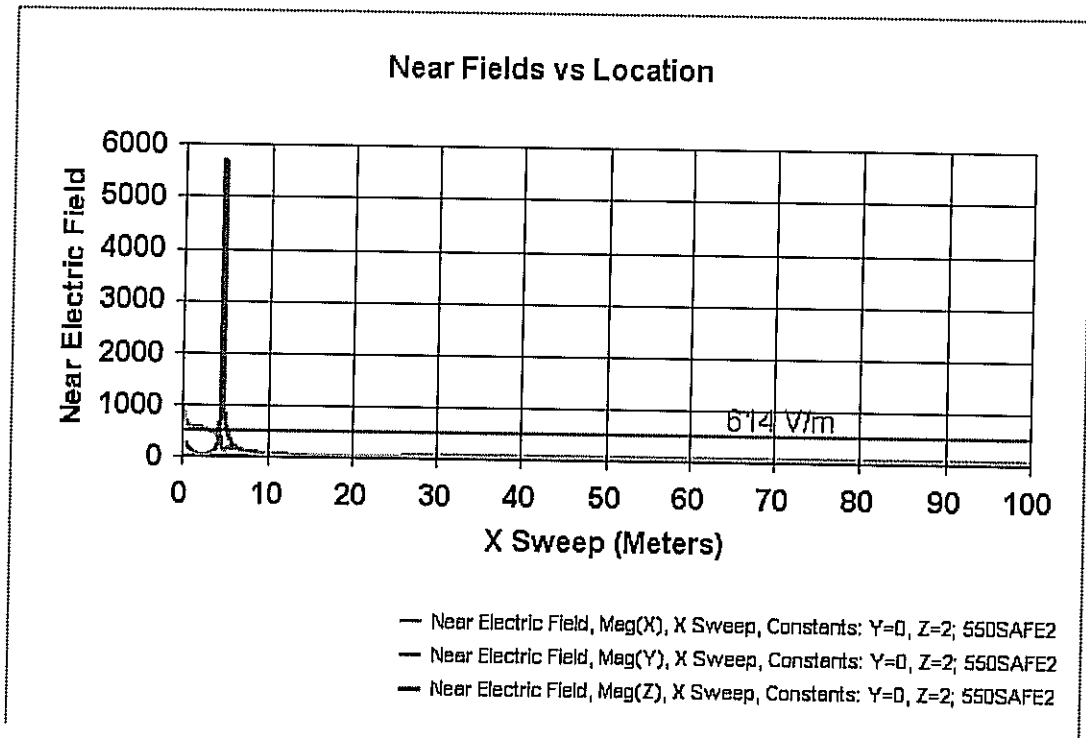


Figure 32 - Electric field directly under top loading wire for 550 kHz at an input power of 50 kW at a height of 2 meters (Permissible level is 614 V/m).

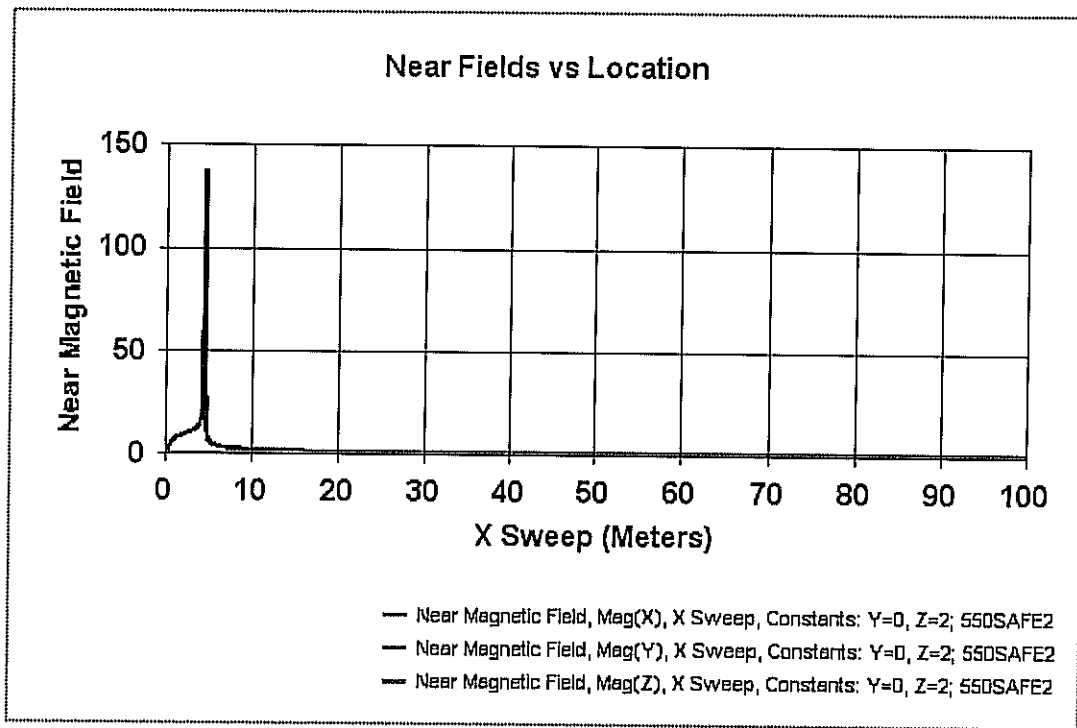


Figure 33 - Magnetic field directly under top loading wire for 550 kHz at an input power of 50 kW at a height of 2 meters (Permissible level is 1.63 A/m, threshold not shown).

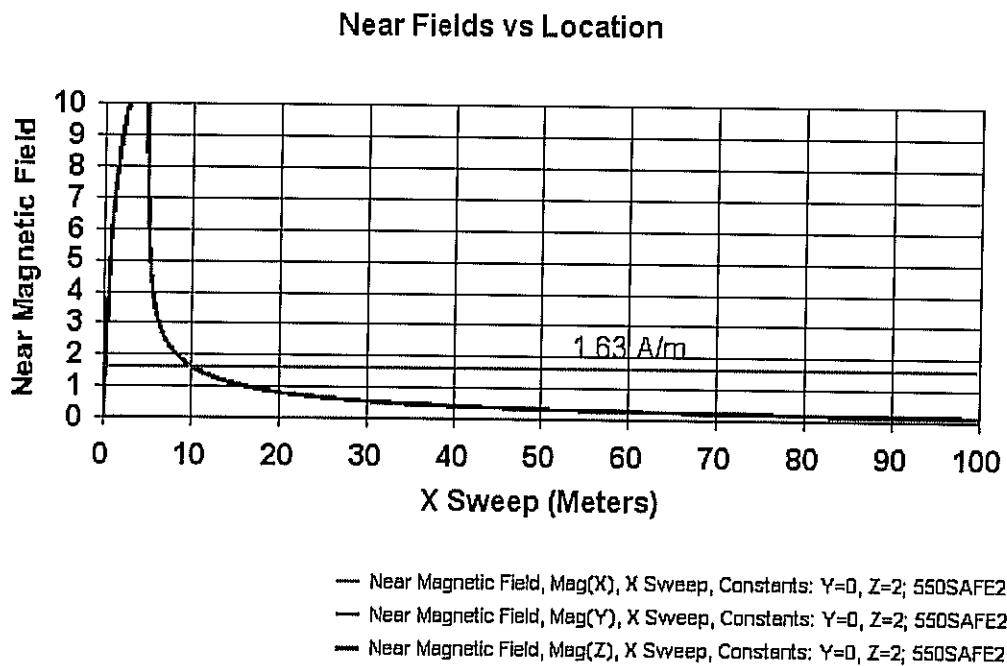


Figure 34 - Magnetic field directly under top loading wire for 550 kHz at an input power of 50 kW at a height of 2 meters (Permissible level is 1.63 A/m).

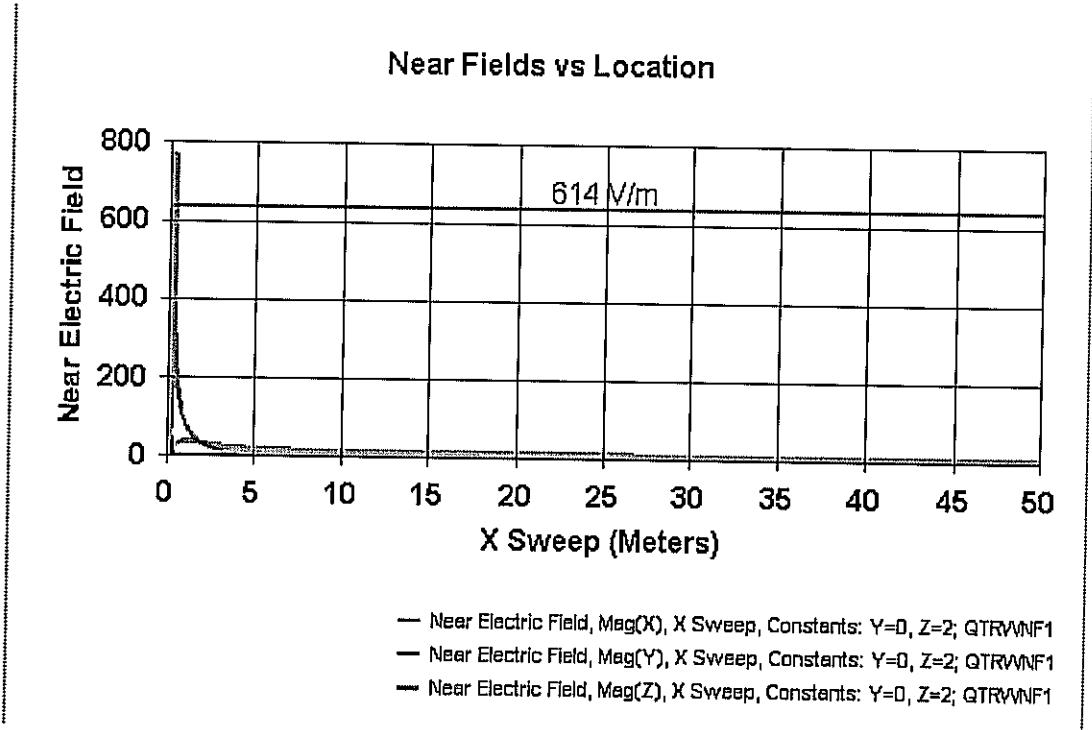


Figure 35 - E-Field plot for 90 degree tower at 1680 kHz at 1 kW along radial at height of 2 meters (Permissible level is 614 V/m).

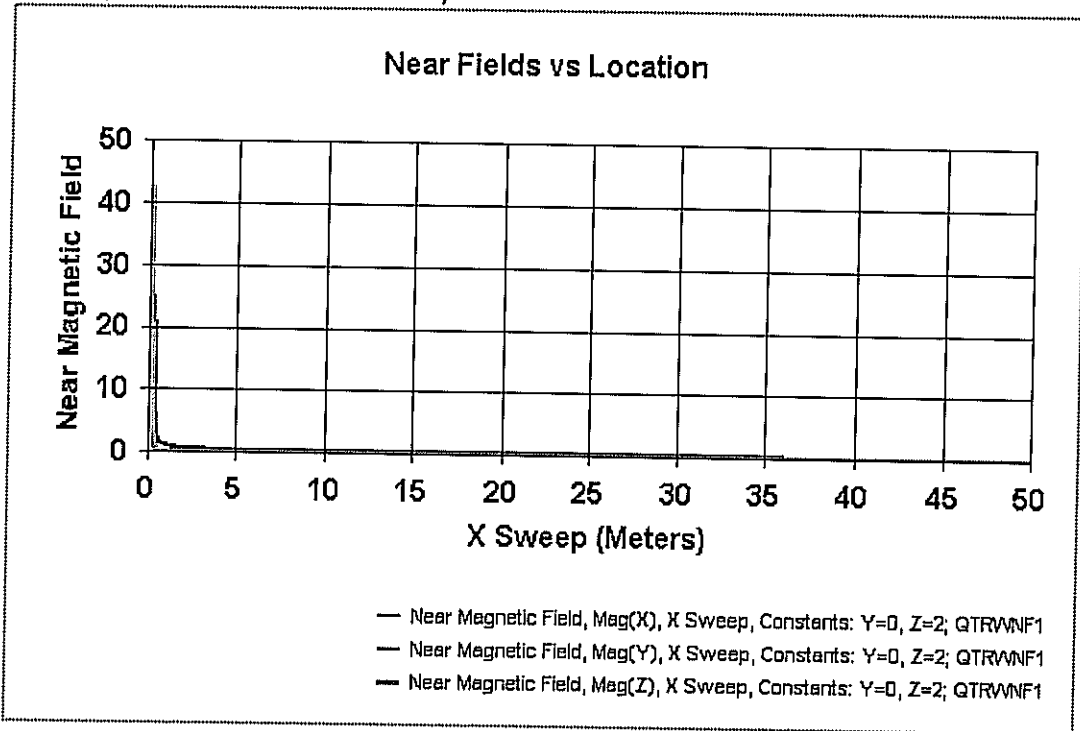


Figure 36 - H-Field plot for 90 degree tower at 1680 kHz at 1 kW along radial at height of 2 meters (Permissible level is 1.63 A/m).

Appendix 1

Ground Parameter and Frequency Variation Study
For KinStar Antenna and Quarterwave Tower

Modeling Results Data

1680 kHz – KinStar A - Transmission Line Match

Conditions	Relative Permittivity	Conductivity (S/m)	NEC Calculated RMS Field at 1km for 1kW input power (mV/m)	Correction Factor from Thin Monopole NEC Model	Calculated Unattenuated RMS Field at 1km for 1kW input power (mV/m)
Perfect with Ground Screen			293.54	-	293.54
Good	15	0.03	273.43	1.069	292.29
Average	15	0.005	215.67	1.365	294.39
Poor	15	0.001	116.56	2.477	288.72
Very Poor	15	0.0001	93.95	3.040	285.61

1680 kHz – KinStar B - Common Top/Bottom Lumped Element Match

Conditions	Relative Permittivity	Conductivity (S/m)	NEC Calculated RMS Field at 1km for 1kW input power (mV/m)	Correction Factor from Thin Monopole NEC Model	Calculated Unattenuated RMS Field at 1km for 1kW input power (mV/m)
Perfect with Ground Screen			293.36	-	293.36
Good	15	0.03	270.6	1.069	289.27
Average	15	0.005	212.8	1.365	290.47
Poor	15	0.001	116.3	2.477	288.08
Very Poor	15	0.0001	94.0	3.040	285.76

1680 kHz - Quarterwave 18" Tower – 146.37 Feet Tall

Conditions	Relative Permittivity	Conductivity (S/m)	NEC Calculated RMS Field at 1km for 1kW input power (mV/m)	Correction Factor from Thin Monopole NEC Model	Calculated Unattenuated RMS Field at 1km for 1kW input power (mV/m)
Perfect with Ground Screen			318.75	-	318.75
Good	15	0.03	297.53	1.069	318.06
Average	15	0.005	233.18	1.365	318.29
Poor	15	0.001	128.67	2.477	318.71
Very Poor	15	0.0001	104.83	3.040	318.68

Correction factor calculation – from thin monopole model

	Attenuated 1 km Field	Unattenuated Field	Calculated Correction Factor
Good	293.59	313.88	1.069
Average	229.91	313.88	1.365
Poor	126.73	313.88	2.477
Very Poor	103.25	313.88	3.040

1000 kHz – KinStar A - Transmission Line Match

Conditions	Relative Permittivity	Conductivity (S/m)	NEC Calculated RMS Field at 1km for 1kW input power (mV/m)	Correction Factor from Thin Monopole NEC Model	Calculated Unattenuated RMS Field at 1km for 1kW input power (mV/m)
Perfect with ground screen			290.43	-	290.43
Good	15	0.03	283.88	1.014	287.85
Average	15	0.005	255.78	1.139	291.33
Poor	15	0.001	172.36	1.695	292.15
Very Poor	15	0.0001	126.12	2.277	287.18

1000 kHz – KinStar B - Common Top/Bottom Lumped Element Feed

Conditions	Relative Permittivity	Conductivity (S/m)	NEC Calculated RMS Field at 1km for 1kW input power (mV/m)	Correction Factor from Thin Monopole NEC Model	Calculated Unattenuated RMS Field at 1km for 1kW input power (mV/m)
Perfect with Ground Screen			290.30	-	290.30
Good	15	0.03	279.51	1.014	283.42
Average	15	0.005	251.32	1.139	286.25
Poor	15	0.001	171.04	1.695	289.91
Very Poor	15	0.0001	125.36	2.277	285.44

1000 kHz - Quarterwave 18" Tower – 245.9 Feet Tall

Conditions	Relative Permittivity	Conductivity (S/m)	NEC Calculated RMS Field at 1km for 1kW input power (mV/m)	Correction Factor from Thin Monopole NEC Model	Calculated Unattenuated RMS Field at 1km for 1kW input power (mV/m)
Perfect with Ground Screen			317.68		317.68
Good	15	0.03	307.27	1.014	311.57
Average	15	0.005	277.26	1.139	315.80
Poor	15	0.001	189.93	1.695	321.93
Very Poor	15	0.0001	140.35	2.277	319.58

Correction factor calculation – from thin monopole model

	Attenuated 1 km Field	Unattenuated Field	Calculated Correction Factor
Good	307.47	311.92	1.014
Average	273.85	311.92	1.139
Poor	184.06	311.92	1.695
Very Poor	136.96	311.92	2.277

530 kHz – KinStar A - Transmission Line Match

Conditions	Relative Permittivity	Conductivity (S/m)	NEC Calculated RMS Field at 10 km for 1kW input power (mV/m)	Correction Factor from Thin Monopole NEC Model	Calculated Unattenuated RMS Field at 1km for 1kW input power (mV/m)
Perfect with ground screen			28.388	-	283.88
Good	15	0.03	28.007	1.0814	302.87
Average	15	0.005	23.33	1.2234	285.41
Poor	15	0.001	10.826	2.7849	301.49
Very Poor	15	0.0001	4.2671	6.7906	289.76

530 kHz – KinStar B - Common Top/Bottom Lumped Element Feed

Conditions	Relative Permittivity	Conductivity (S/m)	NEC Calculated RMS Field at 10 km for 1kW input power (mV/m)	Correction Factor from Thin Monopole NEC Model	Calculated Unattenuated RMS Field at 1km for 1kW input power (mV/m)
Perfect with Ground Screen			28.665		286.65
Good	15	0.03	28.226	1.0814	305.24
Average	15	0.005	22.662	1.2234	277.24
Poor	15	0.001	10.653	2.7849	296.67
Very Poor	15	0.0001	4.1932	6.7906	284.74

530 kHz - Quarterwave 18" Tower – 464 Feet Tall

Conditions	Relative Permittivity	Conductivity (S/m)	NEC Calculated RMS Field at 10 km for 1kW input power (mV/m)	Correction Factor from Thin Monopole NEC Model	Calculated Unattenuated RMS Field at 1km for 1kW input power (mV/m)
Perfect with Ground Screen			31.401		314.01
Good	15	0.03	30.23	1.0814	326.91
Average	15	0.005	25.043	1.2234	306.37
Poor	15	0.001	11.775	2.7849	327.92
Very Poor	15	0.0001	4.698	6.7906	319.02

Correction factor calculation – from thin monopole model

	Attenuated 10 km Field	Unattenuated Field	Calculated Correction Factor
Good	28.837	31.185	1.0814
Average	25.491	31.185	1.2234
Poor	11.198	31.185	2.7849
Very Poor	4.5924	31.185	6.7906

Appendix 2

Elevation Pattern Ratio Comparison Between NEC-4.1 And
73.160 Calculation Formula For Selected Licensed AM
Broadcasting Antennas

**Comparison of Elevation Field Ratios
1680 kHz 18" Face Guyed Tower Monopole**

Angle	NEC-4.1 Prediction	73.160 Calculation	Percent NEC Error between 73.160 and NEC-4.1
0	1	1	0
10	0.97725	0.977886	-0.06497621
20	0.912001	0.914259	-0.24699648
30	0.812156	0.816497	-0.53155512
40	0.688781	0.694639	-0.84337481
50	0.551768	0.558941	-1.28325901
60	0.410828	0.417794	-1.66718741
70	0.27107	0.27656	-1.98483826
80	0.134391	0.137414	-2.19952011

**Comparison of Elevation Field Ratios
700 kHz WLW Blaw-Knox Tower**

Angle	NEC-4.1 Prediction	73.160 Calculation	Percent NEC Error between 73.160 and NEC-4.1
0	1	1	0
10	0.936057	0.933598	0.263305243
20	0.766383	0.75709	1.227487314
30	0.545881	0.526416	3.697673407
40	0.336205	0.303337	10.83540992
50	0.183008	0.131218	39.46931114
60	0.103505	0.026061	297.1629107
70	0.070655	0.018339	285.266962
80	0.039787	0.019898	99.95096892

**Comparison of Elevation Field Ratios
1680 kHz Halfwave Guyed Tower Monopole**

Angle	NEC-4.1 Prediction	73.160 Calculation	Percent NEC Error between 73.160 and NEC-4.1
0	1	1	0
10	0.936152	0.940704	-0.48385188
20	0.766105	0.781863	-2.01537124
30	0.543208	0.570865	-4.84468971
40	0.327374	0.361148	-9.35183726
50	0.162953	0.191854	-15.0641815
60	0.071734	0.079347	-9.59439182
70	0.044627	0.020366	119.1225034
80	0.027587	0.000251	10884.29397

**Comparison of Elevation Field Ratios
1680 kHz 20-Ft Base Halfwave Self Supporting Tower**

Angle	NEC-4.1 Prediction	73.160 Calculation	Percent NEC Error between 73.160 and NEC-4.1
0	1	1	0
10	0.9416	0.941733	-0.01409596
20	0.784996	0.78546	-0.05911828
30	0.576513	0.57735	-0.14507243
40	0.368538	0.369635	-0.29671267
50	0.199657	0.200816	-0.57720268
60	0.08625	0.087276	-1.17592284
70	0.025409	0.02616	-2.86826635
80	0.002887	0.003279	-11.9653009

**Comparison of Elevation Field Ratios
1680 kHz Blaw-Knox Halfave Tower**

Angle	NEC-4.1 Prediction	73.160 Calculation	Percent NEC Error between 73.160 and NEC-4.1
0	1	1	0
10	0.9416	0.941733	-0.01409596
20	0.784996	0.78546	-0.05911828
30	0.576513	0.57735	-0.14507243
40	0.368538	0.369635	-0.29671267
50	0.199657	0.200816	-0.57720268
60	0.08625	0.087276	-1.17592284
70	0.025409	0.02616	-2.86826635
80	0.002887	0.003279	-11.9653009

EXHIBIT A

A Novel Short AM Monopole Antenna with
Low-Loss Matching System

Technical Proceedings of the
IEEE Broadcast Symposium, October 2002

SEE PDF FILE ATTACHMENT

KINSTAR_IEEE_ARTICLE.PDF

A Novel Short AM Monopole Antenna with Low-Loss Matching System

James K. Breakall, Ph.D.

Department of Electrical
Engineering,
The Pennsylvania State
University,
University Park, PA, USA
jimb@psu.edu

Michael W. Jacobs

STAR-H Corporation,
State College, PA, USA
mike@star-h.com

Alfred E. Resnick, P.E.

Broadcast Consultant
Paoli, PA, USA
alresnick@ieee.org

G. Yale Eastman

STAR-H Corporation
Lancaster, PA, USA
yale@star-h.com

Milton D. Machalek, Ph.D.

STAR-H Corporation
Lancaster, PA, USA
milt@star-h.com

Thomas F. King

Kintronic Laboratories, Inc.
Bristol, TN, USA
tking@kintronic.com

Abstract

A number of reduced-size antennas for AM broadcasting have been presented over the years, but all have suffered from limitations inherent in presenting attractive impedances over the desired operating bandwidth to the transmitter. In this work, we present NEC-4.1 Method of Moments modeling results of a novel technique of using multiple independently fed short vertical elements in close proximity to increase the real impedance of an electrically short antenna while retaining the radiation pattern characteristics of a short monopole antenna. Atop each short vertical element is a horizontal loading structure to get the proper current distribution for radiation. The arrangement of elements provides a number of independent input impedances. By parallel combination of these independent input impedances, with the use of appropriate efficient matching techniques, the real part of the input impedance is effectively increased. This antenna exhibits a vertical height of approximately 0.05 wavelengths, resulting in a substantial height reduction from a quarterwave monopole radiator and the elimination of the need for lighted tower structures for AM antenna systems, resulting in reduced construction costs and increased community acceptance of new AM antenna systems. These antennas can also be used in arrays for directional AM patterns, and are fully compatible with the bandwidth requirements of AM stereo or IBOC transmission.

Keywords – low-profile antenna, cage monopole, monopole, short antenna, reduced size antenna, AM antenna, MF antenna

INTRODUCTION

The benefits and limitations of short monopole antennas for MF broadcasting are well known and have been covered thoroughly in the recent literature [1]. We have

developed a method of combining the top-loaded monopole antenna over a ground plane with low-loss inexpensive impedance matching techniques to create an antenna with a vertically polarized omnidirectional radiation pattern with very good efficiency and impedance bandwidth performance. This antenna is expected to meet all FCC performance criteria and be capable of substitution for a standard quarterwave monopole for any power level, while having a height above ground of approximately 0.05 wavelengths. The unattenuated field strength generated by this antenna will be similar to that of a short monopole, on the order of 299.8 mV/m at 1km with 1kW of input power, only a slight penalty from the typical 313.6 mV/m value for the quarterwave antenna. With the reduced height, such an antenna can be situated much closer to the community being served, resulting in improved coverage, or it can be located on a wider range of available properties, with less community opposition, thus reducing site acquisition costs. The antenna itself can be constructed with standard overhead line construction techniques, and will not require obstruction lighting in most applications. STAR-H Corporation currently has a patent application for this antenna and its key concepts pending in both the US and international markets.

ANTENNA CONCEPT AND THEORY

It is well known that creating a cage monopole of vertical wires to increase the diameter of the radiator can increase the bandwidth of a short vertical antenna. If the vertical conductors of a short cage monopole are separated and excited individually in phase, then for a constant input power level the impedance of each monopole is increased. If there are n monopoles, then the impedance of each is now n times the original impedance of a single monopole, if the power is held constant, since the current is divided n ways. This configuration is shown in Figure 1. Providing that the monopoles are closely spaced and symmetrical, as

when on even points on a circle with a radius that is small compared to a wavelength, all the radiated fields will add in phase and the far-field pattern will be essentially identical to that of a single monopole radiator.

This multiplication of the radiation resistance can be shown by considering that for a single radiating element:

$$P_{in} = I_{in} V_{in} = I_{in}^2 Z_{in} = \frac{V_{in}^2}{Z_{in}} \quad (1)$$

If we hold the input power constant and neglect the losses, for the antenna system of Figure 1,

$$P_{in} = n \frac{I_{in}}{n} V_{in} = n \left(\frac{I_{in}}{n} \right)^2 Z_{in}' = n \frac{V_{in}^2}{Z_{in}'} \quad (2)$$

where $\frac{I_{in}}{n}$ is the input current for each individual radiator and Z_{in}' is the impedance of each cage wire monopole.

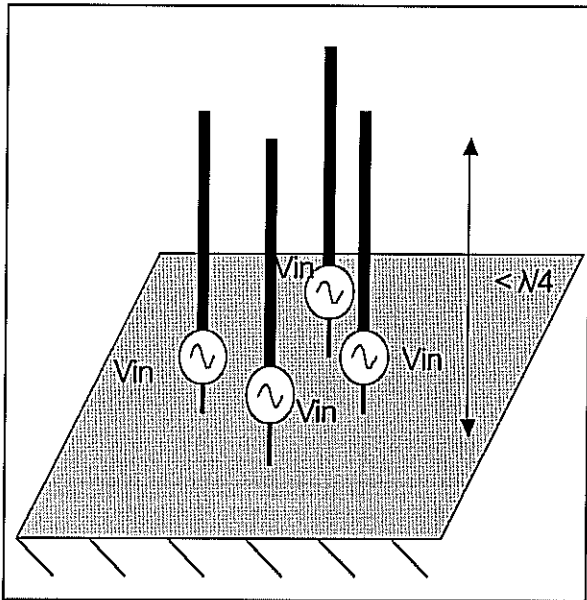


Figure 1. Cage monopole of vertical radiators closely spaced with independent voltage sources.

Solving for the input impedance of one individual monopole in the cage (Z_{in}') gives:

$$Z_{in}' = n \frac{V_{in}}{I_{in}} \quad (3)$$

If we use short monopoles for the cage, we also can use an analytical expression for the input resistance of a short monopole, neglecting the mutual impedance between the vertical elements, which will be small because of their reduced size (NEC modeling confirms this). For a $1/20^{\text{th}}$ wavelength monopole (assuming we can achieve a constant

current distribution on the short monopole), the radiation resistance is:

$$R_{\text{radiation}} = 160\pi^2 \left(\frac{l}{\lambda} \right)^2 \quad (4)$$

$$R_{\text{radiation}} = \frac{\pi^2}{2.5} = 3.95 \Omega$$

where l is the length of the monopole and λ is the wavelength. This compares with a resistance of approximately 36 ohms for a quarterwave monopole. Of course, for the shortened monopole, a substantial reactive component will also be present. This ideal current distribution can be approximated by adding top loading, in the form of horizontal wires or other structures, to the short monopole elements, as shown in Figure 2. Adjustment of the dimensions of these antenna elements can be made to tune the antenna to resonance, so that the reactive components are zero. For other electrical heights, the input impedance can be calculated. Some values are shown in Table 1.

Table 1. Radiation resistance versus height for a monopole with constant current distribution.

Height (λ)	$R_{\text{radiation}}$ (Ohms)
0.01	0.16
0.04	2.52
0.08	10.1
0.1	15.8

We can see that by choosing the height and the number of radiators in our cage monopole, we can achieve substantial control of the input impedance. For example, a cage of four 0.08λ monopoles would result in each having a radiation resistance of approximately 40.4 ohms. This analysis is neglecting the mutual coupling effects, which computer modeling shows to be quite minimal if the element height is small.

The remaining task is to bring these independent input impedances together and to match them to a single 50-ohm source (or load, as the antenna is reciprocal), since we do not wish to use n separate transmitters. One attractive way of doing this is to use the quarterwave transmission line transformer and connect these in parallel.

This is shown in Figures 3 and 4. With the ability to control the input impedance of each radiator, we can select an impedance which can use commonly available 50 or 75 ohm semi-rigid transmission line to implement this with very low loss. A suitable impedance for this four-element example would be 200 ohms at the parallel connection, since four 200 ohm impedances in parallel gives us the desired 50 ohm input impedance at a single feedpoint.

$$Z_{in} = \frac{Z_0^2}{Z_{\text{parallel}}} \quad (5)$$

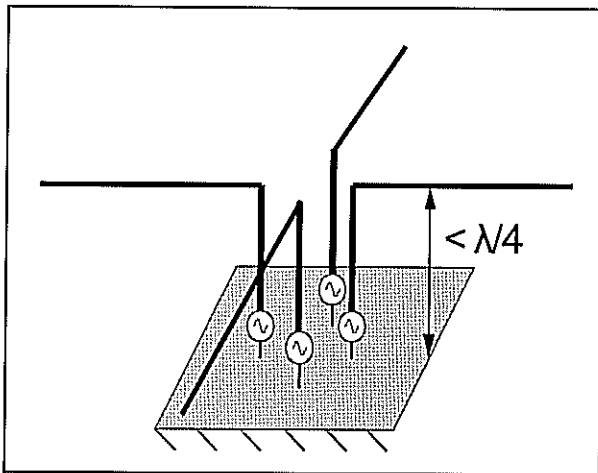


Figure 2. Short cage monopole antenna with independent feedpoints and top loading elements.

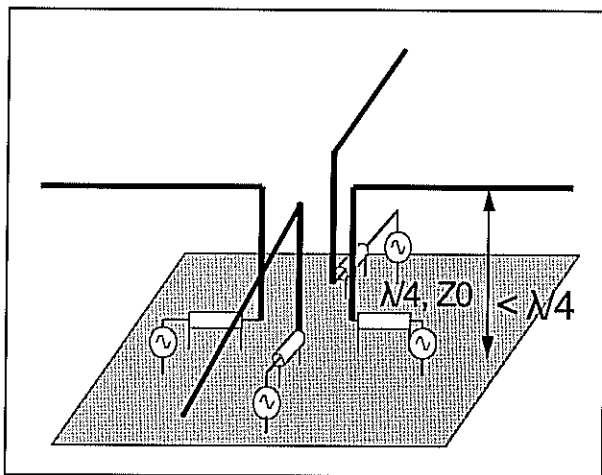


Figure 3. Short cage monopole antenna with addition of quarterwave transformer sections.

Calculating the transformer input impedance using a 50-ohm transmission line yields a value of 12.5 ohms. This 12.5 ohm impedance with $n=4$ for a 4-element antenna corresponds to a short monopole with an impedance of 3.125 ohms. This impedance can be obtained by using an antenna with a vertical height of about 0.044 wavelengths (obtained using Equation 4 or Table 1 above), which is 17.6% of the height of a quarterwave monopole.

For broadcast applications, common low-loss semi rigid coaxial cable can be used for this, and by suitably selecting the line size, the power handling requirements can be met and loss in the transformer section can be kept low for desirable antenna heights. For communications and WLAN applications, smaller sized coax can be used, as can microstrip or other transmission line types. Lumped element matching can also be used if desired, although transmission line transformers are usually less expensive

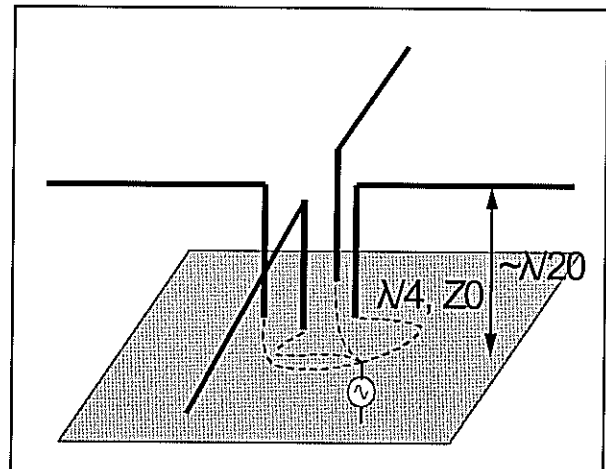


Figure 4. Resulting low-profile antenna with quarterwave matching lines to single feedpoint. Antenna has 50-ohm input impedance.

and easier to construct. The antenna itself can be constructed from stranded aluminum wire conductors as are typically used in the power industry. At many frequencies in the US AM broadcast band, wooden utility poles can serve as the vertical supports.

The radiation pattern from this antenna will be equivalent to that for any reduced size monopole antenna with a nearly constant current distribution, and will be vertically polarized. The fields due to the currents in the vertical radiating elements will add in-phase in the far field, while the currents in the horizontal components will be out of phase and will cancel. This antenna can be constructed with any number of radiating elements, in many different configurations. For broadcasting applications, a conventional 120-radial system is an anticipated requirement to minimize ground losses, although work is underway to develop an elevated radial version of the antenna [2].

NEC MODELING RESULTS

Much of the original development work for this antenna was done using the NEC-4.1 (Numerical Electromagnetics Code) Method of Moments code [3-4], with the GNEC GUI front end and the NECOPT numerical optimizer package for NEC developed at Penn State University [5]. The NECOPT program optimizes the performance of the antenna by automatically varying the parameters of the antenna, such as the height of the monopole, length of the horizontal elements, and radial distance of the monopoles to the center. NECOPT can thus be used to determine the complete antenna dimensions for a particular frequency and bandwidth requirement. Antenna designs consisting of 2, 4, and 8 element configurations have been modeled, using both slanted and level horizontal loading elements. The antenna bandwidth is determined by the number of elements in the antenna, the size of the wires used to make

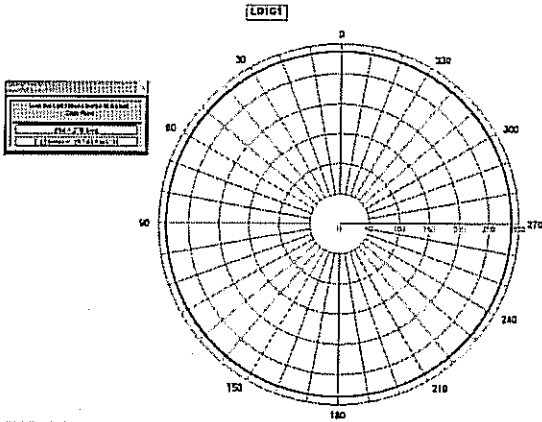


Figure 5. NEC calculated field pattern of 4-element low-profile antenna over perfect ground excluding matching system losses, showing omnidirectional pattern.

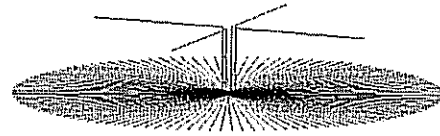


Figure 6. NEC model geometry of low profile antenna designed for 1680 kHz with 120 radial ground screen.

those elements, and the radius of the circle on which the vertical radiators are located.

Additional work has been done to model the antenna performance over ground systems, including the analysis of radial systems and comparison with quarterwave monopole radiators. We have also modeled the antenna performance in a 3-element directional array with particular null requirements.

In anticipation of a full-scale test of this antenna in a configuration for AM broadcast applications, in partnership with Kintronic Laboratories, Inc., of Bristol, TN, we have designed and modeled with NEC an omnidirectional 4-wire version of the antenna at a frequency of 1680 kHz. The model included 120 ground radials and used the Sommerfeld-Norton method for calculating ground effects, and included conductor losses.

For the full-scale test, the antenna will be constructed using 3/8" diameter stranded aluminum conductors suspended between five 55' telephone poles sunk into augured holes and guyed against the strain from the horizontal elements. Semi-rigid foam dielectric 50 ohm coaxial line 7/8" in diameter will be used for the matching transformers. The vertical wire elements will extend to 45 feet above the ground (0.072λ , compared to a quarterwave tower 145.48 feet high), and the horizontal loading wires will be 95 feet in length. The four vertical wires will be evenly spaced on a circle with a radius of five feet. Based on the bandwidth requirements for IBOC transmissions, NECOPT was used to also vary the length of the transmission lines with a goal of maximizing the bandwidth. This resulted in a line length of 38.42 feet with an 89% velocity factor.

The impedance calculated by NEC at 1680 kHz at each vertical feedpoint is $38.3 + j63.3$ ohms. The output impedance after passing through the transmission line transformer will be $194.9 - j8.06$ ohms, which will yield a parallel combined impedance of $48.3 + j1.2$ ohms. NEC's calculated field value at 1 km for 1 kW input over 120 radials and lossy earth is 216.1 mV/m, exclusive of the loss in the matching system. Calculations show that line loss should be less than 0.02 dB, resulting in an attenuated field value of approximately 215 mV/m.

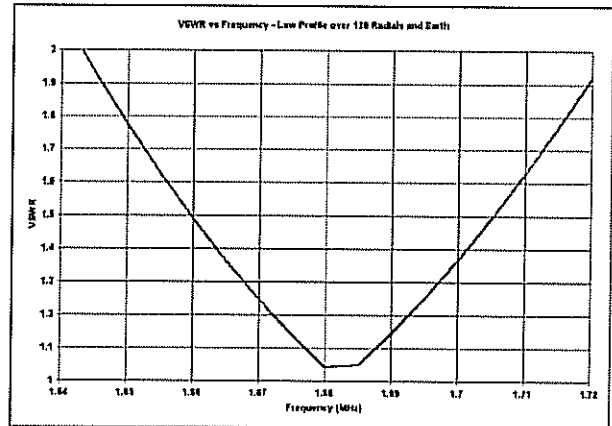


Figure 7. NEC predicted bandwidth for antenna model shown in Figure 5. 1.5:1 bandwidth obtained over 1660 – 1750 kHz.

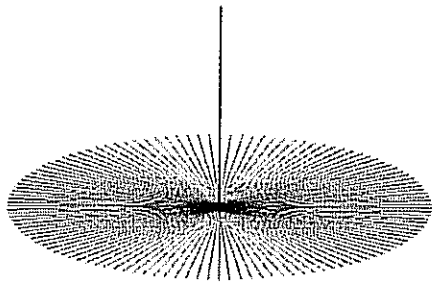


Figure 8. NEC model geometry for quarterwave tower monopole and 120 radial ground screen.

For comparison, NEC was used to model a quarterwave tower monopole at the same frequency and with the same ground system and conditions to yield a calculated value of 233.8 mV/m, without matching system losses. The performance of the low-profile antenna compared with the quarterwave monopole shows that this low-profile is 92.4% as efficient for field strength as the monopole, exclusive of matching system losses. The field values resulting from the low-profile antenna should be entirely sufficient to permit a broadcaster to cover the required service area almost as well as with the much higher quarterwave antenna.

In practice, the use of an optimizer will allow an antenna to be custom designed to meet the bandwidth requirements at any operating frequency. In addition to the transmission line matching system, Kintronic Laboratories is constructing a variable inductor/capacitor tuning unit to place at the parallel line connection for the test antenna to allow a small amount of adjustment for variations due to construction tolerances or other unforeseen effects.

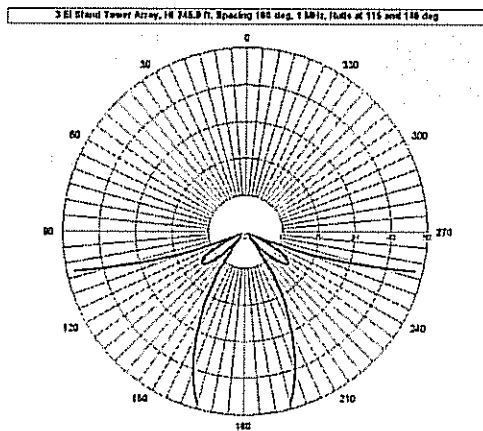


Figure 9. NEC model of directional pattern from 3-tower array.

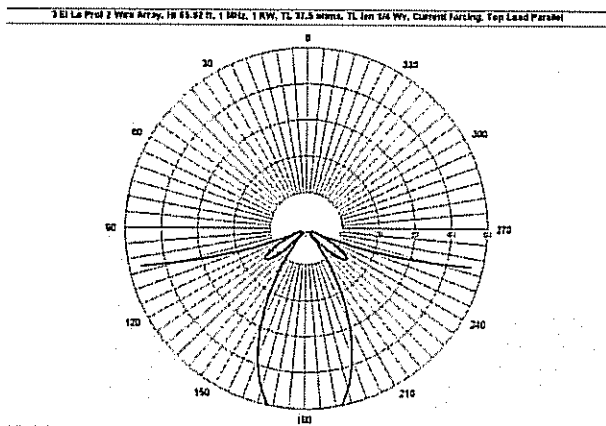


Figure 10. Example of directional pattern using three 2-wire element low-profile antennas to duplicate the pattern obtained with the three-tower array in Figure 9.

Because of the prevalence of directionality requirements on AM broadcast stations in the U.S., we decided to attempt a directional design using this antenna. For this example, nulls were required at 115 and 140 degrees. Comparison was made with a NEC model of an actual 3-tower array with this pattern. It is shown that for this pattern, the low-profile array can be designed to duplicate the directional pattern of the tower array. Figures 9 and 10 show the tower array and low-profile array patterns, respectively. We have used the 2-wire version of the antenna for directional arrays, as shown in Figure 11, to avoid a potential problem with coupling (or mechanical conflict) between horizontal elements of adjacent antennas. Further modeling shows that this may not be a significant problem, allowing the additional versatility and bandwidth of a four-wire version to be used in directional applications.

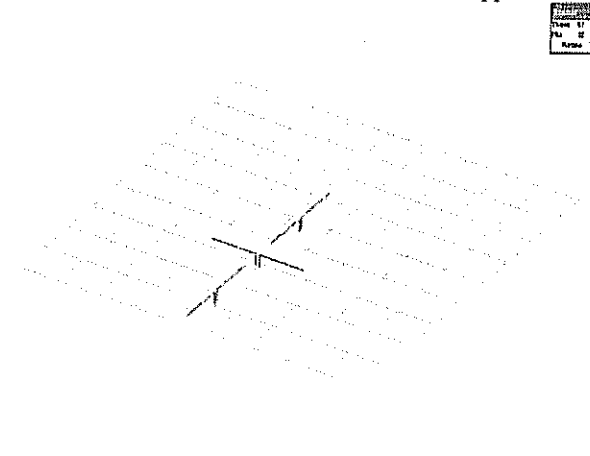


Figure 11 - Three-antenna array used to generate pattern in Figure 10. This array uses 2-element versions of low-profile antennas. Antennas are oriented to minimize mutual coupling between horizontal loading wires.

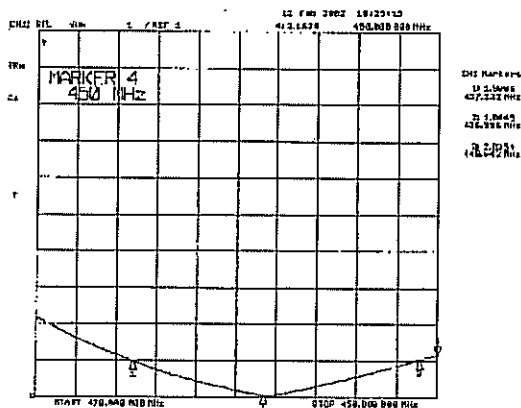


Figure 12. Measured VSWR of a 440 MHz low-profile antenna using 4 wire elements over copper ground plane.

PROTOTYPE TEST RESULTS

Several versions of this antenna have been constructed and tested by STAR-H Corporation, Lancaster and State College, PA. Prototypes have been built and tested at 1.3 GHz, 440 MHz, and 52 MHz using two and four-wire variants of the design. These antennas have served as both prototypes for communications antennas and as scale models for the broadcast version. All have performed as expected based on the computer modeling data. It is anticipated that this will also hold for the full-scale 1680 kHz prototype currently under construction in the Bristol, TN area. Figure 12 shows the VSWR versus frequency for a four-wire version of the low-profile antenna constructed over a circular quarter wavelength diameter copper ground plane, using 0.141" rigid coaxial line for the matching sections.

Comparison testing of the 52 MHz low-profile antenna, shown in Figure 13 on a radial wire ground screen, with a quarterwave monopole on the same ground screen in the same location showed no significant difference of the received signal power levels over path lengths of several miles of irregular terrain. Multipath signal variation adds uncertainty to any measurements in the VHF portion of the spectrum, but the observed data suggests that the performance of the low-profile at any test location was indistinguishable from that of the monopole, verifying the omnidirectional characteristic of the antenna. The VSWR versus frequency plot for this antenna is shown in Figure 14.

Full-scale prototype testing, consisting of comparison field measurements between a quarterwave monopole tower and a 4-wire low-profile antenna over a 120 radial ground screen is anticipated to begin in the September – October, 2002 time frame, with results anticipated shortly after. Ronald Rackley, of du Treil, Lundin, and Rackley,



Figure 13. 52 MHz 4-wire low-profile antenna with 120 quarterwave radial ground wires. Antenna is approximately 8 inches high.

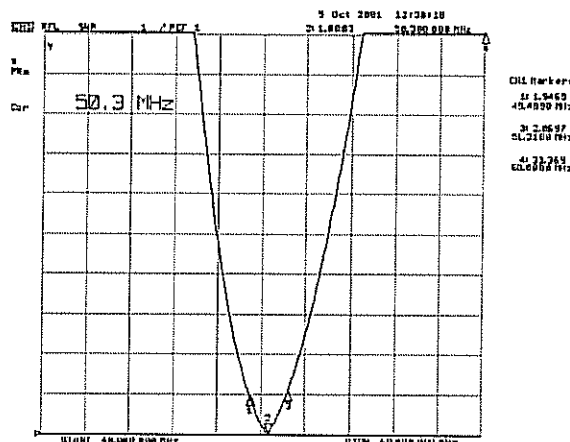


Figure 14. Measured VSWR of 52 MHz low-profile antenna shown in Figure 12. 2:1 bandwidth is from 49.48 to 51.21 MHz.

has been engaged to analyze the measurement data and prepare a report, which will be fully shared with the broadcasting and antenna engineering community upon completion. The report will also be filed with the US Federal Communications Commission in support of a request for review and approval of this antenna for use by AM broadcasters in the United States. Further experiments to implement the directional array concept will be considered in the near future. Parties interested in participating in future testing are urged to contact Mr. Jacobs of STAR-H Corporation.

CONCLUSION

We have presented a novel concept for a practical low-profile antenna that has application at MF frequencies for the broadcasting community. This antenna trades a slight reduction of radiated field intensity for a large reduction of height. Given the expense of locating suitable real estate and meeting land-use regulations and community requirements, the advantage of an antenna that does not require an unsightly tower structure or the expense of aviation obstruction lighting is clear. Even at the low end of the U.S. AM broadcasting band, the antenna height is only approximately 140 feet, compared with 444 feet for a quarterwave antenna. At this height, the antenna in most cases will not require FAA lighting or marking. Since it is constructed using common utility company overhead transmission line methods, the materials and construction of the antenna are reliable, inexpensive, and easy to implement in almost any location using local contractors. Wooden or reinforced concrete poles, or lightweight tower sections or steel utility monopoles can be used as the

vertical supports. Guying of the supports will provide a rugged antenna that can provide reliable service during storms and icing conditions. The antenna can be constructed rapidly, simplifying installation in remote areas, or as an expedient replacement for a fallen tower. It can also be operated in an array to create a directional pattern as required by FCC or other license conditions.

REFERENCES

- [1] V. Trainotti, "Short Medium Frequency AM Antennas", *IEEE Trans. on Broadcasting*, vol 47, no. 3, pp 263-284, September, 2001
- [2] A. Christman, R. Radcliff, R. Adler, J. K. Breakall, A. Resnick, "AM broadcast antennas with elevated radial ground systems", *IEEE Transactions on Broadcasting*, vol 34 no 1, pp 75-77, March 1988
- [3] J. K. Breakall, "Computer modeling of antennas using NEC and MININEC", Proceedings of the 32nd Midwest Symposium on Circuits and Systems, 1990 Page(s): 724 -726 vol.2.
- [4] J. K. Breakall, G. J. Burke, and E. K. Miller, "The Numerical Electromagnetics Code (NEC)," EMC Symposium and Exhibition, Zurich, Switzerland, 1985.
- [5] J. K. Breakall, J. S. Young, R. J. Bauerle, A. I. McDowell and T. A. Erdley, "Numerical Electromagnetics Code Optimization Design Software (NECOPT)," *10th Annual Review of Progress in Applied Computational Electromagnetics*, Naval Postgraduate School, Monterey, CA, 1994.

EXHIBIT B

Summary of Consulting Engineer's Report on Field Proof Testing
and Measured Antenna Efficiency

SEE PDF FILE ATTACHMENT:

KINSTAR_CONSULTING_ENGINEERS_REPORT.PDF

ENGINEERING EXHIBIT
STAR-H EXPERIMENTAL ANTENNA

1680 kHz 0.25 kW ND

January 8, 2003

ENGINEERING EXHIBIT
STAR-H EXPERIMENTAL ANTENNA

1680 kHz 0.25 kW ND

Table of Contents

	Engineering Statement
Figure 1	Summary of Measured Field Strength Data
Figure 2	Radial Average Ratios to Reference Antenna
Figure 3	Tabulation of Measured Field Strength Data
Figure 4	Graphs of Measured Field Strength Data For Quarter-Wave Reference Antenna
Figure 5	Graphs of Measured Field Strength Data For Star H Antenna – Trial A Configuration
Figure 6	Graphs of Measured Field Strength Data For Star H Antenna – Trial B Configuration
Figure 7	Tabulation of Environmental Data

ENGINEERING EXHIBIT
STAR-H EXPERIMENTAL ANTENNA
1680 KHz 0.25 KW ND

ENGINEERING STATEMENT

The engineering exhibit of which this statement is part has been prepared to present and show the analysis of the field strength measurements that were made to determine the effective efficiency of the low-profile mediumwave transmitting antenna – known as the Star-H antenna - that was constructed near the Bluff City, Tennessee headquarters of Kintronic Laboratories, Inc. for that purpose. The station operated on 1680 kilohertz during daytime hours, with a power input of 250 watts, pursuant to an experimental station authorization issued by the Federal Communications Commission.

Two configurations of Star-H antenna, differing with regard to the feedpoint arrangement, were tested. The trial A measurements were made with the Star-H antenna's elements fed through coaxial transmission lines of a length that was selected to provide the desired impedance transformation between their individual feedpoints and the common input point. The trial B measurements were made with the individual feedpoints connected together through a common conductor, without the coaxial cables between the common input point and the individual elements. Details regarding both configurations are in the possession of Kintronic Laboratories, Inc.

In order to form a basis for analyzing the Star-H antenna's effective efficiency, a 146-foot base-fed, series-excited tower was first constructed at the site and a conventional 120-

wire, 146-foot radius radial ground system was installed around it to serve as the reference antenna. Thus, the reference measurements were made with a conventional tower, 90 electrical degrees in height, with a standard 120-radial, quarter-wave ground system.

The field strength measurements that were made on the reference antenna were analyzed in accordance with the "best fit" method outlined in Section 73.186 of the Federal Communications Commission's Rules, using Graph 20 of Section 73.184 to determine the ground conductivity values used in the analysis. The effective efficiency shown on Figure 8 of Section 73.190 - 306 mV/M at one kilometer, unattenuated, for one kilowatt - was assumed for the reference antenna, giving an effective efficiency of 153 mV/M for the 250 watt power that was employed for the tests. As can be seen from the field strength measurement graphs contained herein, that assumption proved to be appropriate.

After the reference antenna field strength measurements were complete, the 146-foot tower was removed and the Star-H antenna was constructed over the same ground system. Field strength measurements were then made for both its trial A and trial B versions, so that their effective efficiencies could be determined by direct comparison with the reference antenna's measured field strengths.

The reference antenna measurements were made in October and the Star-H antenna measurements were made in November, when the temperatures were generally 20 – 30 degrees Fahrenheit lower than they had been at the time of the reference antenna measurements. A tabulation showing data related to the environmental conditions on each of the days that field strength measurements were made is included herein. No ground frost or freezing conditions were present during any of the test operation and, as can be seen from the field strength measurements contained herein, the ground conductivities remained essentially the same throughout the measurement period.

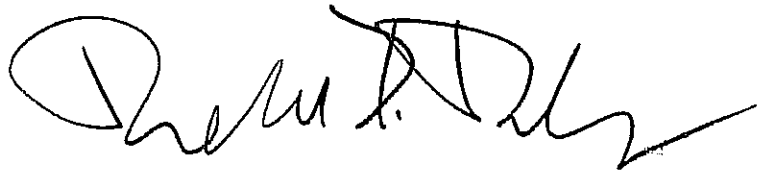
It was noted that the Star-H antenna field strength measurements made several kilometers and beyond from the site appeared to be slightly higher relative to the corresponding field strengths measured for the reference antenna than the closer measurements, indicating a small increase in effective ground conductivity. Such a conductivity change could easily be due to environmental factors related the difference in temperature at the times the three sets of measurements were made, but would be almost insignificant compared to the “winter-summer effect” that is sometimes noted in areas where the ground is frozen for part of the year. To minimize the effect of any conductivity change that might have occurred, only ratios for points within 3.0 kilometers of the site were included in the radial average ratios used to determine the effective efficiency of the Star-H antenna configurations. As the ground conductivities that were used in the graphical analysis of the reference antenna field strength data also provided a good fit for the Star-H antenna configurations’ field strength data - as can be seen from a radial-by-radial comparison of the graphs for the three sets of measurements – they produced no significant ambiguity with the analysis procedure employed herein.

The power was maintained at the 250 watt level while measurements were being made, using the direct method of power determination that is described in Section 73.51 of the Federal Communications Commission’s Rules. Details regarding the antenna input resistance and current measurements that were employed to determine the antenna input power during the tests are in the possession of Kintronic Laboratories, Inc.

The field strength measurements contained herein were made by Mr. Donald Crain, a radio engineer with experience in making such measurements that dates back more than 30 years, working under the direction of the undersigned. He used a Potomac Instruments type FIM-41 field strength meter, serial number 1955, which was most recently calibrated by its manufacturer on January 27, 1997. The meter has more recently been compared with other meters of later factory calibration and found to be in agreement with them. The measurement locations were chosen at distances conforming as closely to the recommendations of Section 73.186 of the Federal Communications Commission’s Rules as practicable – considering the

physical characteristics of the terrain surrounding the transmitter site - using 7 ½ minute topographic maps with the assistance of a GPS receiver that was programmed to have its reference point at the transmitter site. Maps showing the measurement locations are in the possession of Kintronic Laboratories, Inc.

It is clear from the measurement data contained herein that the two configurations of the Star-H antenna that were tested both provide effective field levels approaching that of a conventional quarter-wave antenna. Each was found to have a radiation efficiency well above the minimum values required by the Federal Communications Commission's Rules for class B, C, and D AM radio stations, which are 282 mV/M, 241 mV/M, and 282 mV/M at one kilometer, respectively.

A handwritten signature in black ink, appearing to read 'Ronald D. Rackley', with a long horizontal flourish extending to the right.

Ronald D. Rackley, P.E.

January 8, 2003

STAR-H EXPERIMENTAL ANTENNA
1680 kHz 0.25 kW ND

Unattenuated Field Strength at 1.0 Kilometer

Antenna	Overall Average	Measured 0.25 kW	Calculated 1.0 kW
Reference	-	153 mV/m	306 mV/m*
Trial A	0.994	152 mV/m	304 mV/m
Trial B	0.978	150 mV/m	300 mV/m

* - Agrees with Figure 8 of Section 73.190
of the Federal Communications Commission's Rules

STAR-H EXPERIMENTAL ANTENNA
1680 kHz 0.25 kW ND

Radial Average Ratios to Reference Antenna

Radial (deg. T.N.)	Trial A Average Ratio	Trial B Average Ratio
30	0.981	0.954
90	1.013	0.972
150	0.998	1.027
210	0.990	0.960
270	0.994	0.976
330	0.986	0.980
Overall Average:	0.994	0.978

30 Degree True Radial

Point Desig.	Distance (km)	Reference		Trial A		Ratio (A/Ref)
		Date & Time (local)	Field Strength (mV/m)	Date & Time (local)	Field Strength (mV/m)	
		10/3/2002		11/7/2002		
1	0.25	1022	630	1640	595	0.944
2	0.36	1025	400	1638	385	0.963
		10/8/2002		11/8/2002		
3	0.58	1509	231	1151	225	0.974
4	0.69	1513	188	1154	175	0.931
5	0.80	1432	195	1224	188	0.964
6	1.07	1436	140	1205	138	0.986
7	1.23	1438	115	1207	110	0.957
8	1.33	1440	108	1208	108	1.000
9	1.49	1446	84.0	1210	82.0	0.976
10	1.62	1443	74.0	1212	71.0	0.959
11	2.02	1453	52.0	1228	51.0	0.981
12	2.14	1456	46.0	1231	50.0	1.087
13	2.59	1502	37.5	1233	38.0	1.013
14	2.80	1504	30.0	1234	30.0	1.000
		10/1/2002		11/6/2002		
15	3.12	924	35.0	1344	33.5	
16	3.63	946	25.1	1348	24.5	
17	6.04	931	11.8	1353	11.5	
18	6.92	956	4.10	1356	4.00	
19	8.06	1005	8.40	1408	8.40	
20	9.93	1016	2.65	1438	2.91	
21	10.50	1021	3.25	1441	3.45	
22	11.40	1026	2.42	1446	2.61	
23	12.40	1030	2.25	1449	2.40	
24	16.00	1046	0.425	1509	0.465	
25	18.60	1039	0.435	1505	0.485	
Average Ratio						0.981

30 Degree True Radial

Point Desig.	Distance (km)	Reference		Trial B		Ratio (B/Ref)
		Date & Time (local)	Field Strength (mV/m)	Date & Time (local)	Field Strength (mV/m)	
		10/3/2002		11/22/2002		
1	0.25	1022	630	1216	600	0.952
2	0.36	1025	400	1219	365	0.913
		10/8/2002				
3	0.58	1509	231	1229	210	0.909
4	0.69	1513	188	1232	170	0.904
5	0.80	1432	195	1250	180	0.923
6	1.07	1436	140	1238	135	0.964
7	1.23	1438	115	1240	109	0.948
8	1.33	1440	108	1241	105	0.972
9	1.49	1446	84.0	1243	80.0	0.952
10	1.62	1443	74.0	1244	69.0	0.932
11	2.02	1453	52.0	1257	49.0	0.942
12	2.14	1456	46.0	1259	50.0	1.087
13	2.59	1502	37.5	1302	35.0	0.933
14	2.80	1504	30.0	1305	30.5	1.017
		10/1/2002		11/20/2002		
15	3.12	924	35.0	1158	32.5	
16	3.63	946	25.1	1201	24.3	
17	6.04	931	11.8	1206	11.3	
18	6.92	956	4.10	1559	4.20	
19	8.06	1005	8.40	1602	8.60	
				11/21/2002		
20	9.93	1016	2.65	1114	2.95	
21	10.50	1021	3.25	1110	3.35	
22	11.40	1026	2.42	1057	2.50	
23	12.40	1030	2.25	1104	2.35	
24	16.00	1046	0.425	1044	0.455	
25	18.60	1039	0.435	1038	0.480	
Average Ratio						0.954

90 Degree True Radial

Point Desig.	Distance (km)	Reference		Trial A		Ratio (A/Ref)
		Date & Time (local)	Field Strength (mV/m)	Date & Time (local)	Field Strength (mV/m)	
		10/3/2002		11/7/2002		
1	0.25	1426	530	1412	531	1.002
		10/9/2002				
2	0.35	1037	395	1415	390	0.987
		10/03/2002				
3	0.45	1421	330	1416	330	1.000
		10/9/2002				
4	0.55	1043	242	1420	239	0.988
5	0.65	950	215	1503	210	0.977
6	0.75	1021	255	1509	250	0.980
7	0.88	1004	131	1513	129	0.985
		10/8/2002		11/8/2002		
8	1.73	1553	13.3	907	15.0	1.132
		10/2/2002		11/6/2002		
9	2.60	934	12.0	1338	12.8	1.067
		10/8/2002				
10	3.02	1612	11.5	1340	12.1	
11	5.32	953	5.95	1328	6.15	
12	6.77	1009	3.30	1323	3.59	
13	7.82	1015	2.35	1319	2.62	
14	9.22	1033	2.01	1311	2.11	
15	9.49	1022	1.68	1315	1.71	
16	10.50	1057	1.70	1239	1.95	
17	12.20	1048	0.430	1244	0.480	
18	14.30	1117	0.340	1229	0.375	
19	15.00	1120	0.330	1225	0.385	
20	16.90	1131	0.225	1215	0.260	
Average Ratio						1.013

90 Degree True Radial

Point Desig.	Distance (km)	Reference		Trial B		Ratio (B/Ref)
		Date & Time (local)	Field Strength (mV/m)	Date & Time (local)	Field Strength (mV/m)	
		10/3/2002		11/22/2002		
1	0.25	1426	530	1047	495	0.934
		10/9/2002				
2	0.35	1037	395	1049	375	0.949
		10/3/2002				
3	0.45	1421	330	1051	305	0.924
		10/9/2002				
4	0.55	1043	242	1055	225	0.930
5	0.65	950	215	1011	210	0.977
6	0.75	1021	255	1030	240	0.941
7	0.88	1004	131	1035	125	0.954
		10/8/2002				
8	1.73	1553	13.3	942	14.0	1.057
		10/2/2002				
9	2.60	934	12.0	953	13.0	1.083
		10/8/2002		11/20/2002		
10	3.02	1612	11.5	1610	12.3	
11	5.32	953	5.95	1624	6.10	
12	6.77	1009	3.30	1628	3.65	
13	7.82	1015	2.35	1631	2.65	
				11/21/2002		
14	9.22	1033	2.01	1140	2.10	
15	9.49	1022	1.68	1138	1.69	
16	10.50	1057	1.70	1153	1.85	
17	12.20	1048	0.430	1148	0.470	
18	14.30	1117	0.340	1214	0.360	
19	15.00	1120	0.330	1218	0.395	
20	16.90	1131	0.225	1227	0.265	
Average Ratio						0.972

150 Degree True Radial

Point Desig.	Distance (km)	Reference		Trial A		Ratio (A/Ref)
		Date & Time (local)	Field Strength (mV/m)	Date & Time (local)	Field Strength (mV/m)	
		10/9/2002		11/2/2002		
1	0.25	1049	560	1558	525	0.938
2	0.35	1052	350	1601	340	0.971
3	0.45	1054	285	1604	290	1.018
4	0.55	1057	228	1606	219	0.961
5	0.65	1059	205	1607	202	0.985
		10/8/2002				
6	1.13	1405	84.0	1436	86.0	1.024
7	1.22	1420	54.0	1443	52.0	0.963
				11/8/2002		
8	1.67	1455	45.0	946	46.0	1.022
9	1.88	1451	38.0	942	38.5	1.013
10	2.97	1506	9.20	935	10.0	1.087
		10/2/2002		11/6/2002		
11	4.00	1306	4.30	948	4.30	
12	4.18	1313	5.10	954	5.60	
13	4.67	1318	5.00	1000	5.90	
14	5.57	1328	3.20	1005	3.25	
15	8.76	1348	1.29	1019	1.35	
16	9.45	1346	1.60	1022	1.75	
17	10.20	1352	1.01	1024	1.11	
18	11.00	1411	0.630	1031	0.680	
19	12.00	1358	0.460	1041	0.510	
Average Ratio						0.998

150 Degree True Radial

Point Desig.	Distance (km)	Reference		Trial B		Ratio (A/Ref)
		Date & Time (local)	Field Strength (mV/m)	Date & Time (local)	Field Strength (mV/m)	
		10/9/2002		11/22/2002		
1	0.25	1049	560	1131	550	0.982
2	0.35	1052	350	1134	325	0.929
3	0.45	1054	285	1138	290	1.018
4	0.55	1057	228	1140	225	0.987
5	0.65	1059	205	1143	205	1.000
		10/8/2002				
6	1.13	1405	84.0	1111	88.0	1.048
7	1.22	1420	54.0	1117	51.0	0.944
8	1.67	1455	45.0	910	47.5	1.056
9	1.88	1451	38.0	905	40.0	1.053
10	2.97	1506	9.20	919	11.5	1.250
		10/2/2002		11/20/2002		
11	4.00	1306	4.30	1649	4.45	
12	4.18	1313	5.10	1647	5.80	
13	4.67	1318	5.00	1644	6.00	
14	5.57	1328	3.20	1639	3.40	
				11/21/2002		
15	8.76	1348	1.29	1445	1.35	
16	9.45	1346	1.60	1448	1.78	
17	10.20	1352	1.01	1507	1.15	
18	11.00	1411	0.630	1455	0.690	
19	12.00	1358	0.460	1459	0.500	
Average Ratio						1.027

210 Degree True Radial

Point Desig.	Distance (km)	Reference		Trial A		Ratio (A/Ref)
		Date & Time (local)	Field Strength (mV/m)	Date & Time (local)	Field Strength (mV/m)	
		10/9/2002		11/8/2002		
1	0.25	1316	620	1115	600	0.968
2	0.47	1311	295	1120	285	0.966
3	0.80	1322	80.0	1139	75.0	0.938
				11/7/2002		
4	1.01	1334	118	1616	115	0.975
5	1.11	1332	90.0	1619	88.0	0.978
6	1.21	1330	97.0	1622	93.0	0.959
7	1.31	1327	92.0	1624	95.0	1.033
				11/8/2002		
8	1.59	1338	67.0	1125	70.0	1.045
9	2.36	1350	26.0	1133	27.0	1.038
10	2.83	1355	22.8	1130	22.5	0.987
		10/2/2002		11/7/2002		
11	2.99	1617	15.1	906	15.1	1.000
12	4.39	1628	8.40	914	9.20	
13	9.81	1529	0.720	925	0.840	
14	10.70	1524	0.540	928	0.620	
15	11.30	1429	1.20	935	1.32	
16	11.60	1516	0.880	938	0.980	
17	13.40	1452	0.490	944	0.600	
18	14.70	1458	0.390	950	0.460	
19	16.90	1504	0.600	955	0.670	
Average Ratio						0.990

210 Degree True Radial

Point Desig.	Distance (km)	Reference		Trial B		Ratio (B/Ref)
		Date & Time (local)	Field Strength (mV/m)	Date & Time (local)	Field Strength (mV/m)	
		10/9/2002		11/22/2002		
1	0.25	1316	620	840	590	0.952
2	0.47	1311	295	8942	275	0.932
				11/21/2002		
3	0.80	1322	80.0	1547	70.0	0.875
4	1.01	1334	118	1542	100	0.847
5	1.11	1332	90.0	1540	85.0	0.944
6	1.21	1330	97.0	1538	95.0	0.979
7	1.31	1327	92.0	1536	90.0	0.978
				11/20/2002		
8	1.59	1338	67.0	1708	71.0	1.060
				11/21/2002		
9	2.36	1350	26.0	1529	26.0	1.000
10	2.83	1355	22.8	1526	22.1	0.969
		10/2/2002		11/20/2002		
11	2.99	1617	15.1	1655	15.5	1.026
12	4.39	1628	8.40	1703	9.30	
				11/21/2002		
13	9.81	1529	0.720	1355	0.820	
14	10.70	1524	0.540	1400	0.600	
15	11.30	1429	1.20	1405	1.30	
16	11.60	1516	0.880	1407	0.940	
17	13.40	1452	0.490	1413	0.570	
18	14.70	1458	0.390	1427	0.440	
19	16.90	1504	0.600	1421	0.650	
Average Ratio						0.960

270 Degree True Radial

Point Desig.	Distance (km)	Reference		Trial A		Ratio (A/Ref)
		Date & Time (local)	Field Strength (mV/m)	Date & Time (local)	Field Strength (mV/m)	
		10/9/2002		11/8/2002		
1	0.25	1109	660	958	620	0.939
2	0.35	1112	440	1009	440	1.000
3	0.45	1113	345	1010	350	1.014
4	0.54	1116	305	1012	300	0.984
5	0.66	1132	220	1021	220	1.000
6	0.77	1139	168	1027	168	1.000
7	0.88	1141	150	1029	148	0.987
		10/03/2002				
8	1.00	1106	158	1032	155	0.981
9	1.20	1117	121	1035	121	1.000
10	1.40	1121	82.0	1038	83.0	1.012
		10/9/2002		11/6/2002		
11	2.24	1201	35.5	1110	35.5	1.000
		10/1/2002				
12	2.42	1541	33.0	1107	33.0	1.000
13	2.63	1545	24.5	1115	24.5	1.000
				11/7/2002		
14	3.70	1526	14.3	1131	14.75	
15	4.18	1518	10.5	1126	11.50	
16	4.92	1607	12.1	1136	12.75	
17	5.34	1613	12.3	1140	12.25	
18	6.15	1617	7.80	1222	8.40	
19	7.47	1626	3.05	1228	3.55	
20	8.76	1631	1.85	1234	2.15	
21	9.86	1640	1.10	1238	1.25	
22	10.80	1647	0.780	1243	0.950	
23	13.60	1655	1.00	1251	1.20	
24	14.30	1659	0.960	1257	1.18	
Average Ratio						0.994

270 Degree True Radial

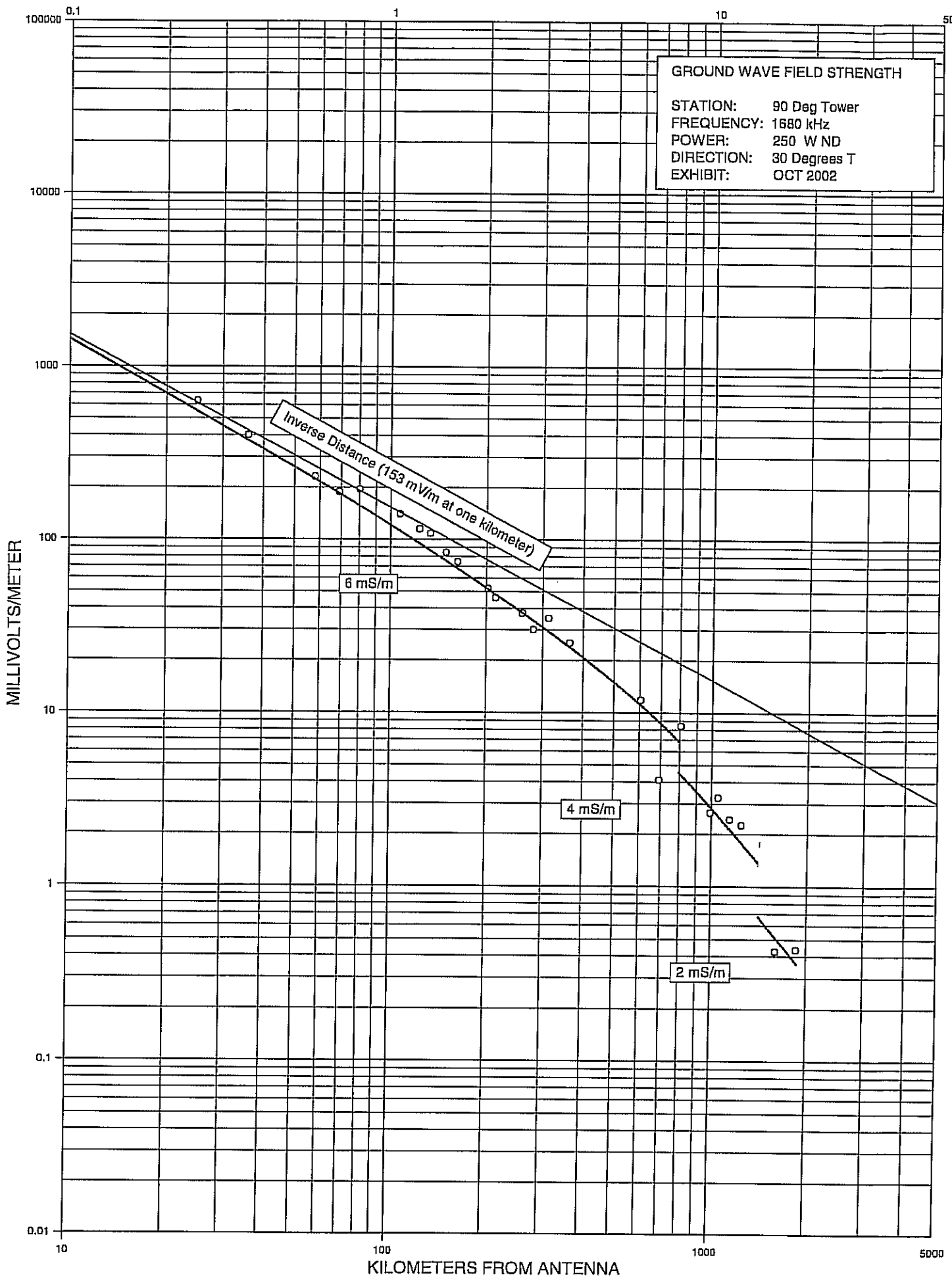
Point Desig.	Distance (km)	Reference		Trial B		Ratio (B/Ref)
		Date & Time (local)	Field Strength (mV/m)	Date & Time (local)	Field Strength (mV/m)	
		10/9/2002		11/12/2002		
1	0.25	1109	660	1150	610	0.924
2	0.35	1112	440	1153	435	0.989
3	0.45	1113	345	1155	330	0.957
4	0.54	1116	305	1157	310	1.016
5	0.66	1132	220	1207	225	1.023
				11/21/2002		
6	0.77	1139	168	1646	165	0.982
7	0.88	1141	150	1644	145	0.967
		10/03/2002				
8	1.00	1106	158	1614	150	0.949
9	1.20	1117	121	1609	111	0.917
10	1.40	1121	82.0	1605	79.0	0.963
		10/9/2002		11/20/2002		
11	2.24	1201	35.5	1227	35.5	1.000
		10/1/2002				
12	2.42	1541	33.0	1230	32.5	0.985
13	2.63	1545	24.5	1234	24.8	1.010
14	3.70	1526	14.3	1244	13.5	
15	4.18	1518	10.5	1248	11.9	
16	4.92	1607	12.1	1255	12.5	
17	5.34	1613	12.3	1335	12.5	
18	6.15	1617	7.80	1339	8.40	
19	7.47	1626	3.05	1344	3.60	
20	8.76	1631	1.85	1358	2.30	
21	9.86	1640	1.10	1354	1.20	
22	10.80	1647	0.780	1403	0.950	
23	13.60	1655	1.00	1411	1.25	
24	14.30	1659	0.960	1415	1.18	
Average Ratio						0.976

330 Degree True Radial

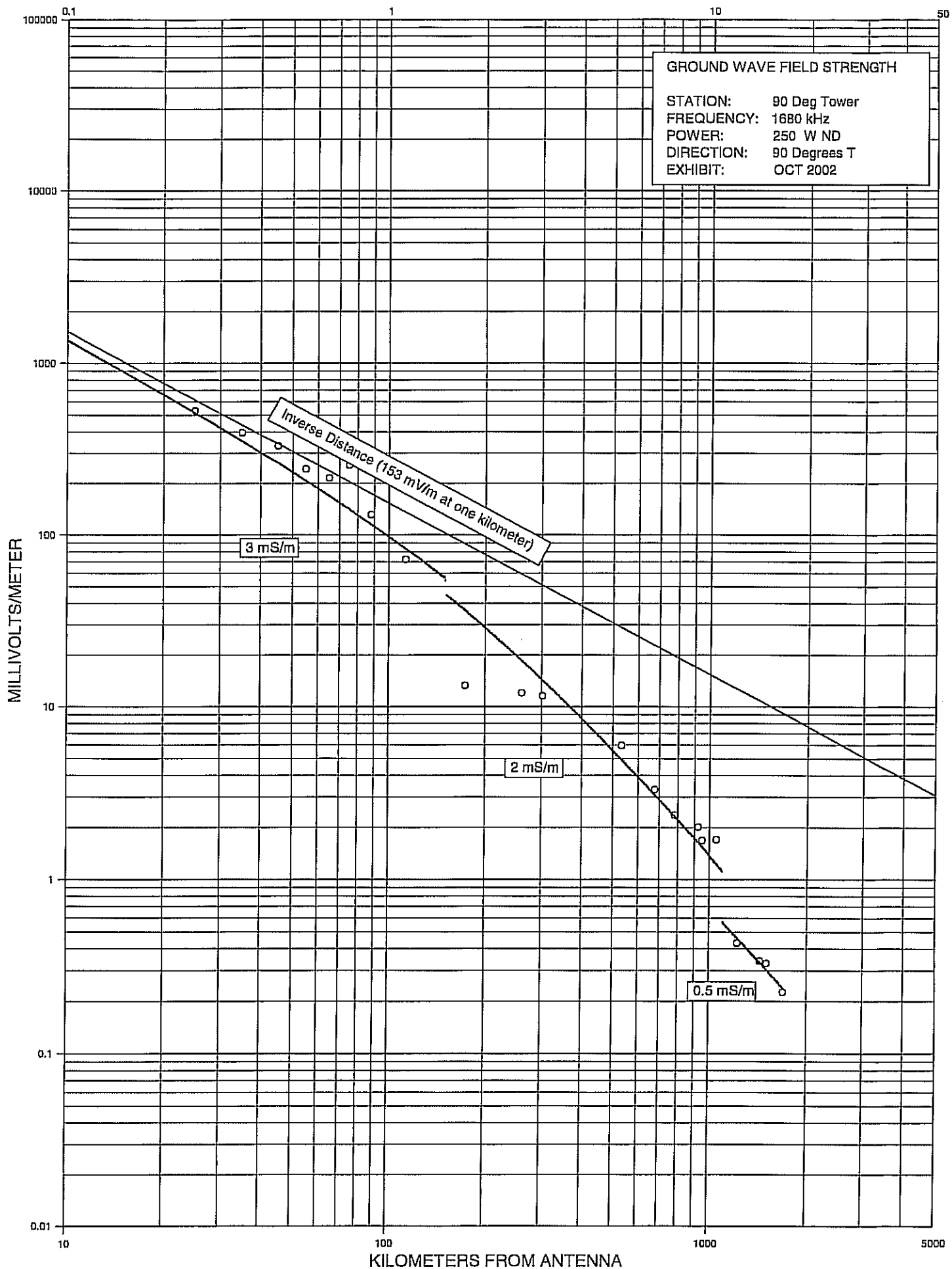
Point Desig.	Distance (km)	Reference		Trial A		Ratio (A/Ref)
		Date & Time (local)	Field Strength (mV/m)	Date & Time (local)	Field Strength (mV/m)	
		10/3/2002		11/2/2002		
1	0.25	1018	605	1631	590	0.975
2	0.45	1015	292	1633	275	0.942
				11/8/2002		
3	0.65	1041	178	1043	178	1.000
4	0.85	1046	180	1046	181	1.006
5	1.05	1050	135	1048	130	0.963
6	1.15	1052	125	1049	121	0.968
7	1.33	1056	78.0	1102	79.0	1.013
8	1.53	1009	70.0	1052	68.0	0.971
9	1.73	1006	47.0	1054	48.0	1.021
10	1.93	1004	37.0	1056	36.5	0.986
11	2.13	1001	33.5	1058	33.0	0.985
12	2.33	957	40.0	1059	40.0	1.000
		10/1/2002		11/6/2002		
13	2.98	1435	26.1	1636	25.9	0.992
14	3.55	1428	19.3	1631	19.0	
15	4.55	1413	10.3	1623	11.0	
16	5.49	1419	6.80	1615	7.20	
17	6.09	1404	6.40	1612	7.00	
18	6.92	1358	5.40	1607	6.40	
19	7.98	1350	3.25	1601	3.85	
20	9.71	1343	1.65	1557	1.89	
21	11.00	1301	0.700	1530	0.880	
22	12.70	1308	0.300	1549	0.315	
23	13.30	1316	0.205	1547	0.240	
24	15.00	1324	0.215	1540	0.245	
Average Ratio						0.986

330 Degree True Radial

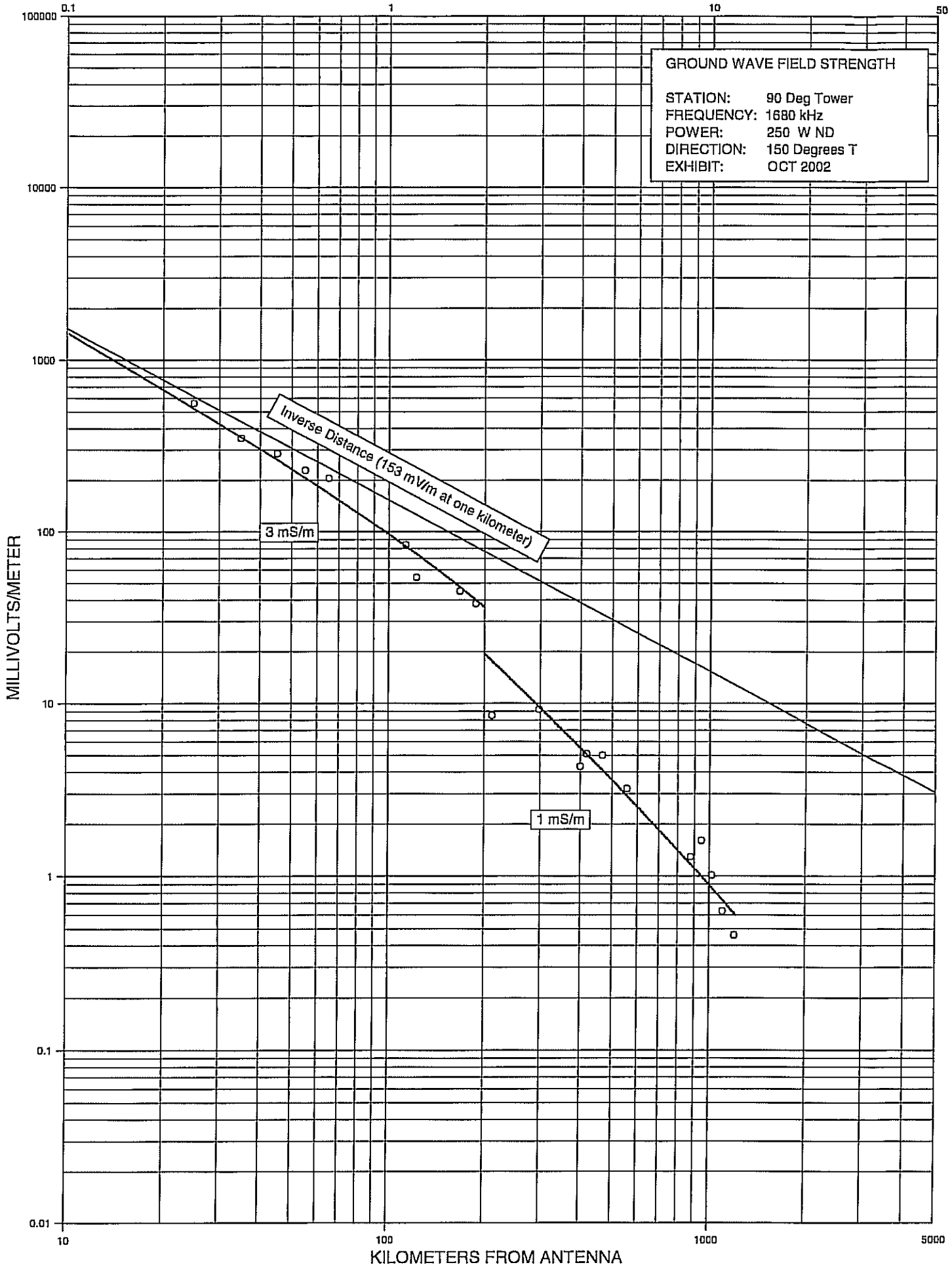
Point Desig.	Distance (km)	Reference		Trial B		Ratio (B/Ref)
		Date & Time (local)	Field Strength (mV/m)	Date & Time (local)	Field Strength (mV/m)	
		10/3/2002		11/21/2002		
1	0.25	1018	605	1657	590	0.975
2	0.45	1015	292	1700	280	0.959
3	0.65	1041	178	1638	181	1.017
4	0.85	1046	180	1636	175	0.972
5	1.05	1050	135	1633	135	1.000
6	1.15	1052	125	1631	120	0.960
7	1.33	1056	78.0	1617	75.0	0.962
8	1.53	1009	70.0	1619	67.0	0.957
9	1.73	1006	47.0	1621	46.5	0.989
10	1.93	1004	37.0	1622	36.5	0.986
11	2.13	1001	33.5	1624	32.0	0.955
12	2.33	957	40.0	1626	39.5	0.988
		10/1/2002		11/20/2002		
13	2.98	1435	26.1	1218	26.5	1.015
14	3.55	1428	19.3	1548	19.5	
15	4.55	1413	10.3	1533	10.5	
16	5.49	1419	6.80	1538	7.30	
				11/21/2002		
17	6.09	1404	6.40	923	7.10	
18	6.92	1358	5.40	907	6.50	
19	7.98	1350	3.25	932	3.90	
20	9.71	1343	1.65	937	1.80	
21	11.00	1301	0.700	942	0.890	
22	12.70	1308	0.300	1009	0.295	
23	13.30	1316	0.205	951	0.250	
24	15.00	1324	0.215	959	0.260	
Average Ratio						0.980

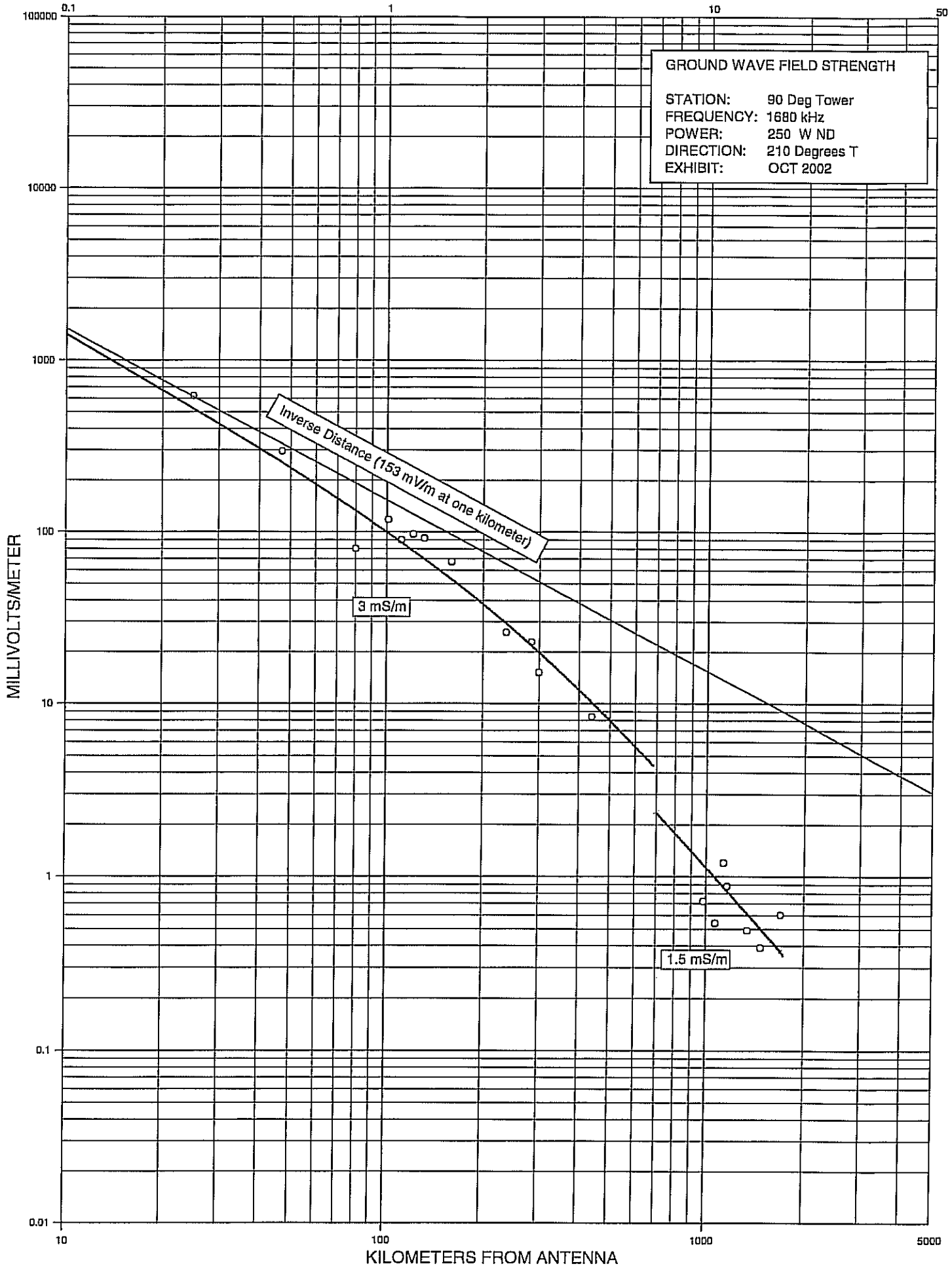


KILOMETERS FROM ANTENNA

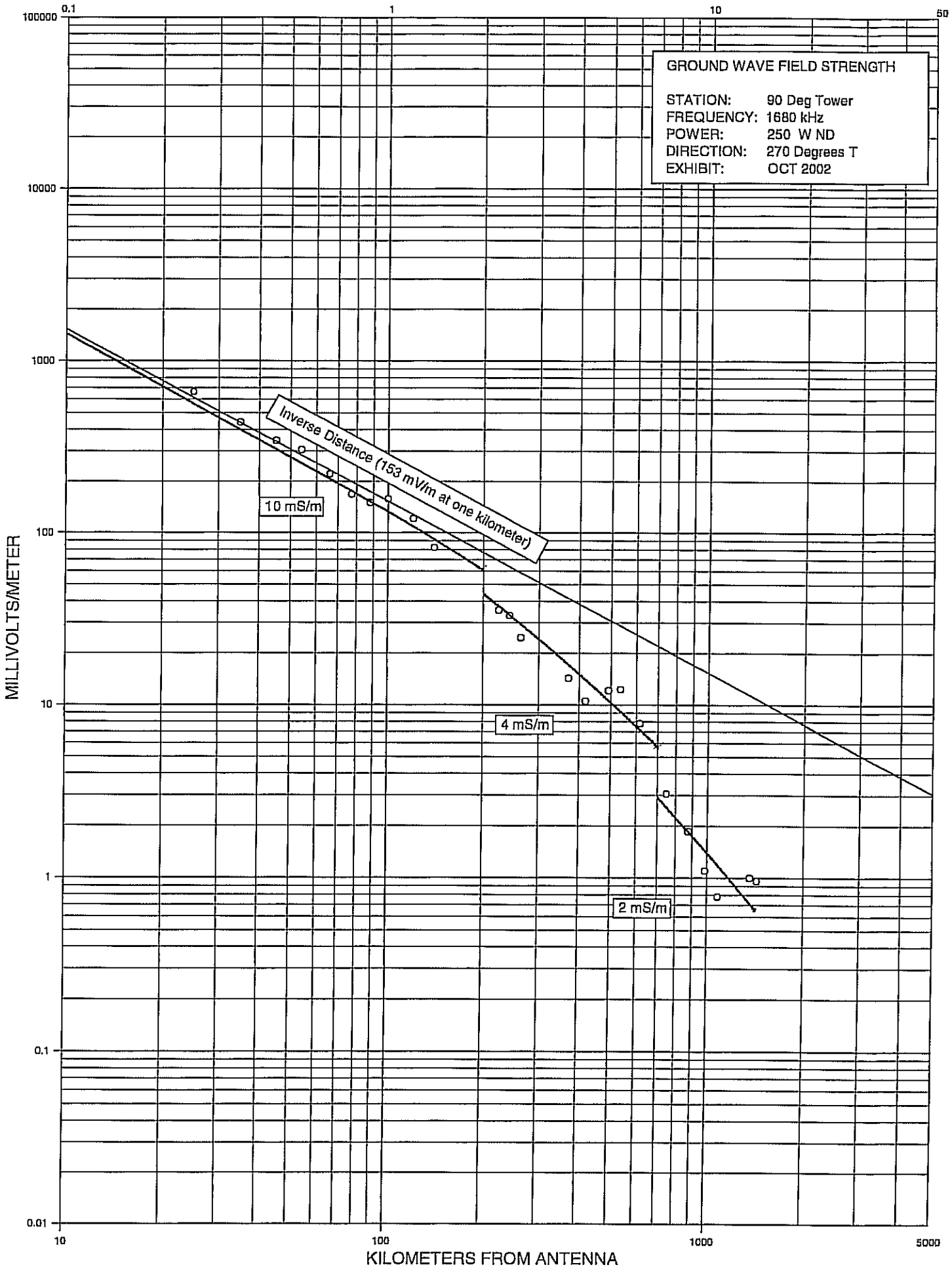


KILOMETERS FROM ANTENNA

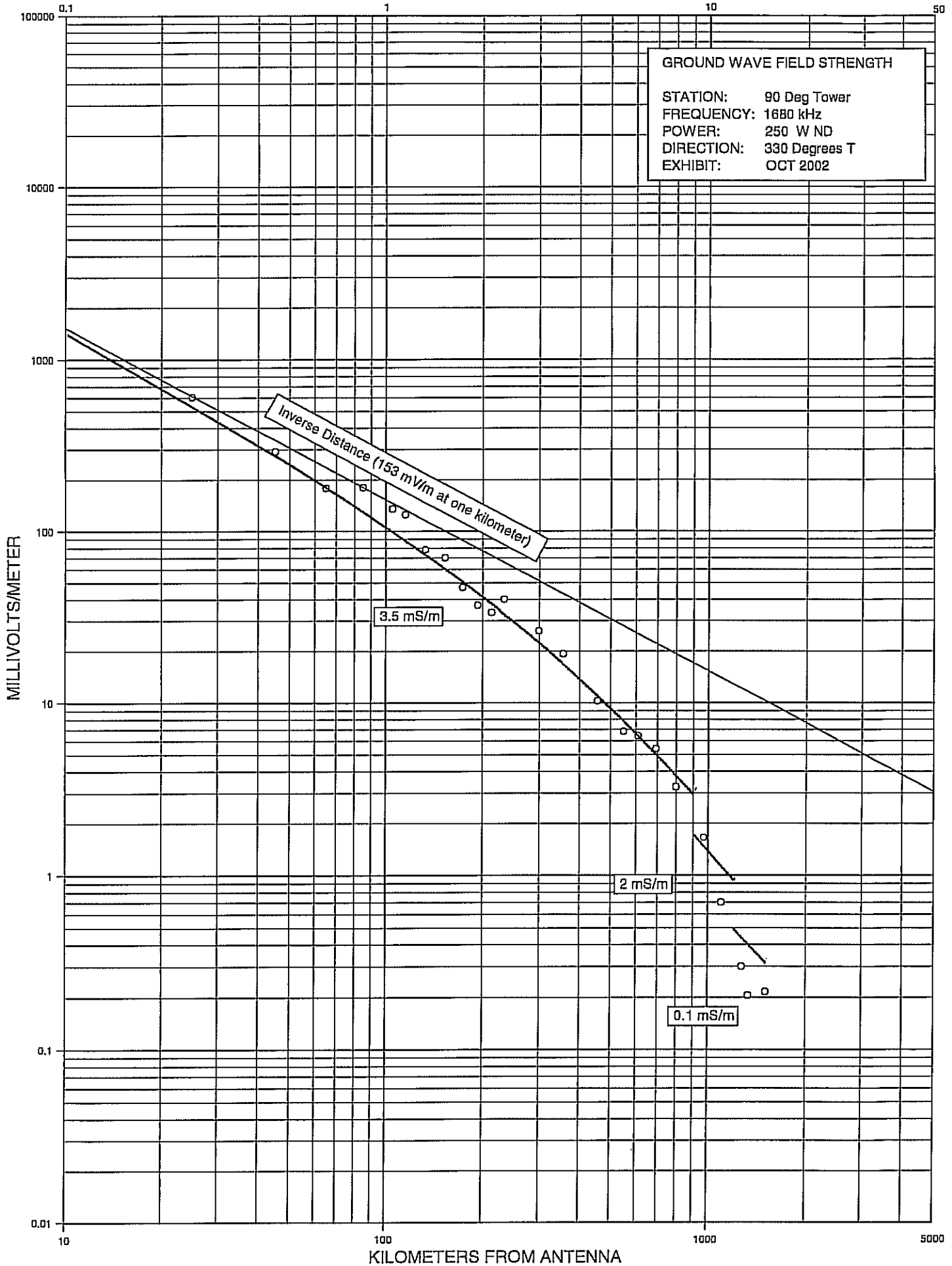




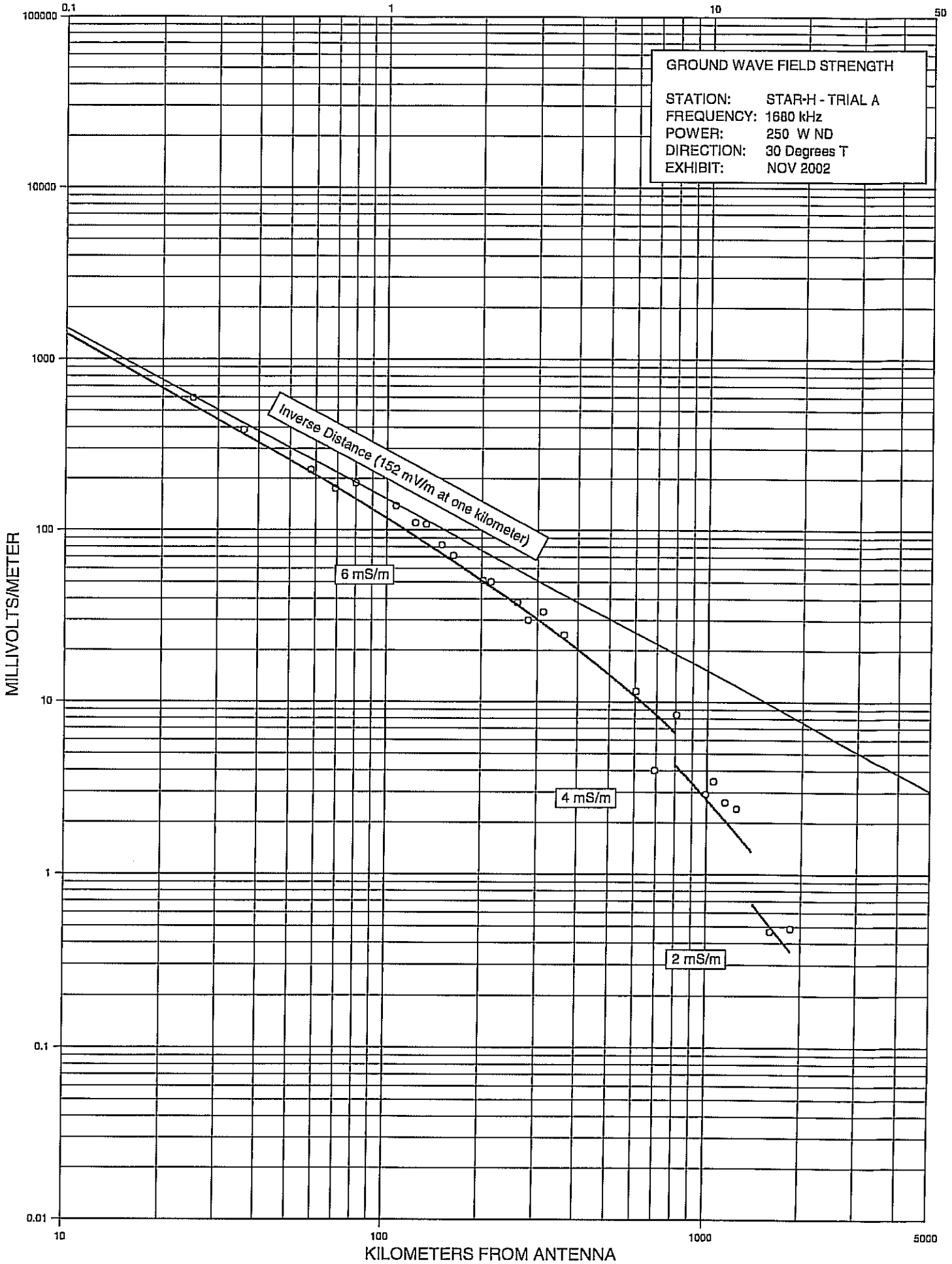
KILOMETERS FROM ANTENNA



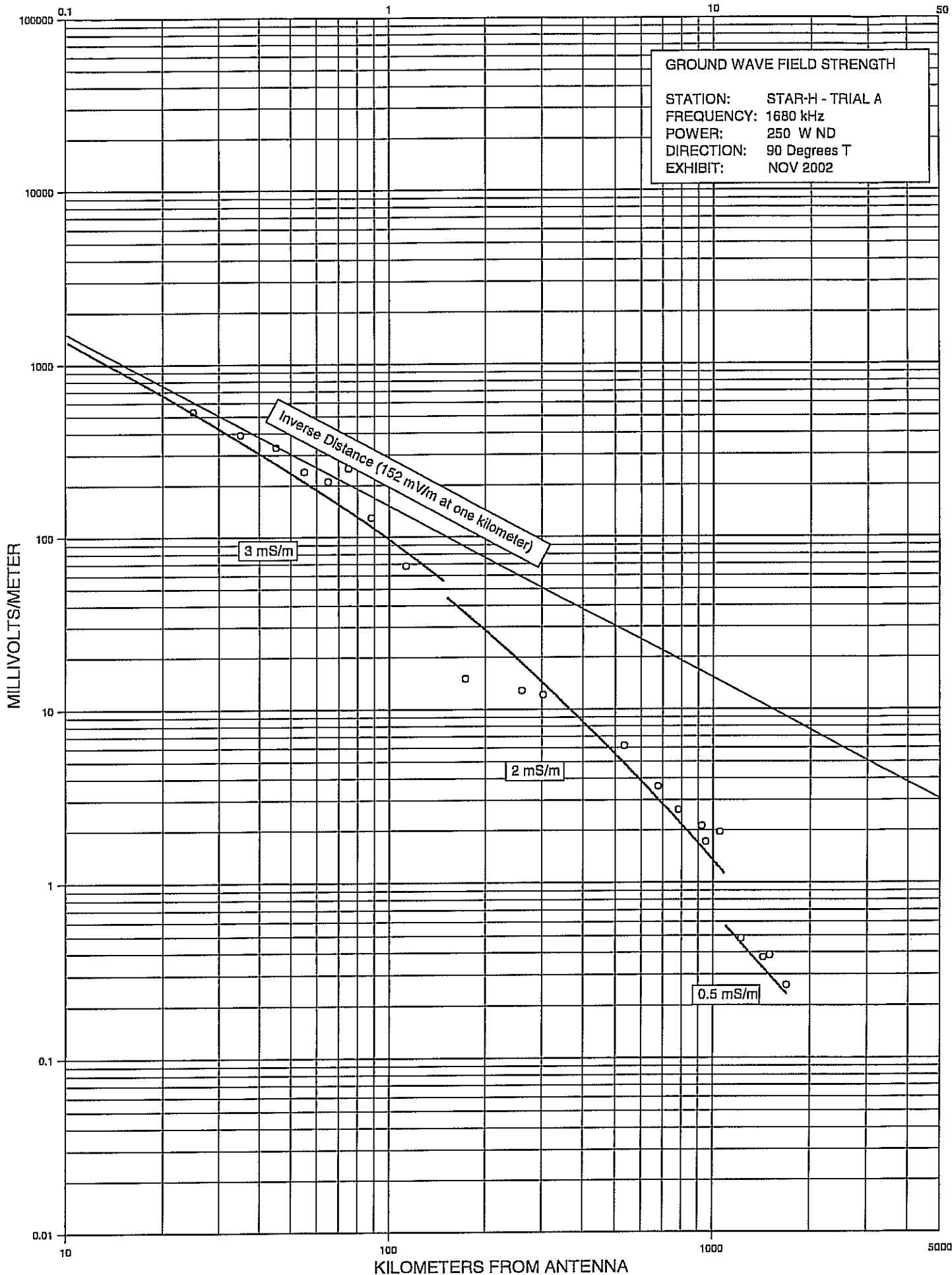
KILOMETERS FROM ANTENNA

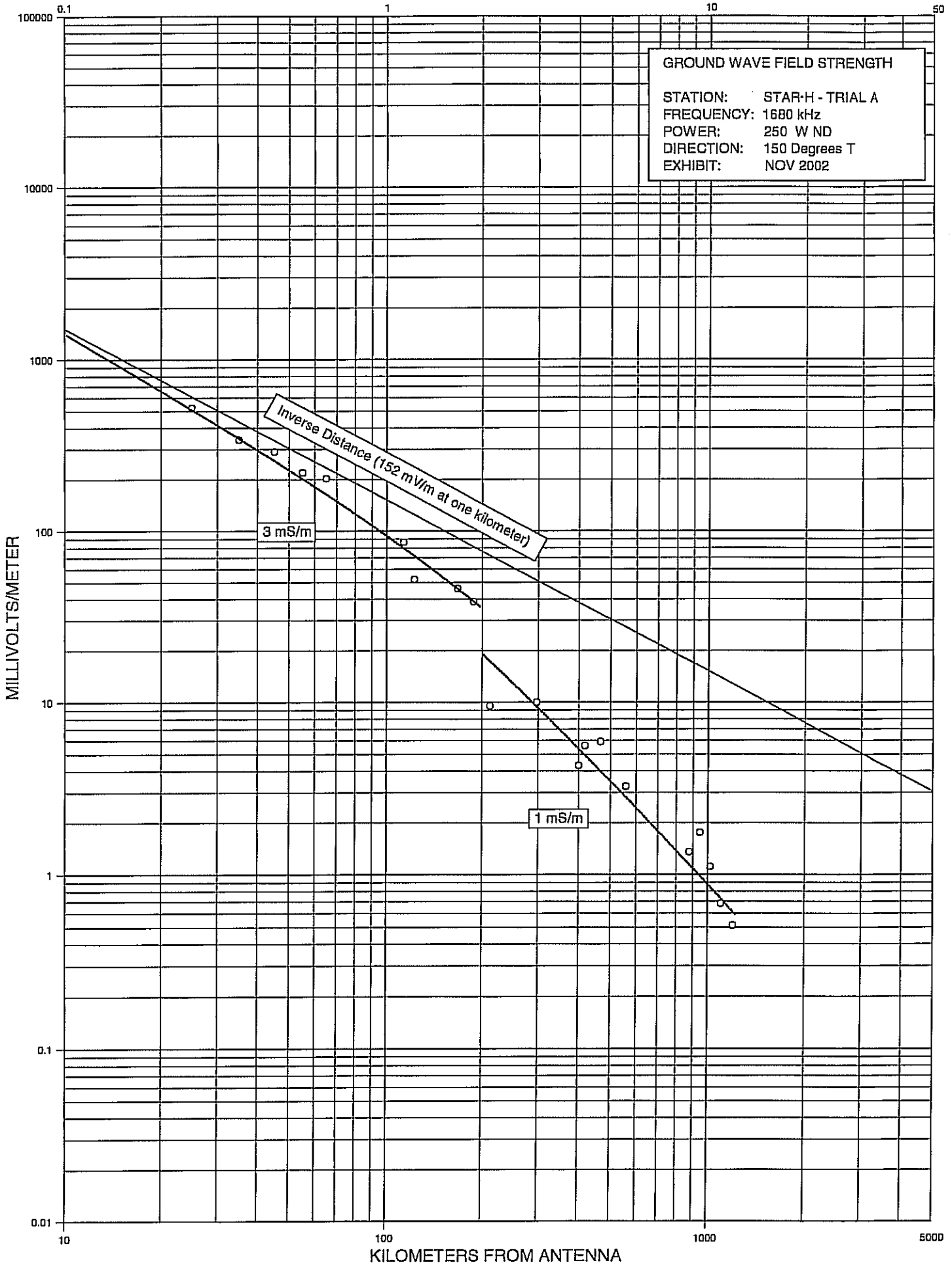


KILOMETERS FROM ANTENNA

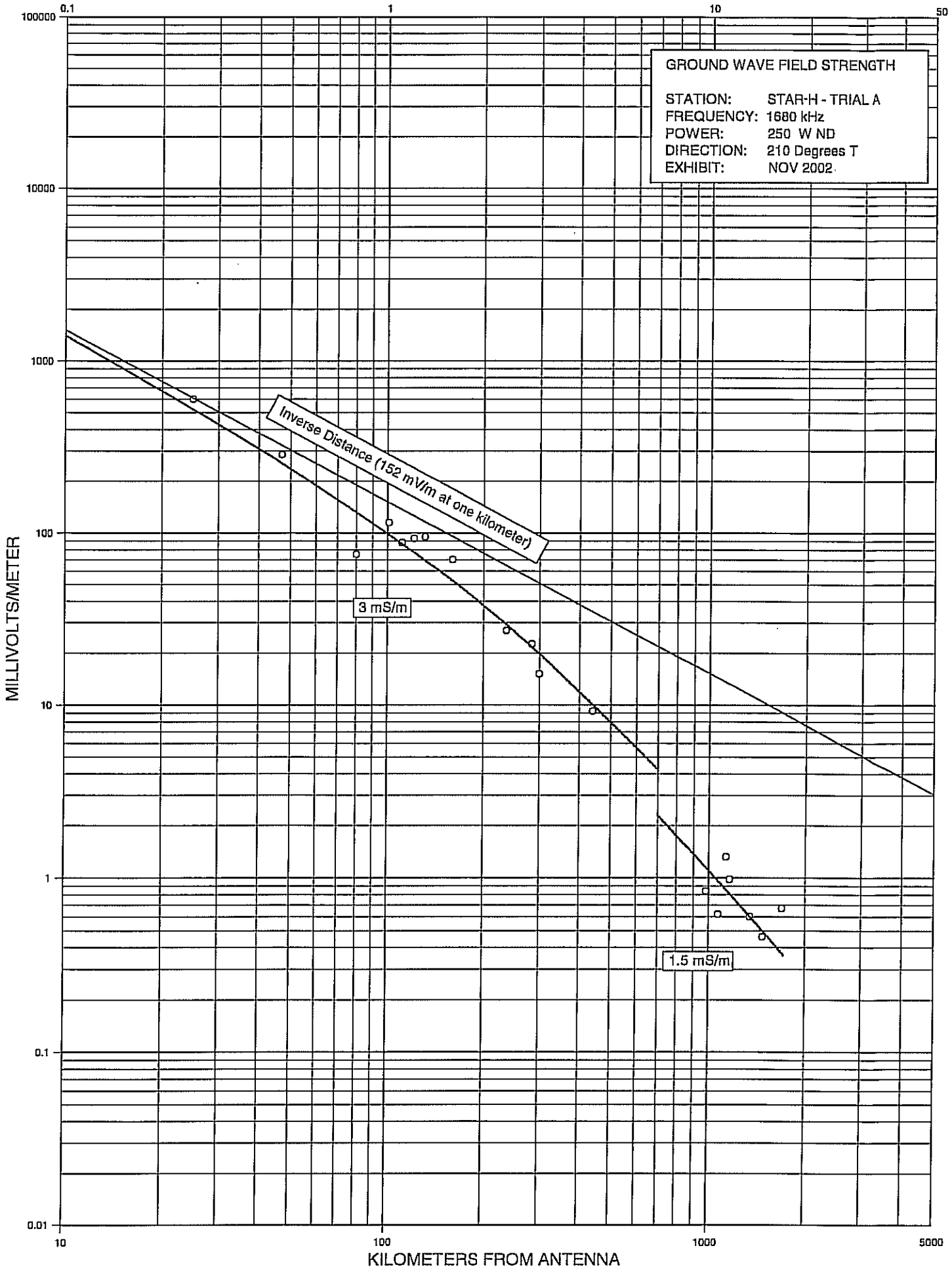


KILOMETERS FROM ANTENNA

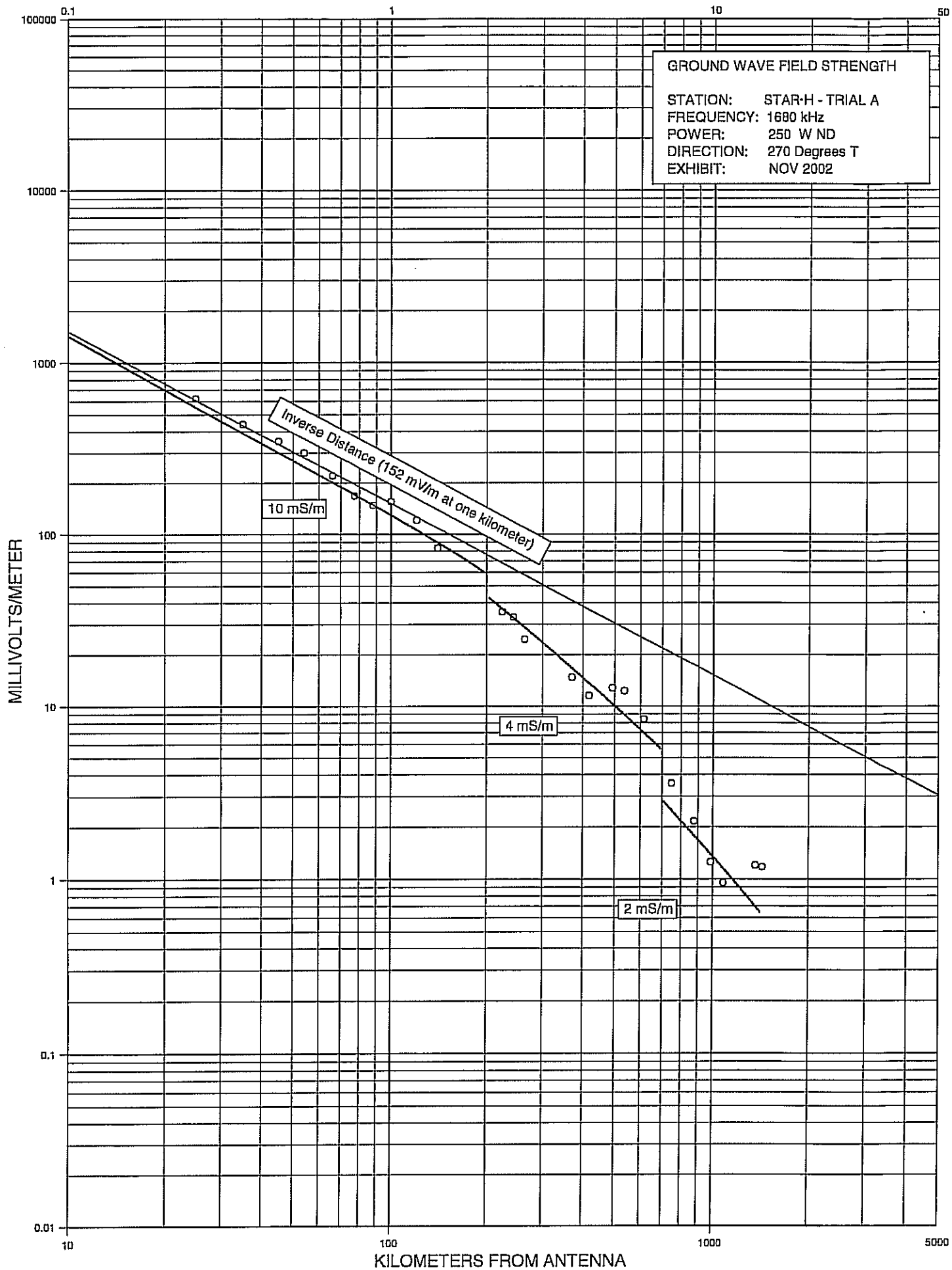




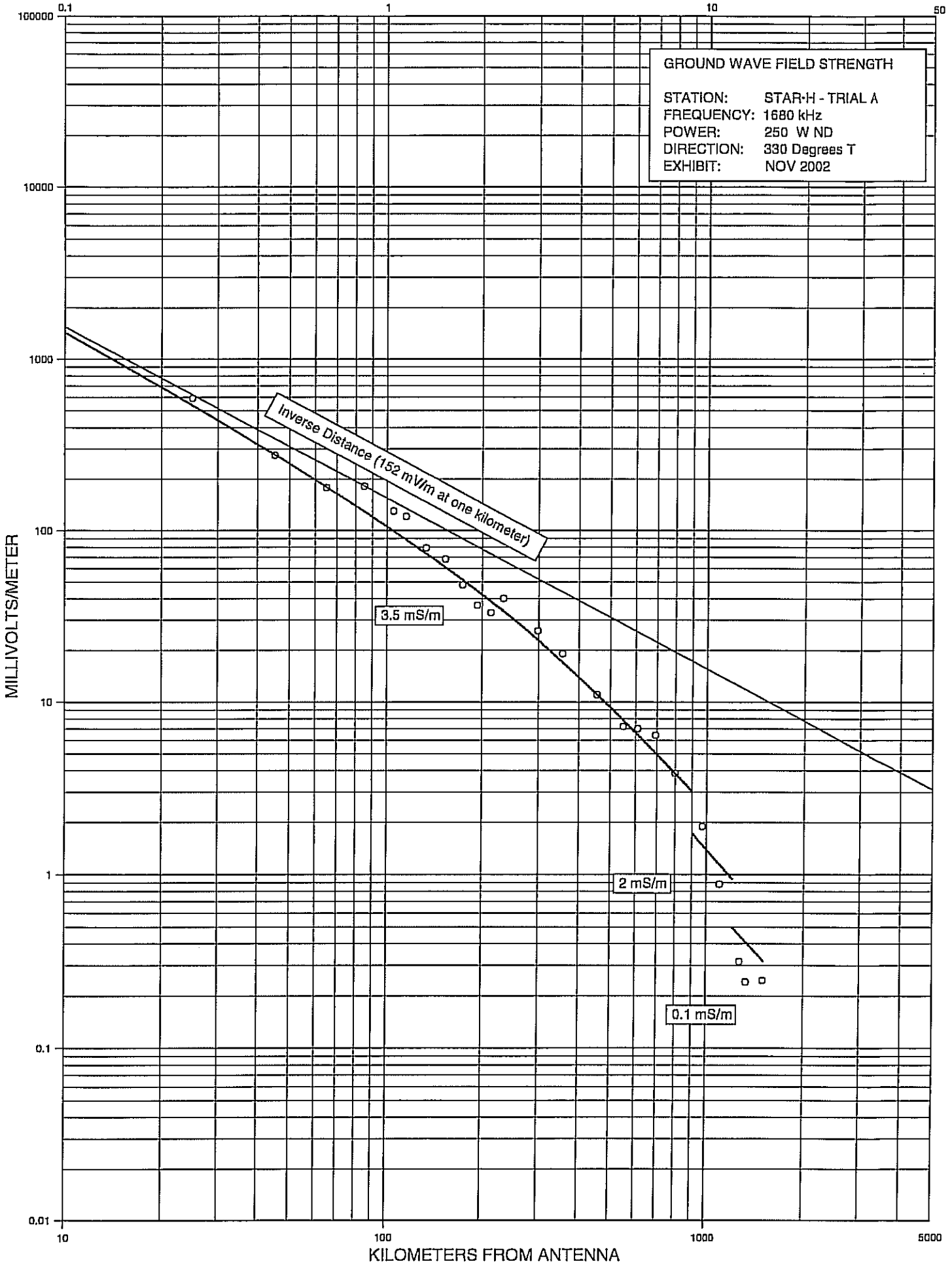
KILOMETERS FROM ANTENNA



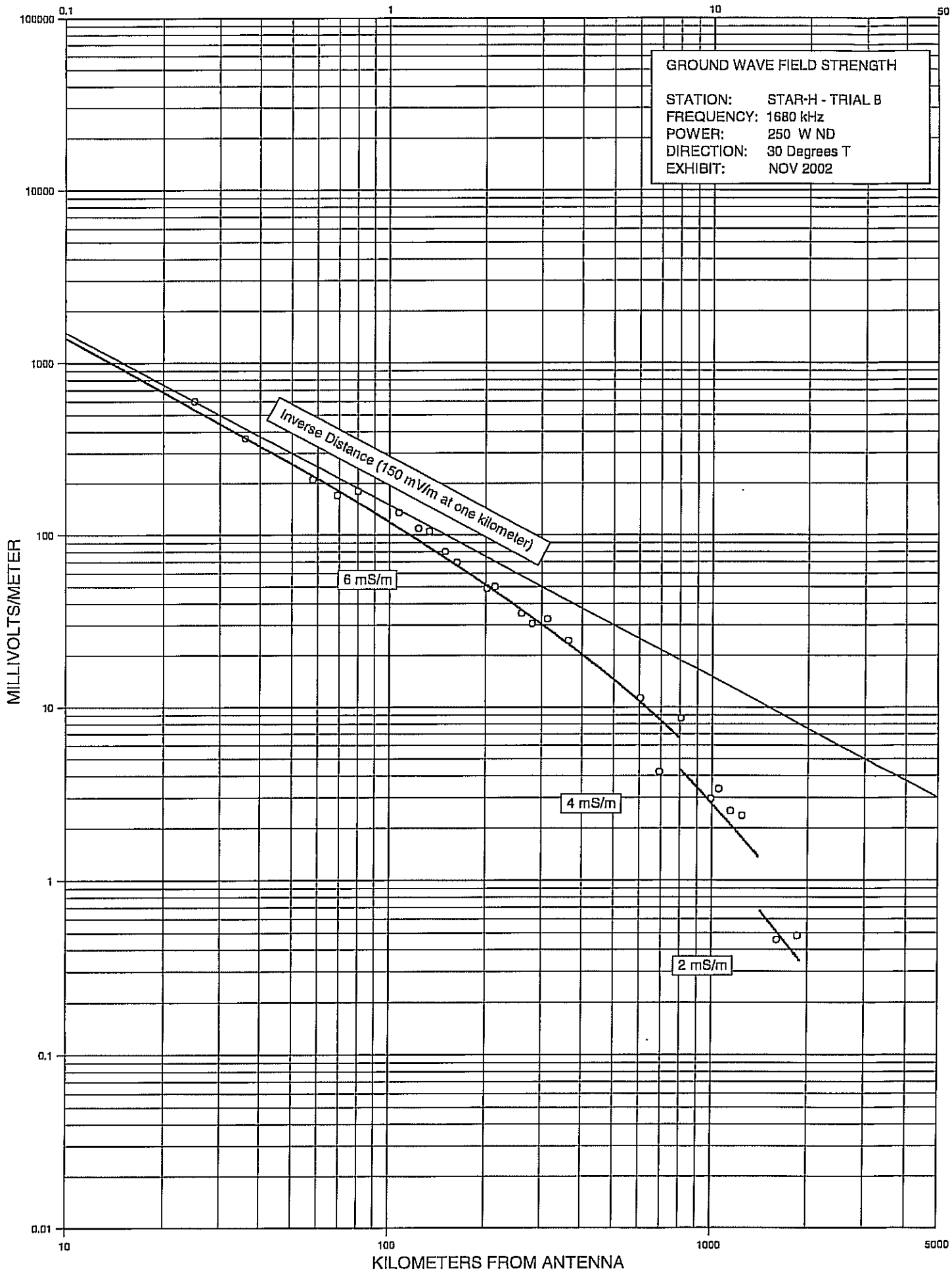
KILOMETERS FROM ANTENNA



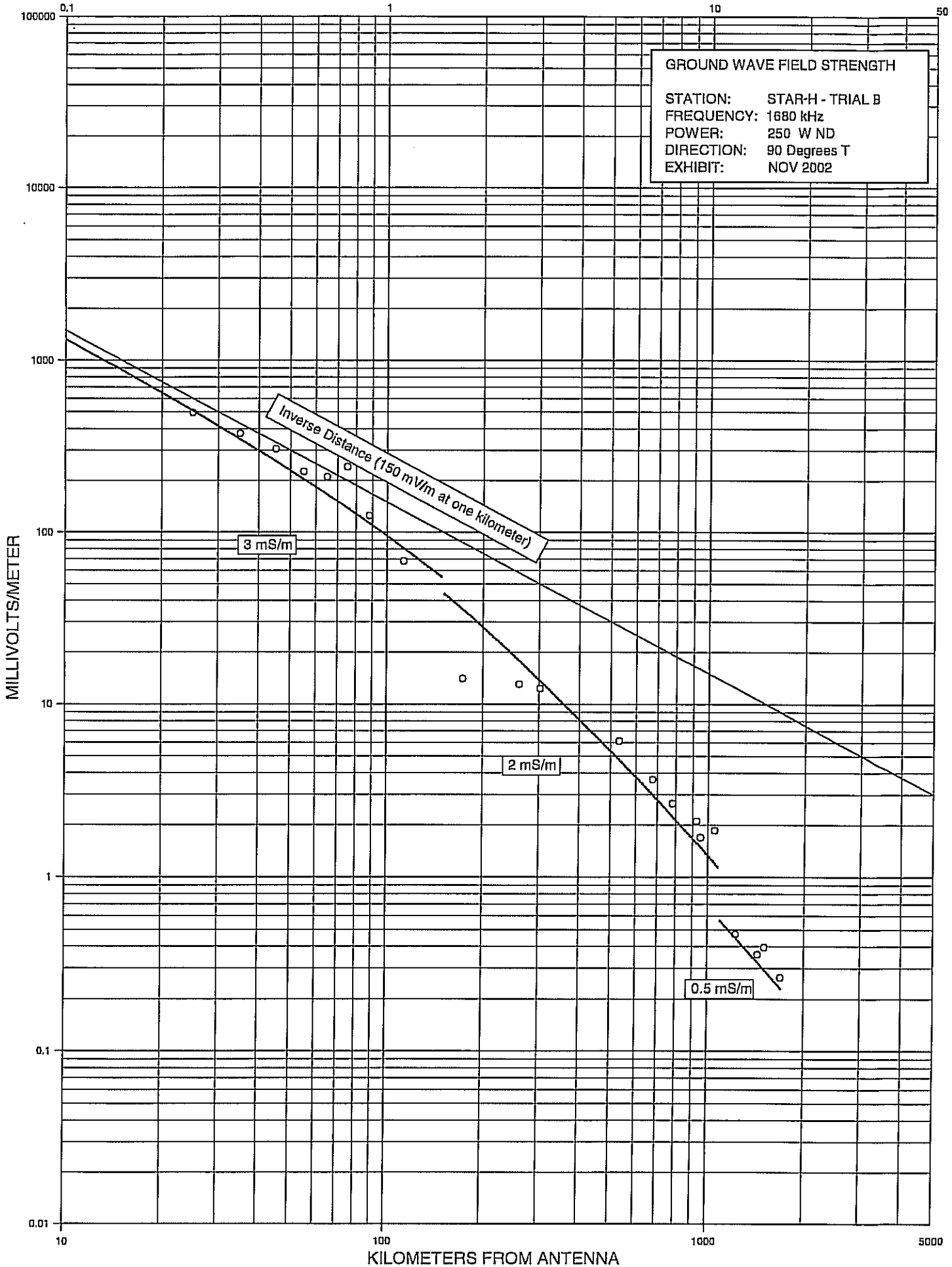
KILOMETERS FROM ANTENNA

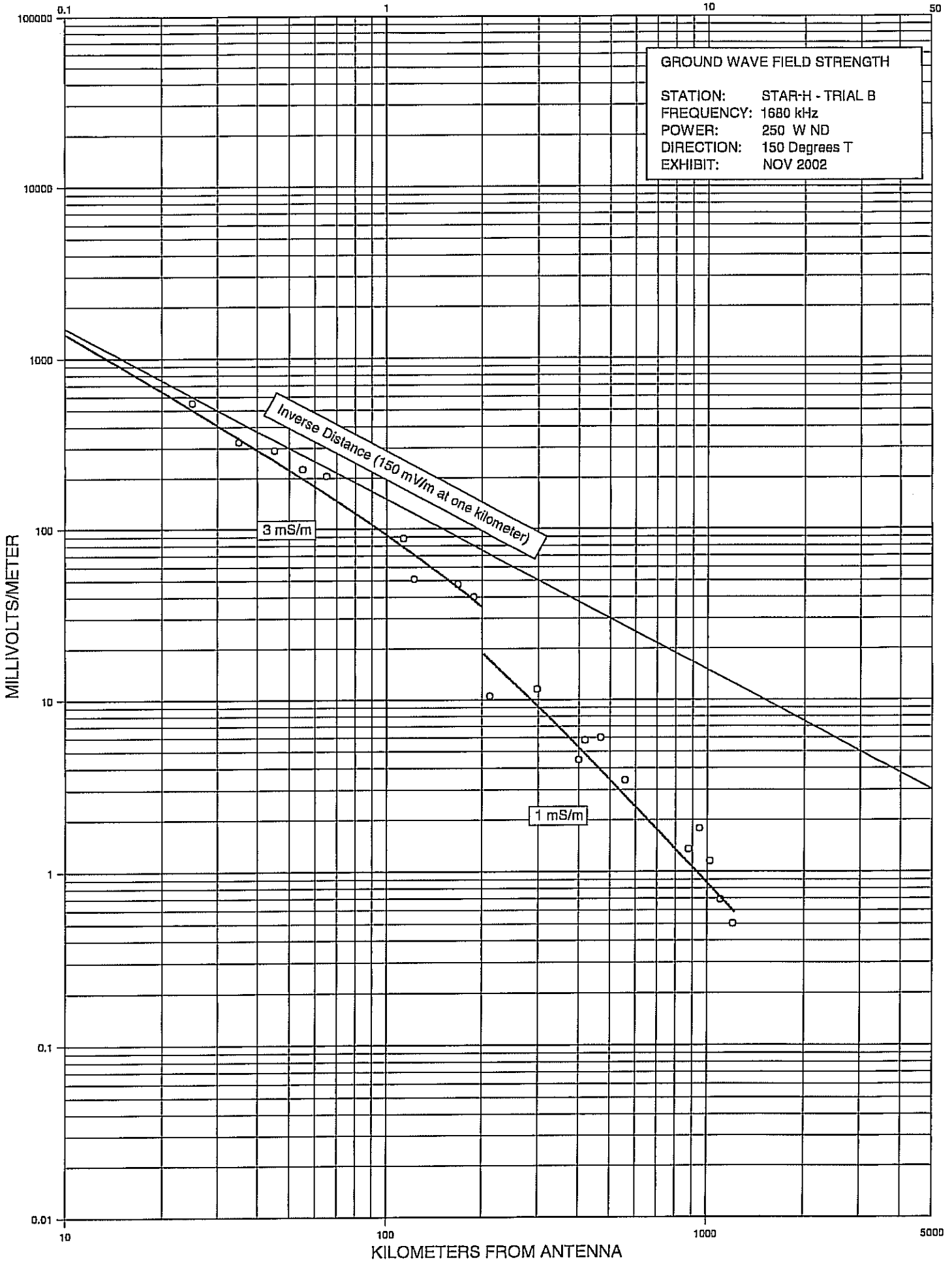


KILOMETERS FROM ANTENNA

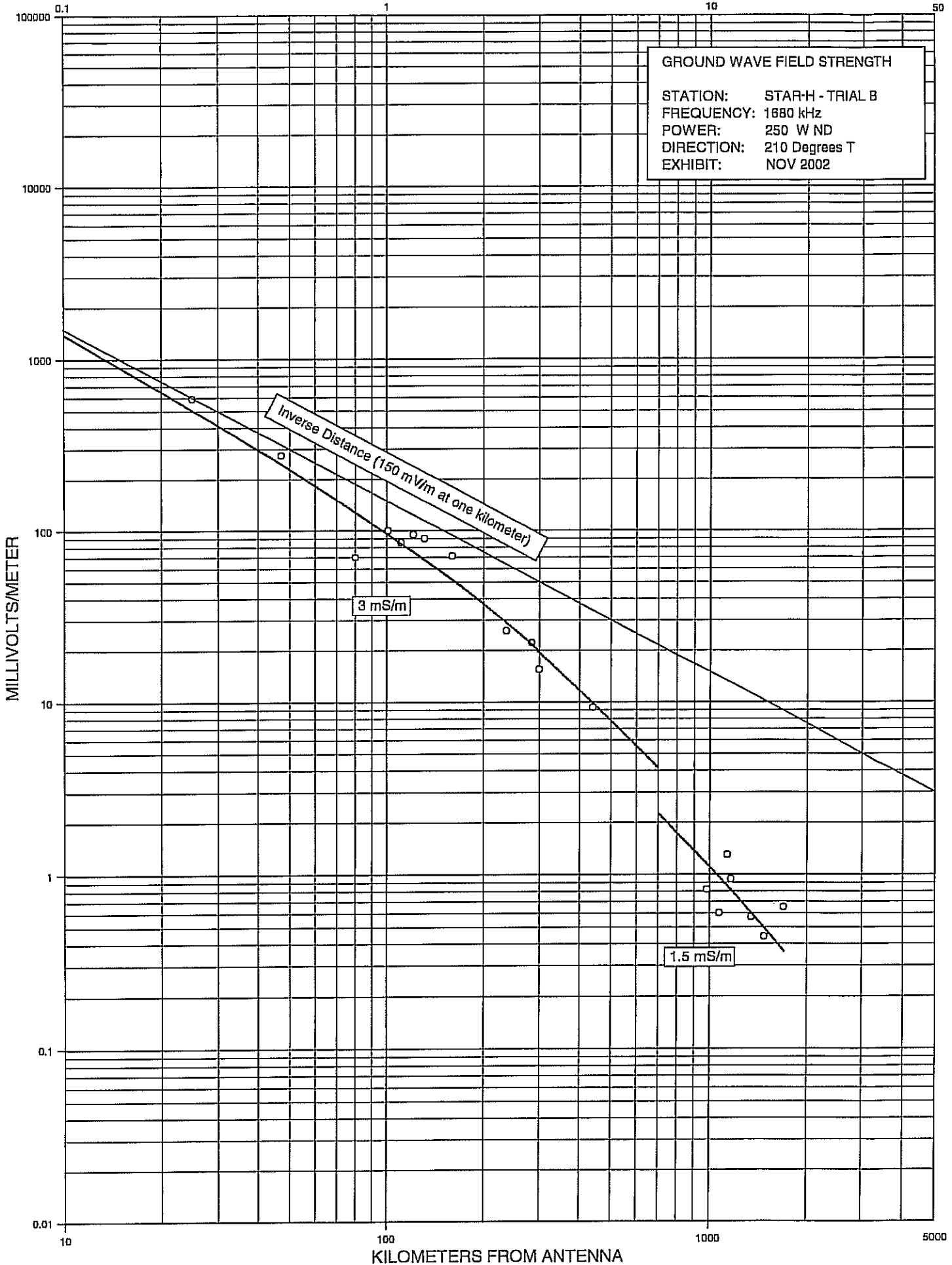


KILOMETERS FROM ANTENNA

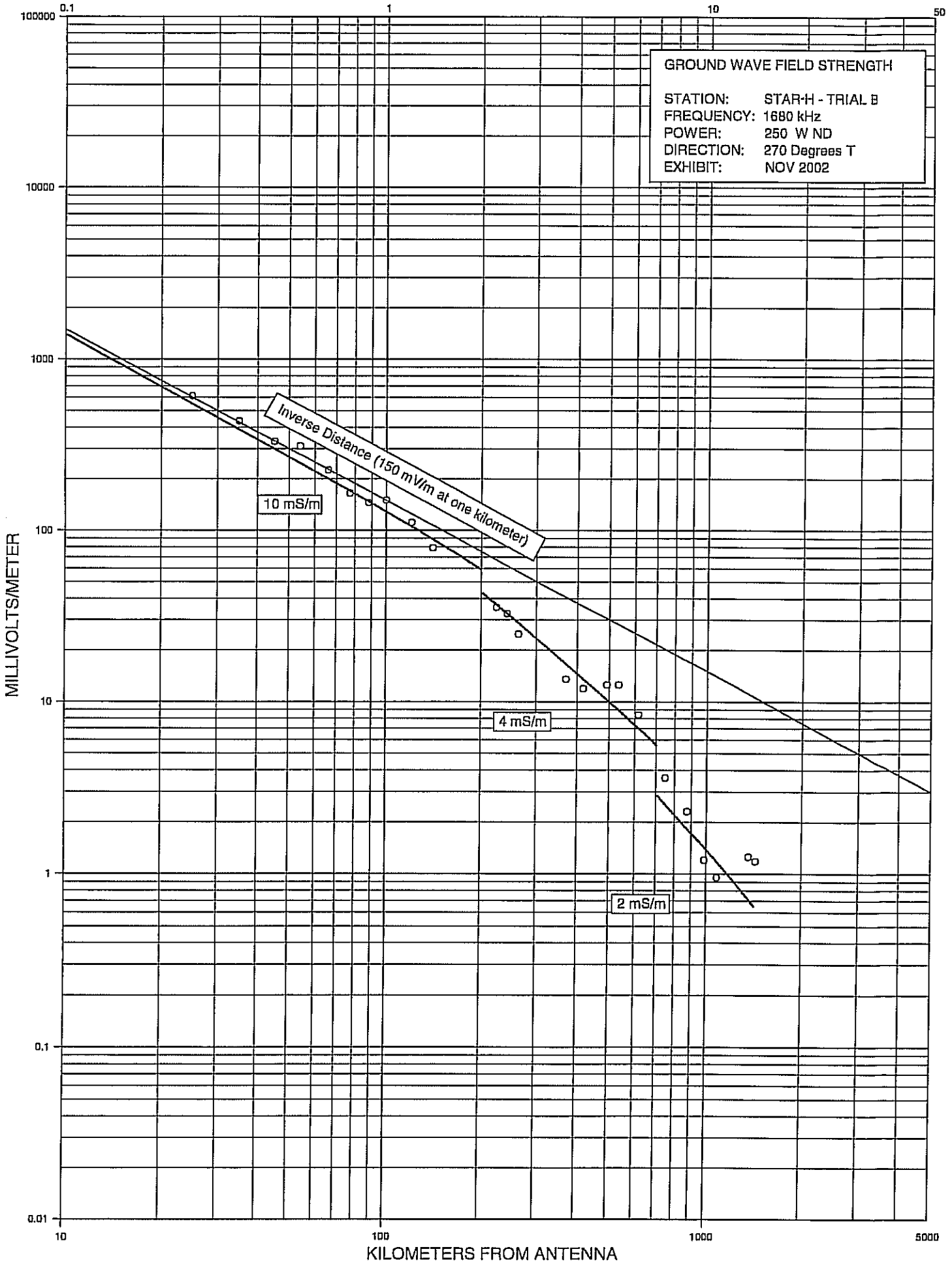




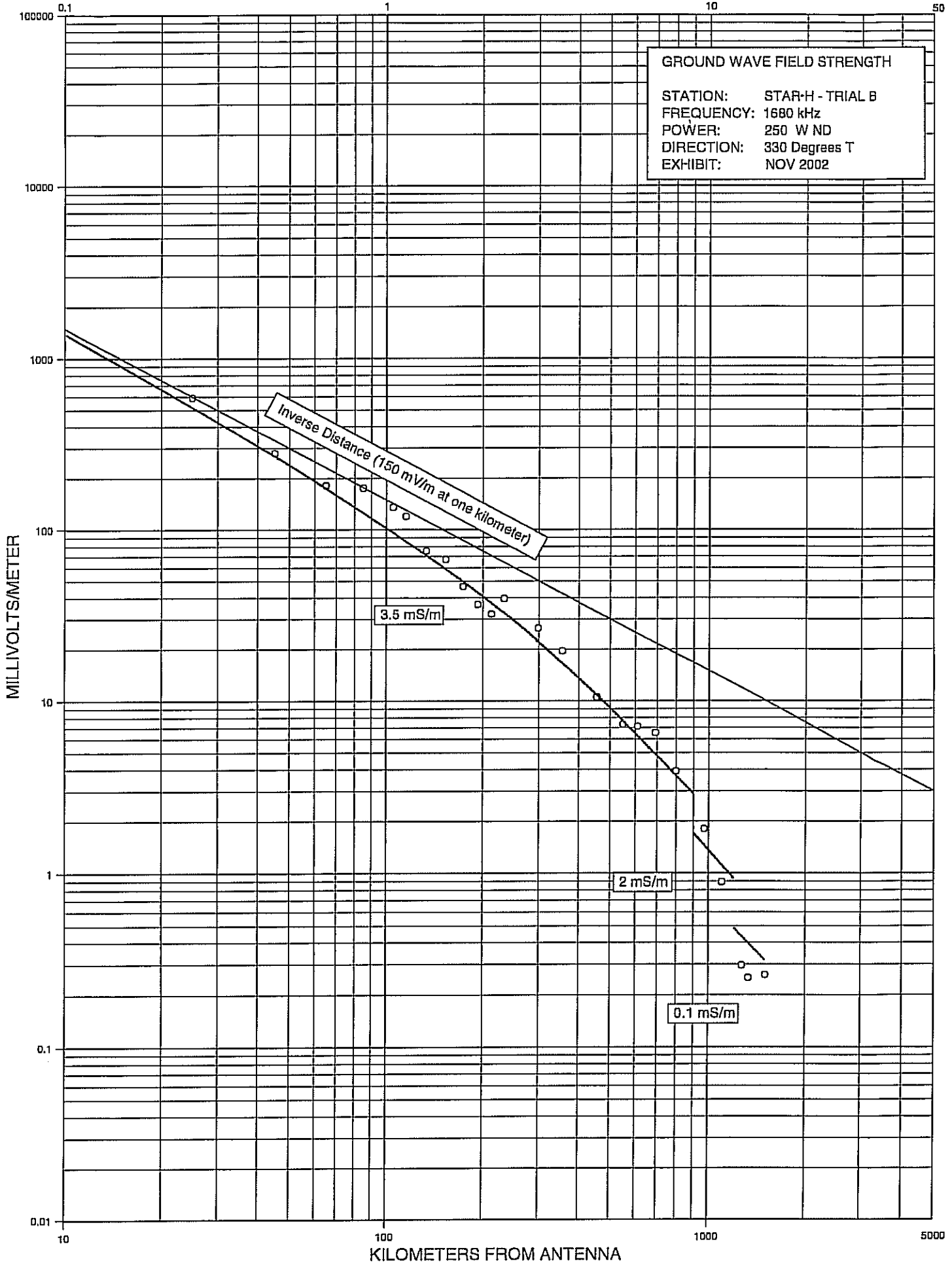
KILOMETERS FROM ANTENNA



KILOMETERS FROM ANTENNA



KILOMETERS FROM ANTENNA



STAR-H EXPERIMENTAL ANTENNA
1680 kHz 0.25 kW ND

Tabulation of Environmental Data

Antenna	Date	Max. Temp. (deg. F)	Total Rainfall (inches)
Reference	10/1/02	83	0.00
Reference	10/2/02	84	0.00
Reference	10/3/02	86	0.00
Reference	10/8/02	73	0.00
Reference	10/9/02	76	0.25
Trial A	11/6/02	54	0.25
Trial A	11/7/02	50	0.00
Trial A	11/8/02	63	0.00
Trial B	11/20/02	57	0.01
Trial B	11/21/02	54	0.04
Trial B	11/22/02	45	0.10